October 2014

Passive Geo-Location of a Radio Frequency Transmitter

Justin Daniel Rice
Worcester Polytechnic Institute

Patrick Lenti Boudreau
Worcester Polytechnic Institute

WORCESTER POLYTECHNIC INSTITUTE

MIT LINCOLN LABORATORY

MAJOR QUALIFYING PROJECT

Passive Geo-Location of an RF Transmitter

10/21/2014

Student Authors: Patrick Boudreau & Justin Rice

Project Sponsor: MIT Lincoln Laboratory

Project Faculty Advisor: Professor Edward A. Clancy

Project Sponsor Advisor: John Meklenburg

This work is sponsored under Air Force Contract #FA8721-05-C-0002. Opinions, interpretations, conclusions and recommendations are those of the author and are not necessarily endorsed by the United States Government.

Abstract

This project, completed at MIT Lincoln Laboratory will explore accurate timing in a system to passively geo-locate a radio frequency transmitter based on the time the transmitted signal arrives at two separate receivers. Two GPS disciplined oscillators (GPSDOs) will be used to keep precise time at both receivers and these units will be the focus of this report. First, the two GPSDOs were tested against one another and the difference between the timing signal outputs of each GPSDO was compared. Then the GPSDOs were placed in the full system and lab tests were conducted, focusing on their performance. Finally, a field test was conducted to determine the feasibility of these receivers as actual field units.

Statement of Authorship

In this project, Justin Rice and Patrick Boudreau worked to characterize the GPS disciplined oscillators and design and perform a test of the entire two-receiver geo-location system. Both partners contributed to all aspects of the project specifically running tests in the lab and designing and conducting the field test. Beyond this, Patrick focused on building the enclosure for both GPS disciplined oscillators, while Justin focused on processing the data and writing the MATLAB scripts to do so.

Acknowledgements

John Meklenburg advised and supervised us for the entirety of this project. John provided useful insight into the techniques and hardware utilized, as well as providing general assistance.

Ryan Lewis was a key person in building and testing the FPGA cards, as well as providing insight into the hardware as well as general assistance.

Jeffrey Blanco was a very helpful individual in assisting us with the entire MQP process as well as providing general assistance.

Dave Scott in TOIL, at MIT LL, for assisting us with making the enclosure for our GPSDO units.

Finally, our WPI advisor, Professor Ted Clancy, was vital in providing us assistance with our report as well as providing insight into our project.

Executive Summary

Project Overview

The goal of this project was to build and test a system with two receivers that geo-locates a moving transmitter. The target was emitting pulses at radio frequencies (RF) that were acquired by both receivers. Based on the difference between the time of arrival of the signal at both receivers, the target's location was estimated. There were three main objectives to meet in order to achieve this goal. First, the mathematics involved with locating the target had to be justified and understood. The second objective was to focus on clock synchronization between two receivers using a Global Positioning System (GPS) disciplined oscillator (GPSDO). The third objective was to integrate the necessary hardware needed in order to test the system on a small scale. The testing was primarily done inside the lab.

While it was important to meet these objectives, it was also essential to understand the requirements of the project. The requirements for this geo-location system were based on this system's future integration with other Group 105 projects, at MIT Lincoln Laboratory (MIT LL). This system needed to utilize the target's transmitted RF signal as an input to output the target's location to a user. Based on the system's output, the target should be located within 1.5°, in both azimuth and elevation, from the view of one receiver 70% of the time when the target is on a flight path 75 km or 100 km away from the receiver setup. The receiver setup consisted of two receivers that were separated by 2 km, which was another requirement set by the group. The long-term goal for the flight path and receiver setup is pictured in Figure 1, where flight of the target will either be on the line that passes through DC or BA. Under these constraints, each objective will be addressed.

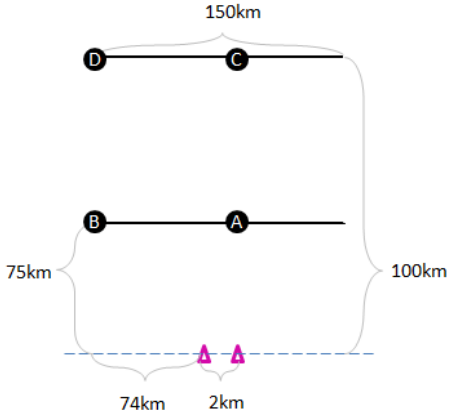

Figure 1: 75 km and 100 km flight paths with some extreme points marked as A, B, C, & D, which encompass all possible distances from the receivers.

The algorithm for locating the transmitter is based on the time difference of arrival (TDOA). The TDOA solution for each pair of receivers is a hyperbola, where the two receivers are the foci of the hyperbola. For each pair of receivers in the system, a hyperbola was computed. When there are multiple pairs of receivers, the hyperbolas created will intersect at the predicted location of the transmitter. In the case of this system, there were two receivers, hence one hyperbola, but there was also a known flight path for the transmitter. This system's predicted location of the transmitter comes from the

intersection of the single TDOA hyperbola and the known flight path. It is also important to note that the predicted location of the transmitter is based on a two dimensional approximation in a three dimensional space.

The hardware element of most interest to Group 105 during this project was a GPSDO. Since the location algorithm was dependent on the time, it was critical to keep precise clocks at each receiver. To keep this precise time, there was a GPSDO at each receiver and they were used to synchronize the clocks. The GPSDOs synchronize the local clocks in the receiver to Coordinated Universal Time (UTC) so that both receivers are precise to one another. The GPSDOs synchronize clocks by receiving signals from the GPS called a pulse per second (PPS). The local oscillator on the GPSDO synchronizes with the PPS signal through a phase locked loop. The output of the phase locked loop is a time accurate to ±30ns UTC RMS; an accuracy that is acceptable for this system. The second part of the hardware objective was to integrate the hardware provided by Group 105. Figure 2 shows the general block diagram of the hardware.

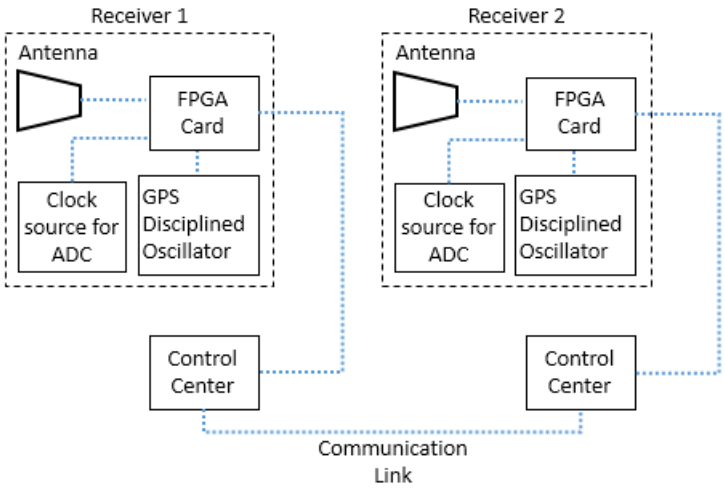

Figure 2: Two-receiver geo-location system block diagram test setup.

A laboratory test was conducted with delay lines to simulate distances. The first setup was a zero TDOA case, where the length of the cable between a power splitter attached to a signal generator and each of the receivers was equal. Therefore, the signal had to propagate through the same length of cable to each receiver, which means the signal should arrive at both the receivers at the same time. Other lengths of cables were tested to determine if the system behaved as expected. The time of arrival of the signal at the receiver as well as the associated time of day was saved to a text file at the control center, which was on a laptop. The TDOA was computed using the two times of arrivals.

The system was setup in the field in order to test its operation in a small-scale realistic scenario. For the field-test it was important to consider the separation of the two receivers and the transmitter. The geometry of the test was determined based on the timing errors between the two GPSDOs, and their corresponding distance errors. The allowable distance errors based on the 1.5° angle requirement were also crucial to planning the field test. The field test was not conducted on the desired scale of the eventual system; rather, a smaller test was chosen to test the system's performance.

Results

Clock Synchronization Findings

The second column of Table 1 shows maximum allowable distance errors at various points on the flight path, pictured in Figure 1. The maximum allowable distance errors were derived from the 1.5° requirement and then were compared to the results of multiple receiver timing errors converted into distance errors. The shaded blocks in the 75 ns and 90 ns columns are values that exceeded the maximum limit.

Table 1: Allowable error at different extreme points along the flight path, as well as distance error associated with different timing errors from GPSDOs. The shaded regions represent results that are too large.

Extreme points along flight path	Maximum allowable distance error (km)	Total distance error (km) with corresponding timing error between GPSDOs					
		15 ns	30 ns	45 ns	60 ns	75 ns	90 ns
A	0.98	0.17	0.34	0.50	0.67	0.84	1.01
B	1.96	0.48	0.95	1.43	1.90	2.38	2.86
C	1.31	0.22	0.45	0.67	0.90	1.12	1.35
D	2.04	0.44	0.88	1.31	1.75	2.19	2.63

Table 2 shows the averages of statistics for 11 two-hour captures of the differences between the two PPS signals, one from each GPSDO, on the oscilloscope. Ideally, both PPS signals should arrive at the same time and there should be no time difference. But, according to the data sheet, 68% of the time the GPSDO may be different from UTC by 30 ns. So, when taking into account the error accumulated by both cards the results in Table 2 are better than the data sheet specifications. That is because the difference between the two is ±30 ns 61.6% of the time while if these errors added linearly the difference should be ±30 ns 34% of the time.

Table 2: Average of statistics of time difference between pulse per second (PPS) signals.

Total Runs	Mean (ns)	Standard deviation (ns)	Percentage of time differences within ±60 ns	Percentage of time differences within ±40 ns	Percentages of time differences within ±30 ns
11	11.0	34.0	90.5%	73.5%	61.6%

In-Laboratory Test

Before the outdoor field test, two 16-hour tests were run in the lab. During both tests, the system was setup in the manner seen in Figure 2, except that instead of transmitting the signal through antennas the signal was transmitted through a coaxial cable. From the signal generator, the simulated transmitter, the signal passed through a 3 ft coaxial cable into a power splitter and from there through a cable to each receiver's input.

The first test was a zero TDOA case, where the setup consisted of 6 ft cables from the power splitter to each receiver. Since the distance that the signal had to travel to each receiver was the same, the time the signal arrived at each receiver should have been the same and the ideal TDOA would be zero seconds. However, with our setup, the average value of the TDOA over the 16 hr test was 105 ns as seen in Figure 3.

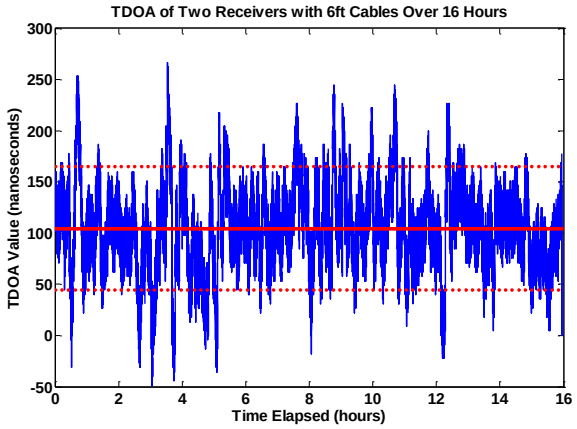

Figure 3: The solid red line represents the average value of the TDOA, 105 ns. The red dashed lines represent the expected deviation from the mean of ±60 ns based on GPSDO measurements.

The second test performed added 150 feet of cable between the power splitter and one of the receivers. This test was conducted in order to determine if the system behaved as expected. Assuming the 105 ns average TDOA seen in the initial test was a constant offset between the receivers, this test should provide a TDOA value of 180 ns less than the zero TDOA test. The 180 ns value results from the propagation delay through the cables used, which was 1.2 ns/ft. The actual result of the test showed that the average TDOA was 201 ns less than the zero TDOA case. This result is 21 ns away from the expected result. The spread around the mean is what is expected from the performance of the GPSDOs. The results are shown in Figure 4.

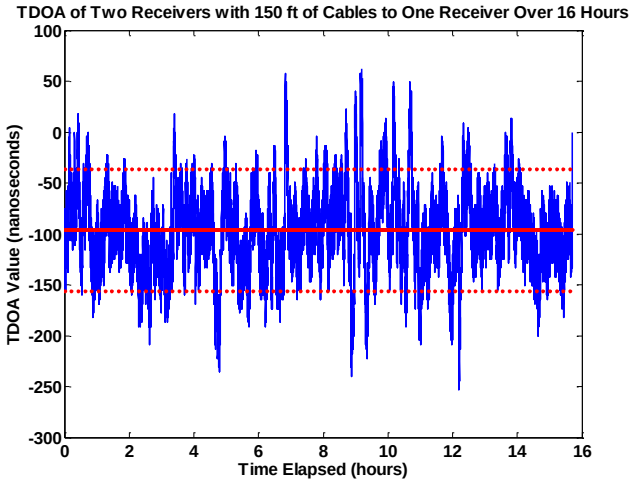

Figure 4: The solid red line represents the average value of the TDOA, -96 ns. The red dashed lines represent the expected deviation from the mean of ±60 ns based on GPSDO measurements.

Field Test

Due to Federal Communications Commission (FCC) restrictions on transmission power and equipment availability, we conducted the test at 2.4 GHz and separated the receivers by a distance of 50 meters. The time of arrival of the transmitted signal at one receiver decreased linearly as time passed, whereas the other receiver had time of arrivals that stayed around the same value. These results were unexpected when compared to the laboratory test results. There are many reasons for this discrepancy such as, environmental conditions, actual receiver separation, or the signal propagating through air as opposed to a coaxial cable.

Conclusions

This project set out to integrate and test a two-receiver geo-location system with a particular focus on clock synchronization between the receivers. We determined that the difference between the GPSDOs' PPS outputs were within ±60 ns 90% of the time. Once the GPSDOs were determined to operate within the 1.5° requirement over 70% of the time, laboratory testing was performed. During testing a 105 ns offset was observed. Other than this offset, the system was still performing within the 1.5° requirement.

The full system was then tested in the field, but the results were inconclusive and a decision was made that there were too many source of error to pursue further field-testing in the limited time available. After reviewing the results, another decision was made to perform further testing in the laboratory in order to better understand the system. The secondary laboratory testing provided results that were contradictory to the initial testing. The results proved that the 105 ns offset initially seen was not a constant offset between the receivers. Further testing procedures to determine the source of the error were determined for future work, but the exact source of the error is still unknown.

Table of Contents

Table of Figures

Table of Tables

1. Introduction

In military operations it is important to know the location of all enemies and allies. A widely used technique to keep track of all targets in the field is radar ranging. Radar ranging is an active technique in which a radar system transmits pulses of energy at radio frequencies (RF) and receives those pulses, which have been reflected by objects in the system's field of view. Depending on the characteristics of the return, an operator can determine what kind of object the pulse reflected off of and where that object is located.

To use radar ranging to geo-locate an object, an entire radar system must be constructed. The entire system includes a receiver, transmitter, and signal processing. Though this kind of system can be very effective, a full radar system is costly and may be unnecessary. If the target of interest has a powerful radar system it is possible to geo-locate that target by its emitted radar pulses.

The Airborne Radar Systems and Techniques group, Group 105, at Massachusetts Institute of Technology Lincoln Laboratory (MIT LL), is interested in the development of a system to passively geo-locate an RF transmitter. The RF transmitter is assumed to be traveling along a known flight path, and Group 105 would like to know its exact location on the flight path at a given point in time. This system will compliment other projects currently ongoing in Group 105.

The requirements for this geo-location system, as provided by Group 105, were based on this system's future integration with other Group 105 projects. This system should receive the target's transmitted RF signal, at Ku band, and use it to output the target's location to a user. Based on the system's output, the target should be located within 1.5°, in both azimuth and elevation, from the view of one receiver 70% of the time when the target is on a flight line 75 km or 100 km away from the receiver setup. When the target is on either flight line, the receiver setup will consist of two receivers that are within 2 km of each other. The scope of this project was limited to integrating and testing each component in the system. A field test was conducted, but it was done on the order of meters as opposed to the full scale.

Time difference of arrival (TDOA) was the method chosen to passively geo-locate an RF transmitter while meeting Group 105's requirements. TDOA utilizes the difference in the time that a signal is received at different locations. With the two-receiver requirement, TDOA was the most viable option to locate the transmitter passively. TDOA requires very precise timing measurements; therefore two GPS disciplined oscillators (GPSDO) were purchased to synchronize the clocks at both receivers. The GPSDOs were accurate to Coordinated Universal Time (UTC) to within tens of nanoseconds.

In order to utilize TDOA and the GPSDOs to locate an RF transmitter, two receivers were placed at separate geographical locations. Each of the receivers included an antenna to receive the signal, a down-converter to down-sample the received RF signal to an intermediate frequency (IF), a field programmable gate array (FPGA) card to sample and process the signal, a GPSDO to synchronize the clock, and a control center where the receivers were controlled from and the TDOA was computed. Most of the required components are already in Group 105's possession; therefore, the focus of the project was on beginning to characterize the GPSDOs to ensure they met the needs of the system and testing the full system to observe its behavior and how well it operated.

The remainder of the report will be dedicated to discussing the research conducted to understand the method of passive geo-location and the hardware needed to perform the desired solution. First, relevant background information will be covered. Second, the overall design of the system will be covered. Third, the methods followed to characterize the GPSDOs will be discussed in detail and the results reported. Finally, the integration and testing of the full system will be discussed.

2. Background

Many topics were researched in order to understand the requirements for the problem presented by Group 105. This research provided a background upon which to base a proposed solution. The remainder of this section covers two main topics, namely, time synchronization and the existing hardware that was used for the solution.

2.1 Time Synchronization

2.1.1 Keeping Time

Coordinated Universal Time (UTC) is the primary means by which the world sets clocks and time [McCarthy and Seidelmann, 2009]. UTC is kept to within ± 0.9 seconds of International Atomic Time (TAI). TAI is formed from the weighted average of the time kept by over 200 atomic clocks, which are located in laboratories all over the world. The laboratories broadcast a frequency signal with their estimated TAI time code over the Global Positioning System (GPS). A central location produces a weighted average of these times to form UTC [McCarthy and Seidelmann, 2009].

Atomic clocks are the most accurate time and frequency standards, where the most accurate atomic clock in the US is accurate to 1 second in 300 million years [McCarthy and Seidelmann, 2009]. Atomic clocks operate based on atomic physics by utilizing the microwave signal that is emitted by atoms when they change energy levels. Slowing atoms with lasers cools the atoms to near absolute zero temperature where the microwave signal is measured. Next, these cooled atoms are probed in an atomic fountain, which briefly exposes the atoms to a microwave electromagnetic field twice. The atoms are exposed once and then there is a brief pause, a time T, followed by the second exposure. After the second exposure the fraction of the atoms that transitioned energy states in time T is measured. This measurement is the basis for time keeping of an atomic clock. [McCarthy and Seidelmann, 2009]

Not every clock has the accuracy and precision of an atomic clock. A precise clock should always keep the same frequency, and an accurate clock will always display the correct UTC time [McCarthy and Seidelmann, 2009]. Clocks experience a phenomenon

known as clock drift, which affects their precision and accuracy. Clock drift is a phenomenon where a clock appears to run at a slightly different speed than another clock. The reason why clocks experience clock drift is due to many factors, such as quality, stability of its power source, and even ambient temperature. A clock that experiences clock drift will need to be adjusted to display the correct UTC time.

Clock synchronization is an important concept when dealing with multiple systems that need to maintain accurate and precise timekeeping with one another. Not every clock has the accuracy and precision of an atomic clock; therefore it is difficult to maintain synchronization between two clocks. Separated systems with synchronized clocks allow the systems to produce accurate time stamps if there are processes that rely on such information.

To demonstrate the large effect clock error has on spatial measurements, first consider an object that leaves a location where a clock reads 12:34:56, and arrives at another location where that clock reads 12:35:06, after travelling at a constant velocity of 500 meters per second. The velocity equation determines that the object travelled a distance of 5000 meters. If the clocks were inaccurate to one another, even by 1 second, then the computed distance the object travelled would be 4500 or 5500 meters. A small error in time can result in a sizable error in distance.

2.1.2 Synchronizing Two Clocks

There are two important methods for synchronizing a clock with another clock signal. Consider clock A and clock B, where clock B is attempting to synchronize with clock A. The first technique used to synchronize clock B to clock A is to physically reset clock B. Every time clock B's pulse is off of clock A's incoming pulse by an amount greater than the desirable error, clock B can be reset. A limitation to this method is that the reset can only be as accurate as the pulse width of clock B. For example, if clock B is a 225 MHz clock, then, on a reset it will be within 4.44 ns of clock A. The second method for synchronizing two clocks is to adjust the phase of one of the clocks. Again, consider clock B is trying to synchronize to clock A. If clock B is outside of the allowable error its phase can be

increased or decreased slightly to synchronize with clock A. The most common way to synchronize phase is via a phase locked loop (PLL).

The general block diagram for a PLL is pictured in Figure 1. The first block is a phase detector. The phase detector takes in a reference signal and a signal from the local oscillator to compare the phase of each signal. This block then outputs whether the local oscillator needs to increase or decrease its phase. The loop filter takes the information from the phase detector and converts it into a signal that is sent to the voltage controlled oscillator. Depending on the voltage output from the loop filter, the voltage controlled oscillator either increases or decreases its phase. The output of the voltage controlled oscillator is the disciplined output of the system, which means it is synchronized to the reference signal.

There is a feedback portion to this loop, which sends the output through a divider, 1/N in Figure 1, which divides the frequency of the voltage controlled oscillator's output to that of the frequency of the reference signal. By dividing the frequency down to the reference signal's frequency, the voltage controlled oscillator is allowed to oscillate at a different frequency than the reference signal. Hence, if clock A is a 1 Hz clock and clock B is a 100 MHz clock, then the reference signal would be 1 Hz and the disciplined output would be 100 MHz. Clock B's output would also be disciplined with the 1 Hz signal, thus, the divider would have to reduce the 100 MHz signal down to a frequency of 1 Hz.

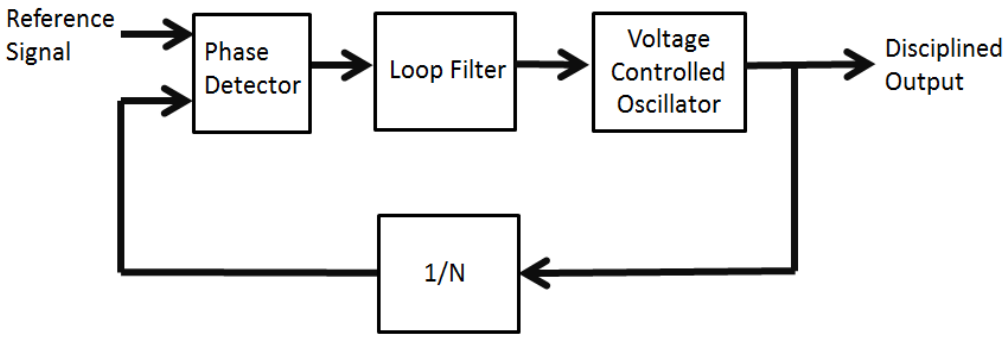

Figure 1: Phase locked loop block diagram.

2.1.3 Synchronizing Time within a Network

2.1.3.1 Network Time Protocol

One method of time synchronization is to utilize NTP. NTP is a networking protocol that allows computers in a packet-switched, variable-latency network to synchronize their corresponding clocks [Mills, 2010]. The intent of NTP is to synchronize the clocks of all computers within a network to be within milliseconds of UTC. Synchronization is usually within tens of milliseconds via public Internet, and can be within one millisecond over a local area network (LAN).

NTP is organized into a hierarchy, where each layer is known as a stratum. The top node, stratum 0, is a high precision timekeeping device such as an atomic clock or GPS clock [Mills, 2010]. Stratum 0 devices are considered to be reference clocks for the rest of the NTP hierarchy. A device that is considered to be stratum 1 will typically have a clock that is synchronized to within a few microseconds of the corresponding stratum 0 device. Stratum 1 devices are considered to be primary time servers.

A stratum 2 device is in turn synchronized over a network to multiple stratum 1 servers. These devices are connected to multiple servers in order to allow the device to assess the quality of the connection and choose the best host from which to base its synchronization. There can be up to a stratum 15 device, where the accuracy of the synchronization is based on the distance from the stratum 0 device, in terms of connections. Stratum 16 is reserved for devices that are unsynchronized.

In order to obtain NTP synchronization, the protocol used is a client-server model or a peer-to-peer model [Mills, 2010]. The client-server model is when the client connection is considered to be the requester of synchronization, while the server is considered to be the reference from which the client synchronizes. The peer-to-peer model is where both ends of the connection consider the other to be a potential time source, from which to synchronize their clock.

There are two methods of NTP synchronization. Both methods involve sending a synchronization packet. This packet is comprised of a 64-bit timestamp that has 32 bits for

seconds and 32 bits for fractions of seconds. This 64-bit timestamp is the number of seconds since January 1, 1990, with a resolution of 233 picoseconds. One method of NTP synchronization involves the server only sending a synchronization packet to a client that requests one. Another method of synchronization is for the server to broadcast synchronization packets periodically while the clients passively listen for these packets and update their clocks when a packet is received.

In order to synchronize the clocks accurately, the round-trip delay between when the client requests a packet and the time the client receives the response needs to be determined. The round-trip delay is used to calculate an offset for the received timestamp. The round-trip delay, δ, can be calculated as follows:

$$\delta = (t_3 - t_0) - (t_2 - t_1) \quad (1)$$

where t_0 is the client's timestamp of the request packet transmission, t_1 is the server's timestamp of the request packet reception, t_2 is the server's timestamp of the packet transmission, and t_3 is the client's timestamp of the response packet reception. The difference between t_3 and t_0 is the time elapsed on the client's end, and the difference between t_2 and t_1 is the time the server spends before a packet is sent.

Utilizing the round-trip delay, an offset can be determined to add to the received synchronization packet to account for the transmission delay. The offset, β, is represented as follows:

$$\beta = \frac{(t_1 - t_0) + (t_2 - t_3)}{2} \quad (2)$$

All of the time variables in Equation 2 are the same as in Equation 1. The difference between t_1 and t_0 is the time between packet-request send and receive, and the difference between t_2 and t_3 is the time between packet-response send and receive. The offset, β, is determined by taking the average between the two transmission delays, assuming that the delays are equal on average. The offset is then added to the timestamp received in the packet, and the computer is synchronized to this new timestamp.

2.1.3.2 Algorithms

A correction algorithm queries a time server for the current time. Once the current time is received, the requesting unit will update its displayed time. One such algorithm is Cristian's algorithm. This method issues a procedure call to query a time server for the current time. When the machine updates its current time based on the time provided by the server, the algorithm also attempts to determine the network and processing delays. The delays are determined in order to adjust the provided time accordingly. These delays are determined through the use of Equation 1. Once the round-trip delay is determined, an offset is calculated with Equation 2 to be added to the provided time by the server. This algorithm, though, assumes that the network and processing delays added to the current time update are accurate as well. [Cristian, 1989]

Another similar method is the Berkeley algorithm. This method assumes that no machine has an accurate time source. Therefore, this algorithm takes the time average of all connected machines, and synchronizes each of the machines to this average [Gusella and Zatti, 1989]. The algorithm also has provisions where it can determine if a machine is too skewed in time from the other machines, and leaves out that specific machine when taking the time average. Both of these algorithms make some assumptions. The Berkeley algorithm assumes that no machine has an accurate time source, when in fact one of the machines may actually be synchronized to a very accurate source.

2.1.4 Keeping Time with GPS

A GPSDO is a card that is used to keep accurate time to the GPS. The GPSDO houses a GPS receiver and a local oscillator. Together these two units output a very accurate time. But, to output that time the GPSDO relies on GPS time.

2.1.4.1 GPS Time

For accurate positioning estimates, it is important that every GPS satellite keep accurate time during every rotation around the earth. Every GPS satellite is equipped with an atomic clock which updates once every orbit. The GPS satellites are in medium Earth orbit, approximately 20,200 km above the Earth's surface. This orbit leads to a revolution period of 11 hours and 58 minutes, half of a sidereal day. A sidereal day is derived from

sidereal time, which is defined based on the Earth's rate of rotation relative to a fixed star. [Lombardi, 2008]

A modern requirement for GPS is that the contribution of each satellite's clock to the receiver location error cannot exceed 1 m. By inverting the speed of light, 3×10^8 m/s, an allowable timing error of 3.3 ns/m is found. Because of the previously mentioned requirement, this error becomes 3.3 ns as the maximum error that a single satellite should contribute to the time error at a receiver.

The Master Control Station (MCS) for the GPS is located at Schriever Air Force Base in Colorado. The MCS is responsible for updating the satellites every orbit. The MCS updates the systems by first gathering satellite data from monitoring stations all over the world. These data are processed in software; implementing a Kalman filter and various errors are calculated for each satellite. The relevant update information is sent to each satellite so it can update in real time. [Allan, 1997]

The GPS time, to which all satellites are synchronized, is different from UTC and TAI. UTC adds leap seconds to correct for rotations of the earth while GPS time does not. In 1980, GPS time was set to UTC and UTC was offset from TAI by 19 seconds. So, the difference between GPS time and TAI is a constant 19 seconds. But, UTC and GPS time do not have a constant time offset because UTC has and will continue to add leap seconds that GPS time will not take into account. [Allan, 1997]

2.1.4.2 The GPS Disciplined Oscillator

A GPSDO is an extremely accurate time reference used in many calibration laboratories across the United States. A GPSDO contains both the benefit of using GPS as a way to keep long-term time accuracy and a crystal oscillator to keep precise time on the short term. Hence, a GPSDO is a very good choice for a system that needs to keep multiple geographically separated clocks synchronized. [Lombardi, 2008]

Accurate time at GPS satellites is critical to accurately locating a GPS receiver on earth. The mechanism by which a GPS ground unit maintains accurate time is by basing its time off of an output from the GPS receiver. This output is called a pulse per second (PPS)

and is a pulse that occurs every second and is accurate to the UTC second within a certain error margin specified by the datasheet of every GPS receiver.

The GPSDO keeps accurate time by synchronizing to the PPS output by the onboard GPS receiver. The receiver acquires the PPS from a GPS satellite. When the GPS receiver outputs a PPS signal, the GPSDO synchronizes the local oscillator to this 1 Hz signal. The way the receiver performs this synchronization is through a servo loop. The type of servo loop most commonly used by a GPSDO is a type of PLL. Pictured in Figure 2 is the kind of loop a GPSDO uses. The microcontroller receives the output of the phase detector and then commands the voltage controlled oscillator (VCO) to either speed up or slow down to match the phase of the received PPS signal. The reason a microcontroller is used in a GPSDO, as opposed to a simple loop filter, is that the microcontroller can compensate for aging of the crystal and ambient temperature, both of which affect the accuracy. [Shera, 1998

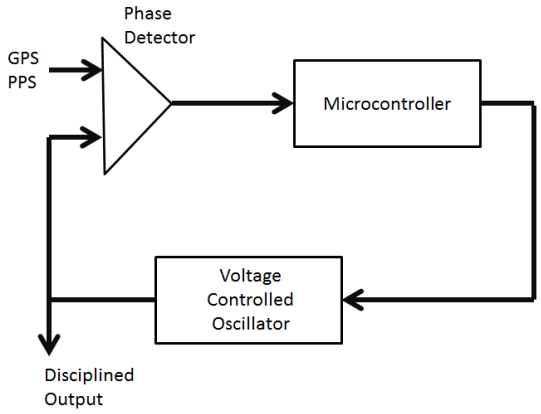

Figure 2: GPS disciplined oscillator block diagram. GPS pulse per second (PPS) reference signal is compared with the output of the voltage controlled oscillator in the phase detector. The microcontroller controls the voltage controlled oscillator, which outputs a disciplined output to be used by another system.

2.2 Geo-location Algorithm

A critical part to the geo-location system is what geo-location algorithm is used. The choice of algorithm determined what information from a signal was needed and the number of antennas at each receiver. In the case of this project, the two-receiver requirement is very influential to the performance of any algorithm.

2.2.1 Time Difference of Arrival

When passively locating a moving transmitter with fixed receivers, a relevant variable to use is the time it takes the signal to propagate from the transmitter to each receiver. Pictured in Figure 3, t_1 and t_2 represent the time it takes a signal to propagate to the corresponding receiver. If the time of transmit and the time of arrival of the signal at each receiver is known, then the distance between the transmitter and each receiver is directly related via the speed of light. Unfortunately, the time of transmission is unknown at the receivers. However, since there are two geographically separated receivers in the setup under consideration, the time difference can be used.

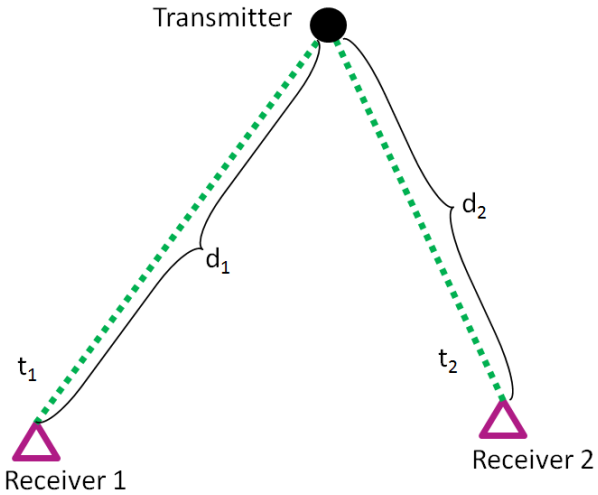

Figure 3: Geo-location with two receivers. The times t1 and t2 represent the time it takes a signal to propagate from the transmitter to receiver one and receiver two, respectively.

Time difference of arrival (TDOA) is the formal name of the aforementioned technique. TDOA is a passive technique that can be used to geo-locate an object in three-dimensional space utilizing the time variable. The remainder of this section will be dedicated to deriving the TDOA equation in a two dimensional plane. The plane under consideration can be rotated to account for any orientation of the three points: one transmitter and two receivers.

The distance difference $\Delta d = d_2 - d_1$, can be calculated from the time difference $\Delta t = t_1 - t_2$. Time is the initial variable that is available, but distance is much more relevant to locating a target. These differences are related as:

$$\Delta d = \Delta t \times c \tag{3}$$

where c is the speed of light.

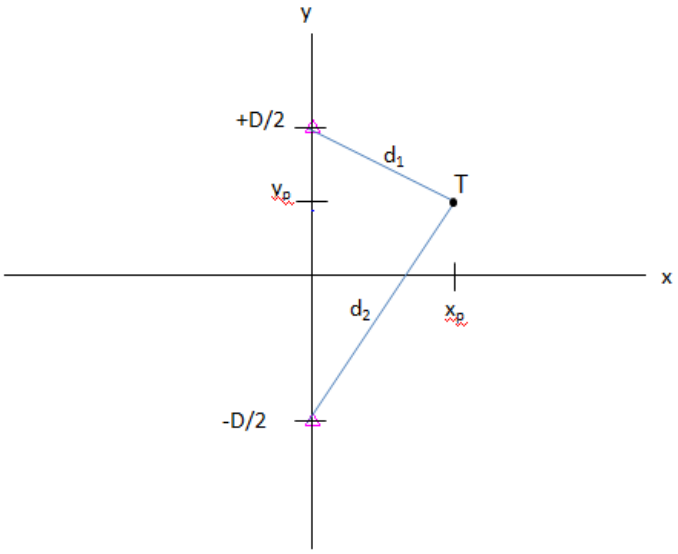

Figure 4: Two receivers D/2 away from the origin along the y-axis. Target point T, at (x_P, y_P).

Setting an arbitrary point (x_P, y_P) for the target allows computation of the distances between the target and the two receivers. In Figure 4, both receivers are located a distance D/2 along the y-axis from the origin and a target point is located at (x_P, y_P). Using Pythagoras's Theorem, the equation for d_1, corresponding to the distance between the transmitter and receiver 1, can be written as follows:

$$d_1 = \sqrt{x_p{}^2 + (D/2 - y_P)^2} \tag{4}$$

The equation for d_2 is derived in a similar way and takes the following form:

$$d_2 = \sqrt{x_p{}^2 + (D/2 + y_P)^2} \tag{5}$$

The derived results for both d_1 and d_2 assume the x coordinate of the transmitter is always greater than the x coordinate of either receiver. In the case under examination though, the time difference is known, not the individual times. The time difference only allows computation of the distance difference, which is expressed as:

$$\Delta d = d_2 - d_1 = \sqrt{x_p{}^2 + (D/2 + y_P)^2} - \sqrt{x_p{}^2 + (D/2 - y_P)^2} \tag{6}$$

Simplifying equation 6 results in:

$$\frac{{y_p}^2}{\Delta d^2/_4} - \frac{{x_p}^2}{D^2 - \Delta d^2/_4} = 1 \tag{7}$$

If the denominator in each term is defined as:

$$a^2 = \Delta d^2/_4 \tag{8}$$

$$b^2 = D^2 - a^2 \tag{9}$$

then equation 7 is simplified to the form of the general equation for a hyperbola opening around the y-axis, which is:

$$\frac{y^2}{a^2} - \frac{x^2}{b^2} = 1 \tag{10}$$

A hyperbola is a curve that consists of two halves, each focused around separate foci. A hyperbola opening around the y-axis with foci at D/2 and –D/2 is pictured in Figure 5. Note that the absolute value of the difference of the distances between each of the two foci of a hyperbola and any point on the hyperbola is always the same. This value is the distance between the vertices of the two halves of the curve. If d_1 is taken to be the distance between receiver one and the transmitter, d_2 the distance between receiver two and the transmitter, and $2a$ the distance between the vertex on both halves of the hyperbola, then the described relationship is written as:

$$|d_2 - d_1| = 2a \tag{11}$$

Rewriting equation 11 with the substitution of Δd for $d_1 - d_2$ results in:

$$|\Delta d| = 2a \tag{12}$$

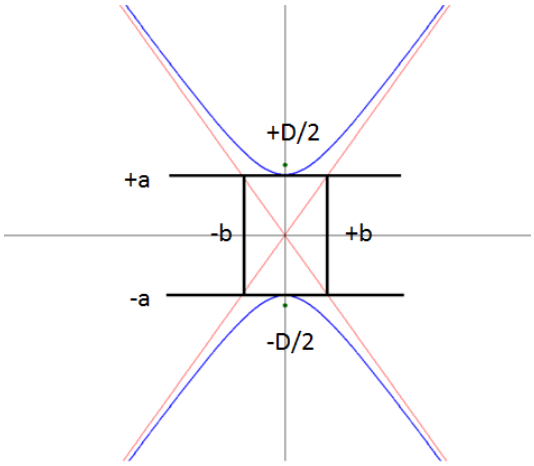

Figure 5: Basic hyperbola with defining variables. Parameter a is the distance to the vertex of each curve from the center of the hyperbola, b defines the slope of the asymptotes, and D is the distance between the foci of the curve. The foci are located at (0, ±D/2) and the vertices are located at (0, ±a).

The values of a and b define the shape of the hyperbola. Visually, the effects of a and b are shown in Figure 5. The vertex of either side of the curve is located a distance of a from the center of the hyperbola. If the origin is the center of the hyperbola opening around the y-axis, as is the case in Figure 5, the vertices are the y-intercepts, located at the points $(0, a)$ and $(0, -a)$. The slopes of the asymptotes are either positive or negative a/b. The slope of the asymptote is responsible for the characteristics of the hyperbola's opening. Returning to Figure 4, a hyperbola is calculated for the estimate as to where the target point is located, and Figure 6 is a representation of this hyperbola. The half of the hyperbola on which the target is located can be determined based on the obtained information. Since Δt was defined as = $t_1 - t_2$, the sign of Δt will indicate which time is lesser, t_1 or t_2. If Δt is positive, then t_2 is smaller than t_1 so the transmitter must be closer to receiver 2, and vice versa.

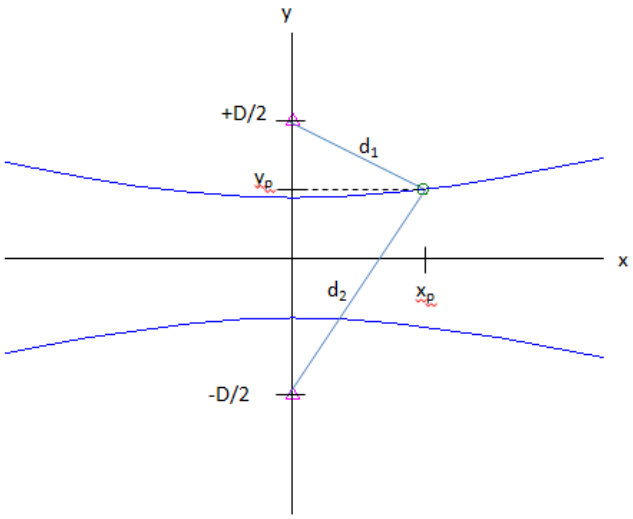

Figure 6: Hyperbola with a target point (xp, yp). The difference of the distance between any point on the curve and the two foci, which are the distances d1 and d2, is always equal to the distance between the vertices of the curve.

This section has shown how relating the TDOA, Δt, to the distance difference, Δd, results in an equation for the TDOA hyperbola. Also the distance between the receivers, D, and the speed of light, c, are needed to find the solution. Substituting Equation 3 into Equation 7 results in an equation for the TDOA hyperbola, which is no longer dependent on distance, rather it is dependent on Δt, a measure obtainable in the field. The result of the substitution is below:

$$\frac{y^2}{\frac{1}{2}(\Delta t \times c)^2} - \frac{x^2}{D^2 - \frac{1}{2}(\Delta t \times c)^2} = 1 \qquad (13)$$

2.2.2 Angle of Arrival

While TDOA outputs location information in the form of a curve, there are other techniques that give more information about the received signal. Some systems provide information about the angle of arrival (AOA) of the signal. With enough receivers spread out over an area, the AOAs will all converge to an estimated target location.

The subsequent subsections describe two techniques that can be used at individual receivers. Once two separate receivers are in the field, a line can be drawn out from each

receiver based on their respective AOA, and the intersection of these lines is the location estimate of the target.

2.2.2.1 Phase-based Angle of Arrival

Phase comparison, a common technique to find an AOA measurement, requires multiple antennas at each receiver. The number of antennas in each array affects the accuracy of the estimated angle. The spacing of the antennas in each array also affects the performance.

The setup of a single receiver with two antennas in the array, R1 and R2, is displayed in Figure 7. If $d_0 << d_1, d_2$, meaning that the antenna spacing is much less than the distance to target T, then the assumption can be made that $\overline{TR1} \parallel \overline{TR2}$, as displayed in Figure 8. Once this assumption is made then angle α is said to be the AOA.

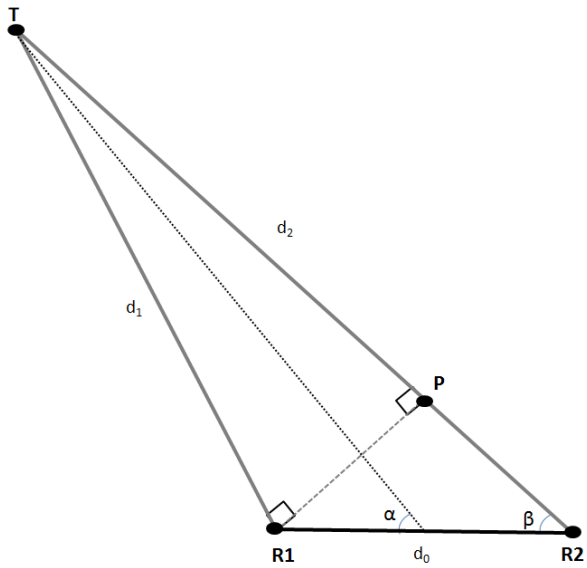

Figure 7: A phase comparison system, where R1 and R2 are the two receivers and T is the target. P is a point chosen along the line $\overline{TR2}$ such that the distance along $\overline{TP}$ is equivalent to d1. Angle α is the angle of arrival and if it is assumed that d1, d2>>d0 then d1 is parallel to d2 intersecting line $\overline{R1P}$. Hence angle β is equivalent to angle α.

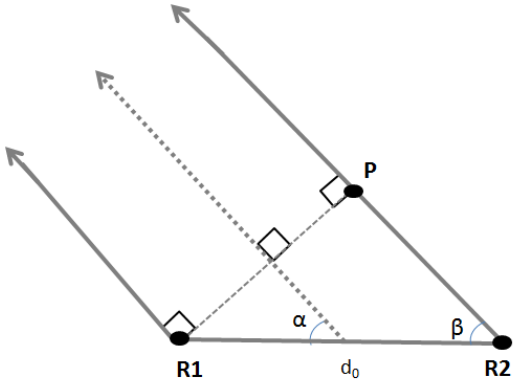

Figure 8: Close up of Figure 7, where $\overline{TR1}$ || $\overline{TR2}$. This figure better shows why angles β and α are equivalent if $\overline{TR1}$ || $\overline{TR2}$.

To calculate angle β, a point P is chosen along the line $\overline{TR2}$, such that the length of $\overline{TP}$ is equivalent to the distance d_1. The purpose of the selection of P is to find a point where the phase of the signal along the path from T to R2 is the same as the phase at R1. The phase will be the same at P and R1 since the signal has travelled the same distance to reach each of these points. Therefore, any difference in phase at the receivers will be due to the extra distance travelled along $\overline{PR2}$. The length of $\overline{PR2}$ is:

$$|\overline{PR2}| = \lambda\left(\frac{\Delta\varphi}{2\pi} + C\right) \tag{14}$$

where λ is the wavelength of the signal; $\Delta\varphi$ is the phase difference, in radians, between the two antennas, which is restricted from 0 to 2π; and C is an integer value. Since $\Delta\varphi$ is restricted from 0 to 2π, C accounts for antenna separation greater than λ.

As observed in Figure 8, a right triangle is formed by $\overline{PR2}$, $\overline{R2R1}$, and $\overline{R1P}$. Since $\overline{TR1}$ || $\overline{TR2}$, and the line formed by angle α is parallel to both of these lines, angle α is equivalent to angle β. Using the right triangle and the length of $\overline{PR2}$ defined in Equation 14, the value of angle β can be obtained with simple trigonometry:

$$\beta = \cos^{-1}\left(\frac{\lambda\left(\frac{\Delta\varphi}{2\pi}+C\right)}{d_0}\right) \tag{15}$$

Since angle β is equivalent to angle α, and angle α is the AOA, Equation 15 can be used to compute the AOA, as long as all of the initial assumptions are met. [Lipsky, 2004]

A limitation of this technique is phase ambiguities, as the value of C is unknown. These ambiguities make this technique less effective if an array of only two antennas is used. To fix this problem, more antennas can be added to the array, or multiple arrays, directed in different directions, can be set into one receiver.

2.2.2.2 Power-based Angle of Arrival

Another common technique to find the AOA of a signal at a receiver is to compare the amplitude of the received signal at multiple antennas in an array. The overall setup is similar to before; however, the array setup is slightly different from a phase-based system's array. When using phase, all antennas in each array are directed in parallel. But, when using the amplitude technique, the antennas in each array must be directional antennas, and are pointed in different directions. Figure 9 demonstrates one option for the setup of two antennas; that is, the two antennas directed 90 degrees away from each other.

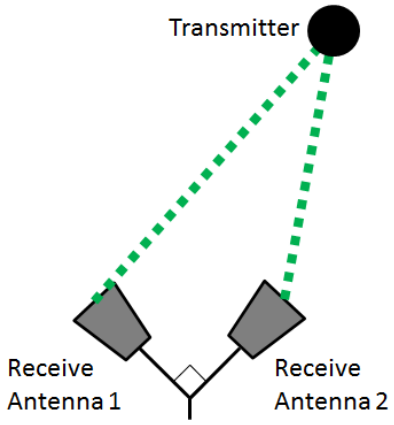

Figure 9: Amplitude comparison antenna configuration. The dashed line represents the direct path a signal would take from the transmitter to each horn antenna. The horn antennas are directed 90 degrees away from one another.

Once the signal is received at both antennas, a power ratio is formed. The ratio is the amplitude received by antenna 1 divided by the amplitude received by antenna 2. This ratio is then compared with values in a predetermined look-up table to find what AOA corresponds to the power ratio. Testing the system with the receiver placed at known locations forms a look-up table, or it is derived from known antenna gain patterns. The accuracy of this look-up table depends on the fact that the antenna pattern must be known and stable. The results of these tests can be compared with the ratio that will occur at each

tested point. Further, more points can be interpolated from these tests to compile a full look-up table. The requirement to implement a look-up table is a limitation of this technique, because the amount of memory in the system determines how large the look-up table can be, hence, how much resolution can be achieved for the AOA.

3. Full Scale Design

Group 105's eventual goal is to build a full scale system that operates a kilometer distances and tracks a target in three-dimensional space. This section will discuss the details of that full scale system. These details are important to understand why the GPSDOs were used as well as to understand the small-scale tests conducted of this system.

First, the geo-location technique will be discussed, explaining how the 1.5° requirement was converted into a distance and then time requirement. The choice of coordinate system will also be discussed as it is important to understand how a three dimensional problem can be solved by a TDOA hyperbola in a two dimensional plane. Second, the specifics of the receiver hardware will be discussed. This section is important because the hardware discussed here was used in the system testing.

3.1 Geo-Location Technique

3.1.1 Converting Angle Requirement to Distance

A requirement for this system was that the system needed to provide the location of the target to within 1.5° in azimuth and elevation, as seen from receiver one, 70% of the time. The angle requirement can be translated into a distance requirement at various distances from the receivers. The distance errors will then determine how much timing error from the GPSDOs can be tolerated by the system in order to operate within acceptable means.

In order to determine what scale of error is acceptable, the requirement introduced as an angle needed to be translated into a distance. Since the output of the system is a location, an error in distance will be easier to understand. Using the calculated location and the actual location of the target will allow a distance error to be determined, which can then be compared to the allowable distance error. The distance error calculated will be referred to as the cross-range in this section. The cross-range is not the distance between the receiver and the transmitter, it is the lateral distance along the flight path from the transmitter's actual location.

Translating the angle requirement into an allowable distance requirement can be done with trigonometry. A representation for two scenarios of the 1.5° angle requirement can be seen in Figure 10 (a) and (b). Angle θ is 0.75°, which is one half of the angle requirement; angle ϕ is utilized to calculate the cross-range, e, which is the acceptable distance error; r is the range to the flight path from the receiver; and w is the distance along the flight path the target has travelled.

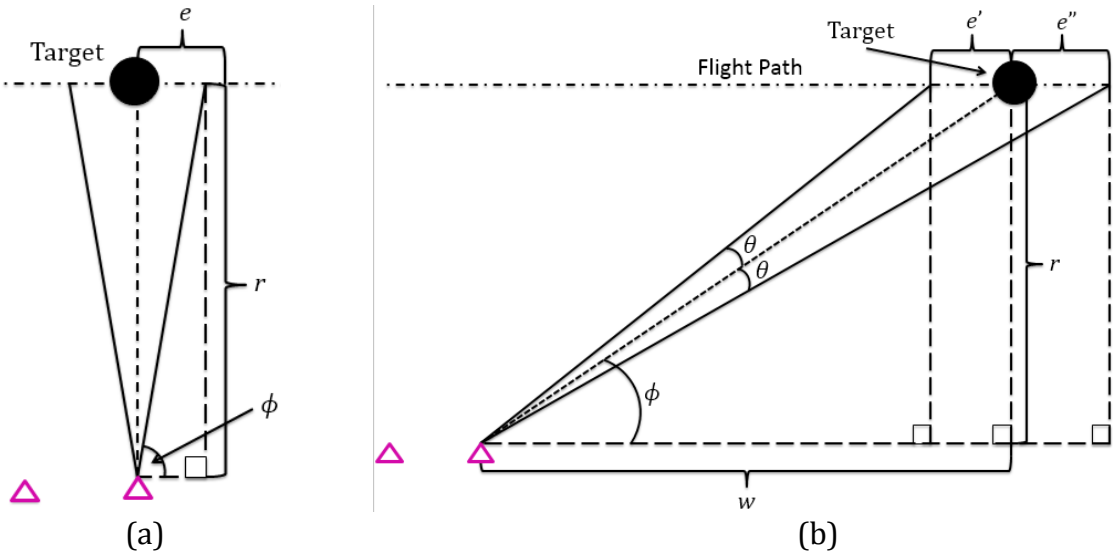

Figure 10: Representations of 1.5° error at different points along flight path. (a) Representation of target that is in-line with receiver. Angle ϕ is 89.25°; r is the distance to the target from the receiver; and e is the cross-range, which is the allowable error. (b) Representation of target at any point not in-line with receiver. Angle ϕ is used to solve the cross-range; angle θ is 0.75°, which is half of the acceptable error; r is the distance from the receiver to the flight path; w is the distance along the flight path from the receiver; and e' and e" are the cross-ranges, or acceptable errors.

The technique used to solve for the cross-range is determined by where along the flight path the target is located. There are two scenarios: when the target is above the receiver, as seen in Figure 10 (a), and when the target is not above the receiver. In the first scenario, the target is in-line with the receiver, seen in Figure 10 (a), and the calculation for the cross-range is simple. Using the following equation, where r is either 75 km or 100 km, and angle ϕ is 89.25° or 90° - θ, the cross-range can be solved.

$$e = \frac{r}{\tan(\phi)} \tag{16}$$

Equation 16 comes from rearranging the tangent equation. Equation 16 is used when either an angle of a triangle or one of the corresponding adjacent or opposite sides is desired and the other two are known. When solving for cross-range, the majority of the time the target is not in-line with the receiver, as seen in Figure 10 (b). This scenario involves more computation, as more information is required to determine the cross-range. The first piece of information required is angle ϕ, which is solved using the following equation.

$$\phi = \tan^{-1}\frac{r}{w} \tag{17}$$

In Equation 17, r is the range between the receiver and the flight path, and w is the distance the target has travelled along the flight path. To determine e', angle θ is added to angle ϕ, and to determine e'', angle θ is subtracted from angle ϕ. The newly determined angles, $\phi + \theta$ and $\phi - \theta$ are used in Equation 16 along with r from Equation 17. The result of Equation 16 is either subtracted from w which solves e', or w is subtracted from the result which solves e''. Equations 18 and 19 below are the solutions for e' and e''.

$$e' = w - \frac{r}{\tan\phi + \theta} \tag{18}$$

$$e'' = \frac{r}{\tan\phi - \theta} - w \tag{19}$$

3.1.1.1 Converting Time Error into Distance Error

There are four extreme points along the flight path as a result of the two ends of the flight path being equidistant from the center of the receiver pair. These extreme points are labeled and shown in Figure 11. All calculations for the cross-range were made from receiver one. The first point, point A, is the closest the target will be to receiver one on the flight path 75 km away. Point B is the furthest point along the 75 km away flight path that the target will be from receiver one. Point C is the closest the target will be to receiver one along the 100 km away flight path, and point D is the furthest point along the 100 km away flight path. Since receiver one is one km off-center, it is closer to one end of the flight path than the other receiver. This dissymmetry is resolved by calculating the cross-range for the end of the flight path furthest from receiver one. This calculation provides a cross-range

that is larger than the cross-range of the other end of the flight path. Therefore, all cross-range values, for the entire flight path, are between the cross-range of the closest point and the furthest point from receiver one. These points have been labeled on top of Figure 12, and can be seen in Figure 11.

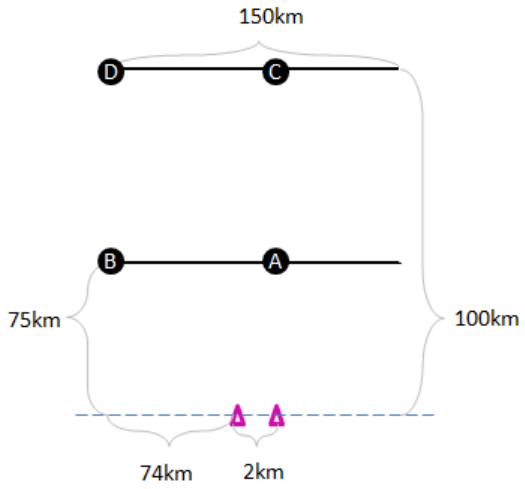

Figure 11: Flight path with extreme points marked as A, B, C, & D

The receivers are setup 2 km apart, as seen in Figure 11. Receiver two is placed 74 km from point B in the x-direction and receiver one is placed 76 km from point B. The receiver placed at 76 km from point B is used as the reference point for calculating the distance between the target and the receivers. This setup puts A a distance of 75 km, B a distance of 106.8 km, C a distances of 100 km, and D a distance of 125.6 km. These distances will be used for calculating the distance error allowance. The distance errors at 75 km and 100 km will be determined using Equation 16 and the other two distance errors will be determined with Equations 17, 18, & 19.

To determine if the system is producing accurate location outputs, different timing errors associated with the GPSDOs need to be considered in the TDOA calculation. The characteristics of the hyperbola's opening determine how much distance error is introduced, and the opening is determined by the TDOA. When the target forms an approximate isosceles triangle with the receivers, as is the case with points A and C from Figure 11, the hyperbola opening is very wide and the TDOA is relatively small. The other case is when the target does not form an approximate isosceles triangle; rather a triangle

with an obtuse angle is formed. In this scenario the opening of the hyperbola is narrower than the previous case and the TDOA is larger.

The value of the TDOA determines how much a small change in the TDOA will affect the hyperbola. When the TDOA is small, slight time variations do not have a large effect on the opening. However, when the TDOA is large, the slight time variations have a more significant effect.

The reason that the effect of small time variations depends on the size of the TDOA relates to how the hyperbola is described. In the equation for a hyperbola, the variable a is equated as the TDOA multiplied by half the speed of light. This constant multiplication would lead to a linear relationship, however, a is then used to find b in the following equation:

$$b = \sqrt{D^2 - a^2} \tag{20}$$

This equation is restated from a previous section, where D is the distance between the two receivers. This equation also shows that there is a nonlinear relationship between a and b. In the case where D is 1, plotting b as a function of a from 0 to 1 results in a quarter of the unit circle. When a is close to zero, b has a small rate of change as it is on the top of the circle. But as a increases, so does the rate of change of b. Since a is directly related to the TDOA through a constant multiplier, b is proportional to the TDOA multiplied by a constant. So when the TDOA is large, small variations change b more than a smaller TDOA because the rate of change of b is greater at larger TDOAs. Therefore, larger TDOAs, resulting from the target on points such as B and D, result in a greater distance error that may be outside of the 1.5° limit. Utilizing the equation for a hyperbola with different TDOAs and different errors introduced by the GPSDOs, the resulting distance errors can be calculated.

$$\frac{{y_p}^2}{\Delta d^2/_4} - \frac{{x_p}^2}{D^2 - \Delta d^2/_4} = 1 \tag{21}$$

where the value for y_p is a constant, either 75 km or 100 km depending on which side of the flight path the target is on; Δd is determined from the TDOA; and D is the distance between

the receivers. The time error introduced from the GPSDOs can be added to the Δd calculation, Equation 3, and then x_p can be evaluated through Equation 21. The resulting value for x_p will not be the actual location of the flight path if a timing error was introduced by the GPSDOs. This amount of acceptable error in x_p will be determined through the use of the cross-range errors.

3.1.1.2 Allowable Distance Error along Flight Path

Using the values calculated for cross-range, calculation described in section 3.1.1.1, as the maximum allowable distance errors, a table of different distance errors associated with timing errors from the GPSDOs was created. The maximum distance errors were calculated for the extreme points along the flight path, and then timing errors between the GPSDOs were introduced into the TDOA calculation in steps of 15ns. The results of these calculations can be seen in Table 1 below. Results that exceed the maximum allowable distance error are shaded.

Table 1: Table of allowable error at different extreme points along the flight path, as well as distance error associated with different timing errors from GPSDOs. Results that exceed the maximum allowable distance error are shaded.

Extreme points along flight path	Maximum allowable distance error (km)	Total distance error (km) with corresponding timing error between GPSDOs						
		15 ns	30 ns	45 ns	60 ns	75 ns	90 ns	105 ns
A	.98	.17	.34	.50	.67	.84	1.01	1.18
B	1.96	.48	.95	1.43	1.90	2.38	2.86	3.33
C	1.31	.22	.45	.67	.90	1.12	1.35	1.57
D	2.04	.44	.88	1.31	1.75	2.19	2.63	3.07

As noted in Table 1, when the time error is 90 ns and the target is at any position along the flight path, then the associated error is greater than the allowed distance error. Clear from Table 1 is that the distance errors associated with a 60 ns timing error are all within the limits of acceptable error. Since the selected data points for allowable error are the maximum and minimum points on the flight path, it can be interpolated that all points

on the flight path have an acceptable error at a time error of ≤ 60 ns. The actual timing error at which all points on the flight path do not fall within the allowable distance error is somewhere between 60 and 75 ns. As long as the GPSDOs can provide a timing difference between the two units to within 60 ns, the system will be able to locate the target to within Group 105's requirements.

3.1.2 Problem Requirements: Coordinate System Choice

The geo-location problem presented is a three-dimensional problem because the x, y, and z coordinates of the target are desired. However, the analytical approach discussed in the background only finds a solution in a two dimensional plane. So, incorporating the time of arrival of the signal at the two receivers that this system uses will only give a location in two dimensions. That is, TDOA at two receivers produces a single equation of a curve in a two dimensional space. If there were three receivers available, then the three TDOA measurements lead to three equations which, by adding the variable into the TDOA equations, can be solved for three variables, x, y, and z, hence three dimensions. When one more receiver is added, to make a total of four, then there will be six TDOA measurements available to make six equations, which creates an over determined system which can be estimated. More receivers allow more hyperbolas to be computed; therefore, a four-receiver system can solve for three dimensions with less computational intensity than a system of three receivers. More information than receiver location and time of arrival is required when solving for three dimensions in a two-receiver system.

A known piece of information in this system is the flight path of the target. A top view of the flight path in relation to the receiver setup is shown in Figure 12. The flight path can be modeled as a straight line segment that is parallel to the line formed through the receivers. The flight path line segment is either 75 km or 100 km away from the receiver line, where the receiver line is the line that contains both of the receivers. Using the hyperbola solution that results from the two-receiver system, the location of the target is obtained by finding the intersection of the curve with the flight path, either on the near line or the far line.

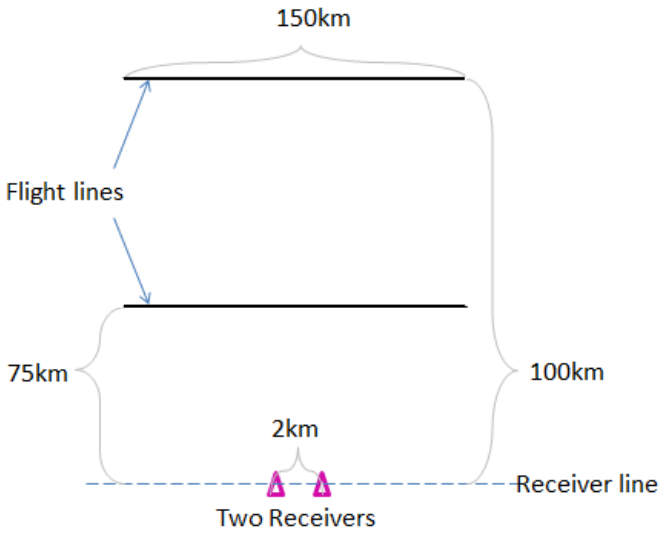

Figure 12: Top view of flight path and receivers. Each side of the flight path is a straight line segment of 150 km, either 75 km or 100 km away from line on which the receivers fall.

The intersection of the flight path line segment and the two receiver TDOA curve still only locates the receiver in a two dimensional plane along the ground. To extrapolate to the third dimension, it may be possible to incline the two-dimensional plane so that it contains the line going through the receivers, as well as a single line of the flight path. A view from the side of this setup is shown in Figure 13. If the two dimensional plane encompassing the TDOA hyperbola was inclined from the ground to be along the D_N line and perpendicular to the plane of the paper, then the distance between the flight path line at 75 km and the receiver line is D_N. If the altitude of the target is 9 km then D_N is equal to 75.54 km, which is obtained using basic trigonometry. The reason for rotating the plane of the TDOA hyperbola is to find the intersection between the hyperbola and the flight path line segment in the new plane. If this location is found, then the location coordinates can be transformed back into the original reference coordinate system based on the 75 km distance along one axis and 9 km distance along another.

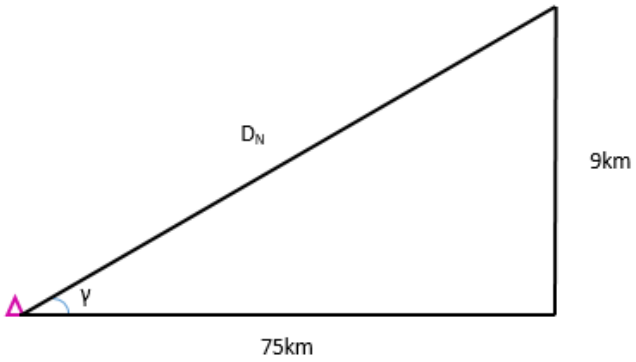

Figure 13: Side view of the flight path and receiver setup, where the hypotenuse of the triangle is a line that is formed that is perpendicular to the receiver line and the flight path line, which is 75 km away, as is displayed in Figure 12.

Inclining the plane to be along the line D_N, hence intersecting with the receiver line and the closer flight line, will allow for accurate geo-location along the near side of the flight path but not the far side. By rotating the plane to be along D_N, the need to consider the z-axis is eliminated for the near flight line. However, if the plane is rotated to be along D_N, then the far side of the flight path, at 100 km away, now has a large offset in the z direction. This offset is shown as Δz in Figure 14. Using the angle γ, originally pictured in Figure 13, the value of Δz can be calculated as approximately 3 km. At this range, the maximum allowable error is 1.3091 km, so an estimate for the far side of the flight path will be inaccurate using a plane rotated onto the line D_N.

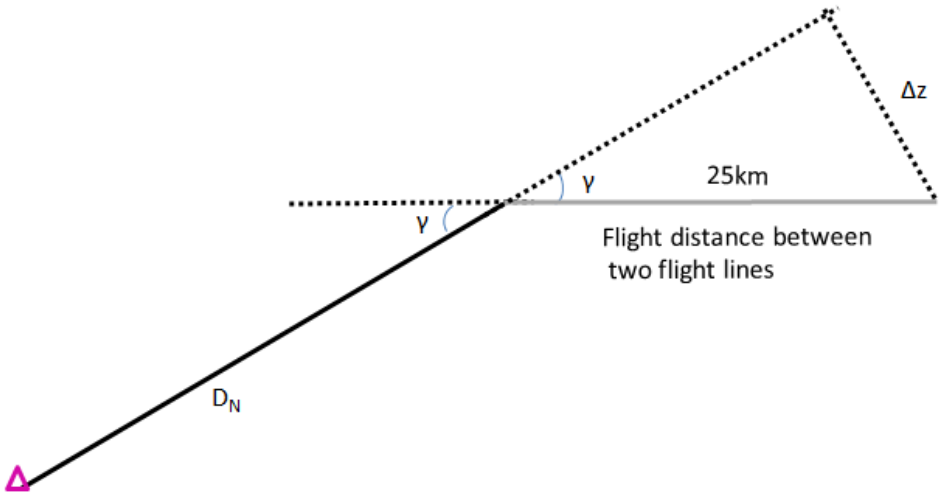

Figure 14: Far side of flight path considered in the rotated plane.

Another option to bypass this unacceptable error is to rotate the plane to the middle of the flight path. Rotating the plane of the hyperbola to the line D_M, as pictured in Figure 15, averages the error measured on each side. Instead of no error on the 75 km flight line and full error on the 100 km flight line, this approach splits the error. Through trigonometry, it can be found that the error, Δz, for both sides of the flight path would be about 1.5 km. An error of 1.5 km is unacceptable at both flight lines; therefore, this approach is also ineffective.

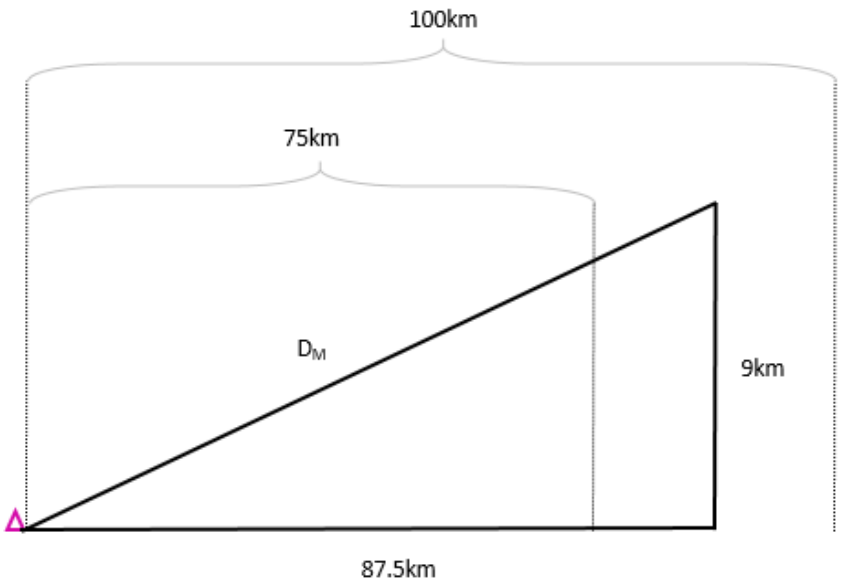

Figure 15: Side view of the flight path. Where the edges are at 75km and 100km, and the shown triangle's hypotenuse terminates in the middle of the flight path, at 87.5km away from the receiver line.

All previous approaches have had errors outside of the acceptable margin for at least one of the flight lines. The solution is to use an adaptive approach that utilizes a different plane for each flight line. That is, a plane that goes through the receiver line and the flight line 75 km away, and a plane that goes through the receiver line and the flight line 100 km away. The challenge of this technique is to know when to switch the plane used for calculation.

By shifting which plane is used, all calculations of the hyperbola can be performed in two dimensions. This simplification makes computation much easier and hence more efficient. Once the calculation to find the intersection of the flight path and hyperbola has

been completed, the results are transformed into the global coordinate plane. This transformation was not computationally intensive and hence it is worth calculating the location by shifting the plane of the two dimensional hyperbola and then transforming the results. Attempting to solve for the location with the equation for a hyperbola in three dimensions was more difficult.

3.1.3 Time Difference of Arrival with Knowledge of the Flight Path

As discussed in the background, TDOA with two receivers allows the possible locations of the transmitter to be narrowed down to one half of the hyperbola. With no further information the space covered by half the hyperbola is the only estimate of the location of the target. However, since our system assumes knowledge of the flight path the intersection of this half hyperbola and the flight path provide a location estimate of the transmitter.

For a simple case let the flight path be modeled as a line that is parallel to the line that the receivers lie on, all in the x-y plane. An example is shown in Figure 16, where it is clear that the flight path intersects the hyperbola at point T. In the case pictured in Figure 16, taking Equation 13, repeated here:

$$\frac{y^2}{\frac{1}{2}(\Delta t \times c)^2} - \frac{x^2}{D^2 - \frac{1}{2}(\Delta t \times c)^2} = 1$$

and substituting x_p into the equation produces a point of intersection when solving for y. The point of intersection, T, is the estimated location of the transmitter.

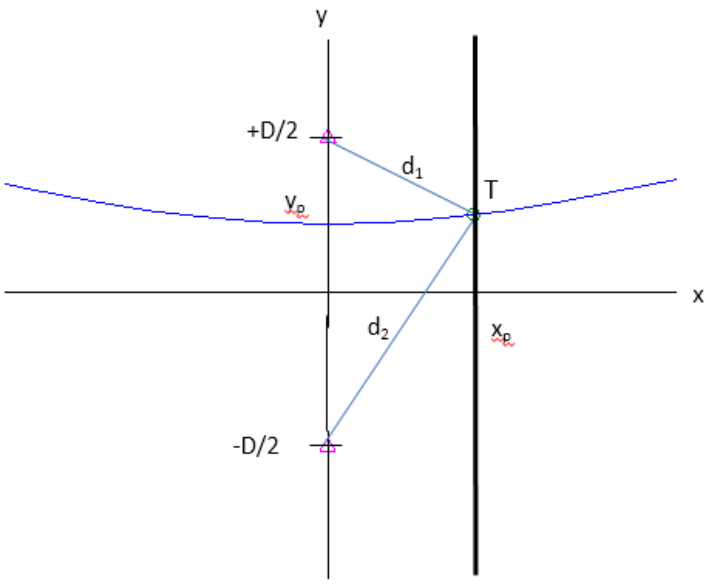

Figure 16: Target point T, at (x_P, y_P). Point T is at the intersection of half the hyperbola and the flight line, represented by the thickest line.

3.2 Receiver Hardware

Group 105 owned some hardware that they wished to utilize for the implementation of this project. This hardware consisted of a front end, which included an antenna and a down-converter; a field-programmable gate array (FPGA) card; and a control center. All of these components were integrated together, along with the geo-location system that was developed, in order to locate and track an RF transmitter in real-time. A block diagram of the full receiver setup is shown in Figure 17.

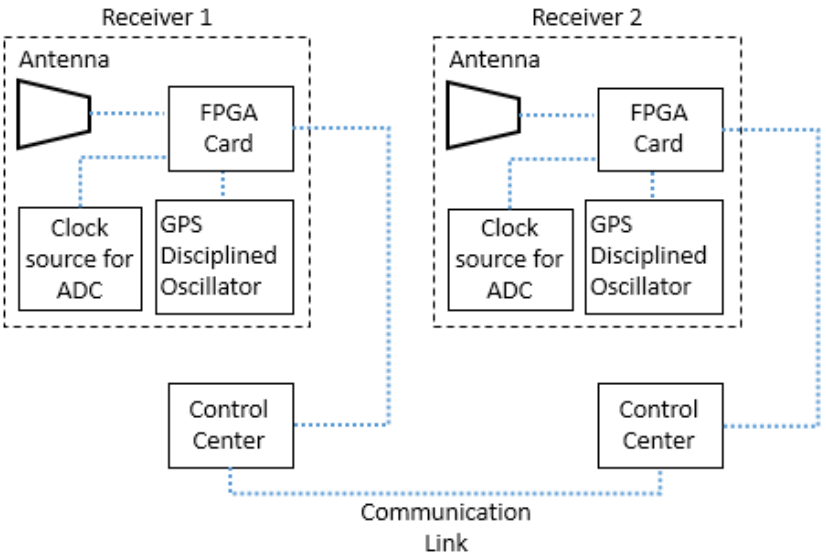

Figure 17: Block diagram of receiver configuration.

3.2.1 Front End

The function of the RF front end is to process a received signal at the initial RF and then convert the signal to an intermediate frequency (IF) where it is easier to process and perform computations on the signal.

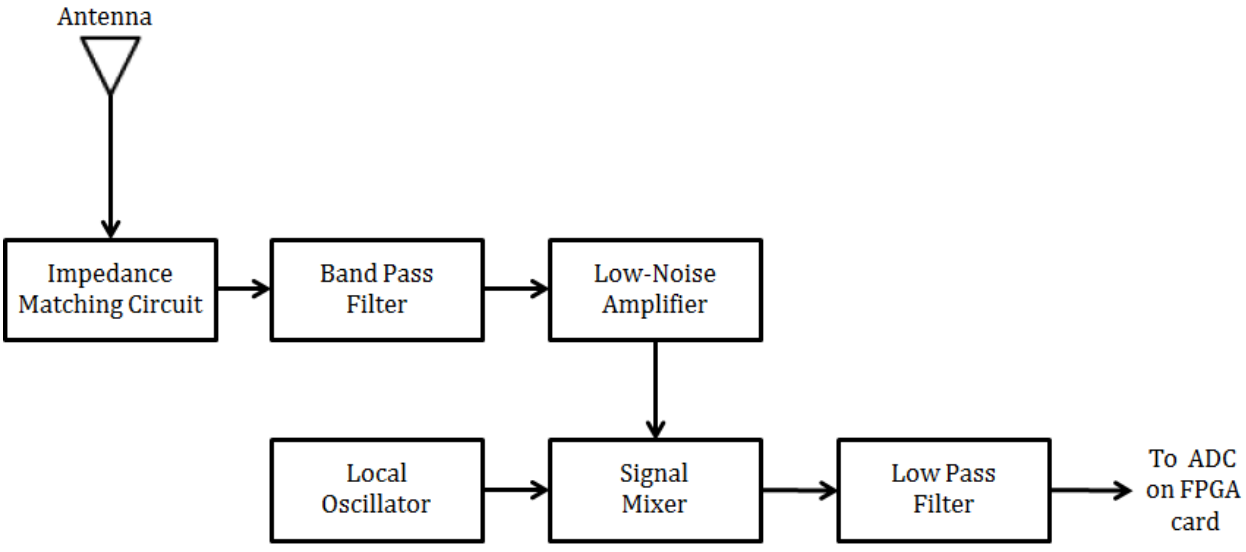

Figure 18: Radio frequency front end block diagram. The antenna is connected to the band pass filter through an impedance matching circuit, and then the output of the filter is passed through a low-noise amplifier. A local oscillator generates a signal at an intermediate frequency to mix with the output of the amplifier, before it passes through a low pass filter, in order to down-convert the received signal.

The first component of the front end is the antenna, which is used to receive a transmitted signal. The purpose of the impedance matching circuit is to transfer the maximum amount of power from the antenna to the rest of the system. The bandpass filter (BPF) rejects all signals outside of the signal frequency band. The low-noise amplifier (LNA) amplifies the power of weak signals while minimizing noise contamination in order improve the signal-to-noise ratio (SNR). The local oscillator generates an offset RF signal from the incoming signal. The signal from the local oscillator is mixed with the received signal in the mixer in order to down-convert the signal from RF to the IF. Finally, a lowpass filter (LPF) reduces any high frequency noise.

3.2.2 GPS Disciplined Oscillator

One of the key components of the system was the GPSDO, which was the means of synchronizing the clocks of the receivers and thus facilitating the ability to acquire an accurate TOA of the signal. The specific GPSDO used for the project was a Microsemi (previously Symmetricom) GPSDO 2650, which can be seen in Figure 19. The GPSDOs do not have internal antennas, so an external antenna was purchased. Each GPSDO had a MMCX connector to receive a 5V GPS antenna. For these GPSDOs, a Parallax Inc. 5V amplified GPS antenna was used. This antenna, pictured in Figure 20, has a 10ft cable, as specified by the manufacturer, and verified in the lab.

Before the GPSDO will output PPS signals it must be locked to GPS satellites. Knowing when the GPSDO is locked and to how many satellites it is locked to is very important. There is an LED on the board that blinks red once satellites are in view and then alternates green and red once the GPSDO is locked to satellites. This feedback is easy to see and understand, but it is binary. However, the GPSDO is capable of reporting the number of satellites that are being tracked as well as their signal strength to a user through the use of a serial connection to a computer. This useful feedback allows the user to determine if the location is sufficient for the GPSDOs to operate at their maximum performance.

The PPS output from the GPSDOs were used to synchronize the clocks at the individual receivers. The PPS signal is output from the GPSDO through a cable harness. There are three output choices for the PPS: A 5V CMOS, LVDS differential pair, and an RS-

232 level output. The specific PPS output used was a RS-232 level signal. This output provided a -6 V to +6 V signal with a pulse width of about 800 ms. The PPS was input into the back plane of the FPGA card through a six-foot, 18 gauge, six-wire cable with a nine-pin RS-232 connection. The rising edge of the PPS output was used to reset a counter in the processing block. The counter was used to determine the relative TOA of the received transmission at each receiver.

Figure 19: Microsemi GPSDO 2650 used for clock synchronization.

Figure 20: Parallax Inc 5V amplified GPS antenna with a 10ft cable that is partially cropped out of the photo at the right edge, and a MMCX male adapter on the end. Photo Courtesy of Digi-Key.

Mounting the GPSDOs inside of an enclosure protected them from being damaged in the field. The enclosure also provided a convenient means of storing and transporting the GPSDOs without risk of physical damage. Each of the GPSDOs was secured in their own

enclosure to be used at each receiver. One enclosure was completely built for the purpose of the GPSDO, while the other enclosure was retrofitted to incorporate the GPSDO.

3.2.2.1 Standalone Box

The first enclosure shown in Figure 21 is a custom 10" x 6" x 3.5" aluminum box obtained from the supply shop at MIT LL. It is a two-piece box, where the two halves slip together in order to form the enclosure. On the outside of the box was an AC power receptacle with fuses and a switch, a female 9-pin RS-232 connector, a power switch on the front of the box, and a small hole for the antenna. The AC receptacle, seen in Figure 22 (a), utilizes fuses to protect the connected components in case of a short circuit, and the fuses used are rated for 250 VAC and 1 A. The female RS-232 connector, seen in Figure 22 (b), had solder leads on the opposite end, which were used for the PPS output from the GPSDO and ground. A male RS-232 cable was attached to the female connector in order to supply the PPS signal to the digital input on the back plane of the FPGA card.

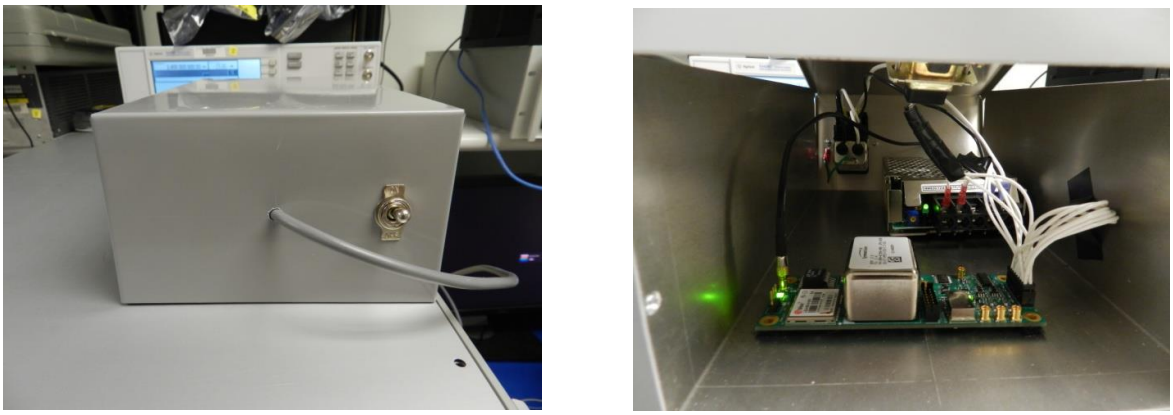

(a) (b)

Figure 21: Enclosure for the GPS disciplined oscillator (GPSDO). (a) The outside of the enclosure. (b) The inside of the enclosure.

(a)

(b)

Figure 22: (a) An AC power receptacle with fuses and switch. (b) RS-232 female connector with solder leads for wiring.

Inside of the box were the GPSDO and a 12 V, 2.5 A, DC power supply, along with all of the necessary wiring. The AC receptacle connected the box to an AC source in order to power the DC power supply in the box. The AC receptacle was wired to the DC power supply through the power switch on the front of the box, and both components can be seen in Figure 23. The DC supply was then wired to the GPSDO, providing +12 V_{DC} to pins 15 and 16 of the power connector, and ground to pins 3, 12, and 14. The PPS output from the GPSDO was provided by pin 10 on the GPSDO's power connector. Pin 10 of the GPSDO was wired to pin 3 of the female RS-232 connector and ground was provided to pin 5 of the connector. Finally, the antenna used by the GPSDO was fed through the extra hole and was utilized outside of the box.

(a)

(b)

Figure 23: (a) A DC power supply rated at 12 V and 2.5 A. (b) A power switch used on the outside of the enclosure.

3.2.2.2 Second enclosure

The second GPSDO was enclosed in an available box that was built for an intern over the summer. This box was built for a similar project that Group 105 is working on; therefore, the box was also used to house the components needed for the TDOA system. The box was custom built to fit inside and attach to a component rack that is owned by the group. Inside of the box is a 12 V, 2.5 A, DC power supply that is connected to an AC source and powers the GPSDO. The DC power supply was already in place; therefore, the GPSDO only needed to be secured inside of the box. The PPS output was similarly wired to a female RS-232 connector, and the power connecter of the GPSDO was wired to the DC power supply. The second enclosure is shown in Figure 24.

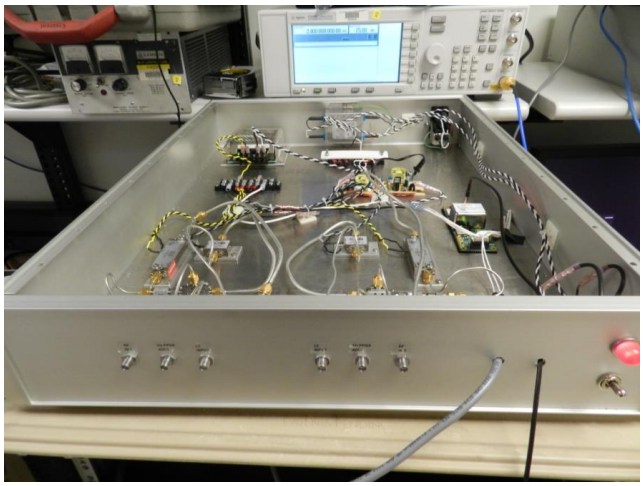

Figure 24: Enclosure used to house the GPS disciplined oscillator (GPSDO).

3.2.3 Field Programmable Gate Array Card

A FPGA is a digital logic integrated circuit that is designed to be configured in the field in custom ways that meet the user's needs. A user utilizes a hardware description language (HDL) to configure the FPGA to re-map the many different connections between programmable logic components, or logic blocks. These logic blocks, usually comprised of a look-up table and a flip-flop, can be configured to perform complex logical operations. The logic blocks can even be configured to act as simple logic gates, such as an AND or XOR. FPGAs typically include memory elements such as flip-flops, or actual blocks of memory, such as RAM. [Trimberger, 1994]

The purpose of the FPGA card in the integrated system is to compute the TOA, based on inputs from the GPSDO and the front end, and send that information to the control center. Group 105 has multiple Tekmicro Gemini-V6 FPGA cards that have three Virtex-6 FPGAs and a 12-bit ADC that samples at 1.8 GSa/s, which is displayed in Figure 25. The Gemini FPGA card also has a 225 MHz clock onboard. Since the ADC samples at 1.8 GSa/s; therefore, signals ≤ 900 MHz can be unambiguously sampled without aliasing occurring. This restriction is why the front end is implemented before the FPGA. The FPGA samples the down-converted IF signal and then sends the requested information about the signal to the command center.

Figure 25: Gemini V6 field-programmable gate array (FPGA) card with 12-bit analog to digital converter (ADC), and three Virtex-6 FPGAs.

Though the role of the PPS was discussed in the previous section, the whole process of acquiring a TOA will be discussed here, where relevant signals are pictured in Figure *26*. . The PPS output from the GPSDO is used to start a counter, which is incremented by the 225 MHz clock on board the FPGA. The counter increments every 4.44 ns on the rising edge of the 225 MHz clock. The received signal, after being digitized by the ADC, acts as a trigger to stop a counter on the FPGA. This count represents the TOA of the received signal relative to the time the PPS was received. The value of the count stored in memory and the associated time of day, accurate to one second, were sent to the control center where it was used to determine the TDOA. The control centers at each receiver were synchronized to the second by placing the laptops next to one another, and manually resetting the clock on one of them to match the other.

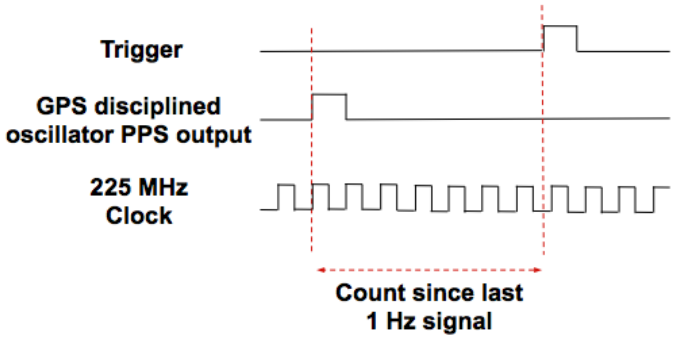

Figure 26: Diagram of how the pulse per second (PPS) signal is used in conjunction with the 225 MHz clock on the FPGA to generate a count once the trigger is received. Count represents the time of arrival (TOA) of the received signal.

3.2.4 Control Center

The control center is software on a laptop computer that allows the user to communicate with the receivers, specifically the FPGA. One control center is needed for each receiver for the intended implementation. Here, the user can request specific information from the receiver about the received signal. One such piece of information about the signal that is very important is that the control center displays to the user when a trigger is received. This display shows a running average of the signal's pulse repetition interval (PRI) and pulse width (PW). Different settings for the receivers can also be set through the control center. These settings consist of different calibrations for the receivers, or changes to how the received signal is converted.

The control center utilizes a graphical user interface (GUI), so control of the receivers is intuitive and easy to use. This interface allowed information to be sent and received from the FPGA card. The TOA was sent as a User Datagram protocol (UDP) packet from the FPGA to the laptop. The control center extracted the TOA from the packets and wrote the information to a text file. The time stamp associated with the TOA measurement was also saved to the text file. In order to communicate this information between receivers, each of the control centers needs to be able to communicate with the other.

3.2.5 Receiver Communication

The two receivers for the proposed solution were located approximately 2 km away from one another. In order to transfer information between the receivers, a communication link needed to be established. Connection across a network allows information to be sent and received between all the connected devices. A few methods of creating a network were researched and evaluated.

3.2.5.1 BlackBerry Tethering

One method of connecting the receivers is to utilize the tethering capabilities of BlackBerry cell phones. BlackBerries can be directly connected to computers to act as a modem, which allows access to the Internet. The connected BlackBerry can then sign into a virtual private network (VPN) to allow access behind the firewall of restricted networks, such as the MIT LL LAN. Connecting to the MIT LL LAN allows secure communication of data to and from the receivers. Unfortunately, acquiring BlackBerries at MIT LL is a time consuming process and was not feasible under the time constraints of this project.

3.2.5.2 Direct Connection to Network

Another method of connecting the receivers is to directly connect them to the MIT LL LAN. This method would be accomplished by placing the receivers close enough to a location where an Ethernet cable can connect the computer to the network. Locations near a window are required because this connection would allow immediate unrestricted access to the capabilities of the MIT LL LAN. Ethernet, which is a twisted pair type of wired connection, can provide data transfer speeds of up to 10 billion bits/second (Gbps). The shortcoming of this method is limitations on where the receivers can be placed. The receivers would be limited to locations next to buildings at MIT LL, as these locations are the only ones with direct LAN connections.

3.2.5.3 Public Wireless Connection

One last method of connecting the receivers is to utilize a public wireless network. If there is access to a wireless network at the locations of the receivers, the computers can communicate via the Internet. This method, similar to the BlackBerry method, does not

allow connection to the MIT LL LAN unless a VPN can be established. Finding access to a public wireless network can also be difficult if a receiver is setup in a remote area.

4. Testing Logistics

The previous section discussed the full scale design of the passive geo-location system. To implement this system on the full scale and test it would be a long and challenging process that is out of the scope of this project. Rather, this project focused on testing the GPSDOs, followed by a lab test of the entire system, and then a small scale field test. These steps are the first that need to be taken to achieve a full scale test and therefore, it was accepted that these steps were an appropriate choice of scope for this project.

This section will elaborate on some of the logistics that were specific to the lab test and small scale test of the system. Specifically, what frequency would be used to transmit, the hardware needed for operation at the specified frequency, and the geometry of the field-test setup.

4.1 Frequency Choice

The front end that was discussed is necessary for the full scale implementation. However, the test of the system was conducted at 2.4 GHz; therefore the front end was unnecessary. The choice of 2.4 GHz was dictated by three factors: hardware operation, regulations, and necessary power at the receiver. These restrictions will now be discussed in further detail.

4.1.1 Hardware Operation

Since Group 105 provided the hardware for the system, any frequency choice had to operate with this hardware. With Group 105's hardware, a received signal is sent through a six-foot coaxial cable into an ADC. The ADC had a 1.8 GHz sampling rate; therefore, every half sampling rate, or 900 MHz, the spectrum will be aliased down to the band from 0 to 900 MHz. Figure 27 shows where a 2.4 GHz sine wave lies in relation to the sampling rate. Since the 2.4 GHz signal is a real signal it is symmetric about the y-axis in Figure 27 below.

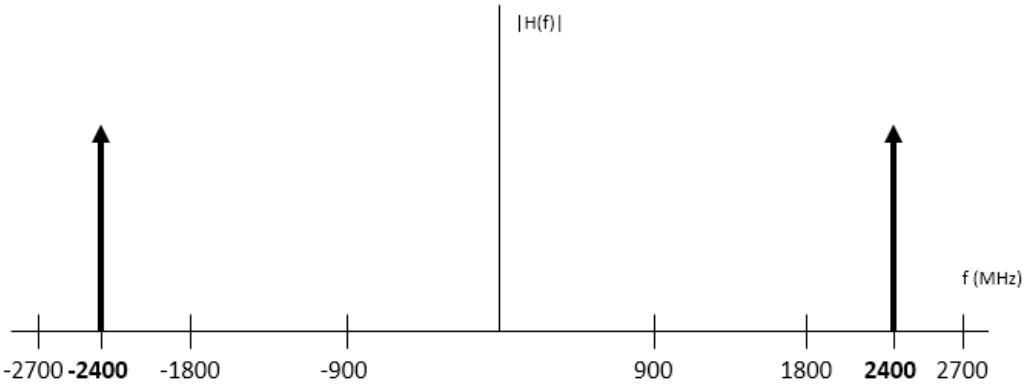

Figure 27: Plot of the 2.4 GHz signal in the frequency domain.

Since 2.4 GHz is greater than the 1.8 GHz sampling rate by 600 MHz, the signal will alias down to 600 MHz. This aliasing is shown in Figure 28. The signal will also be aliased to -600 MHz since it is still real.

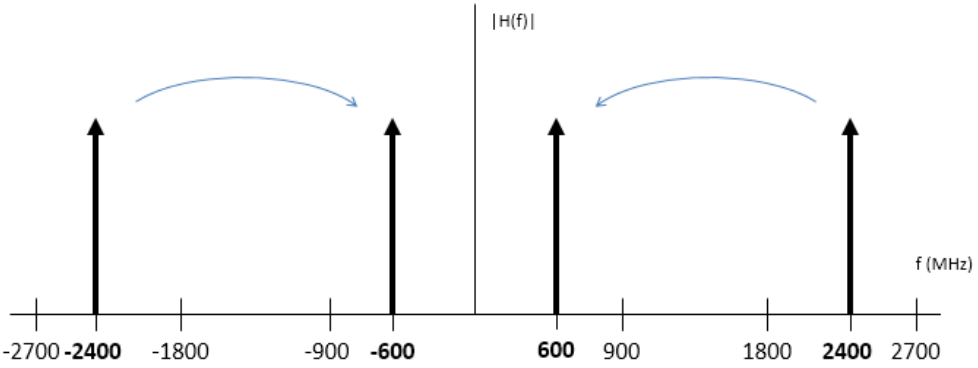

Figure 28: Frequency plot of 2.4 GHz signal aliased down to 600 MHz.

Finally, after the ADC there is a digital bandpass filter that is centered at 450 MHz and is 750 MHz wide. Figure 29 shows the filter and the 2.4 GHz signal aliased down as 600 MHz. From this figure it is clear that the signal is in the pass band of this filter.

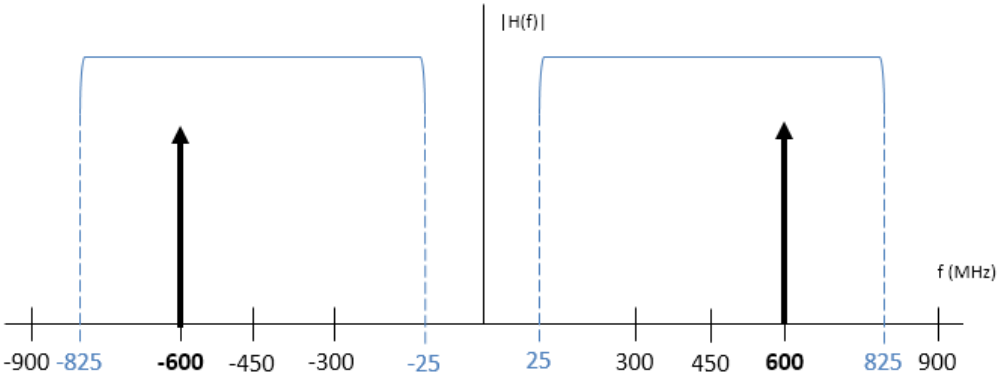

Figure 29: Aliased 2.4 GHz signal in the frequency domain with bandpass filter displayed.

4.1.2 Legal Restrictions

The Federal Communications Commission (FCC) regulates all transmitters in the country and requires transmitting units to file for a license, a process that is very lengthy and time consuming. Fortunately, for low-power, short-range emitters there is an exception made that allows very restricted power emission with no license. The power limit depends on the transmitter frequency.

The FCC set aside a number of frequency bands for industrial, scientific, and medical equipment so the bands are known as the ISM bands. The FCC eventually allowed three of the bands to be used for unlicensed low-power transmission. The rule governing these three ISM bands is that the maximum transmitter output power before the antenna is 1 W, or 30dBm. The ISM band of interest is the middle band, from 2.4-2.4835 GHz. Hence 2.4 GHz is a very practical frequency to choose when considering FCC regulations.

4.1.3 The Friis Transmission Equation

The Friis transmission equation can be used to compute the received power in a system based on many parameters. The Friis transmission equation is a variation of the radar range equation. The equation is written below:

$$P_R = \frac{P_T G_T G_R c^2}{(4\pi R f)^2} \tag{16}$$

where R is the distance between receiver and transmitter, P_T is the transmitted power in watts, P_R is the received power in watts, G_T is the gain of the antenna at the transmitter, G_R is the gain of the antenna at the receiver, and f is the transmitted frequency. The diagram in Figure 30 models the general system where the relevant parameters come from.

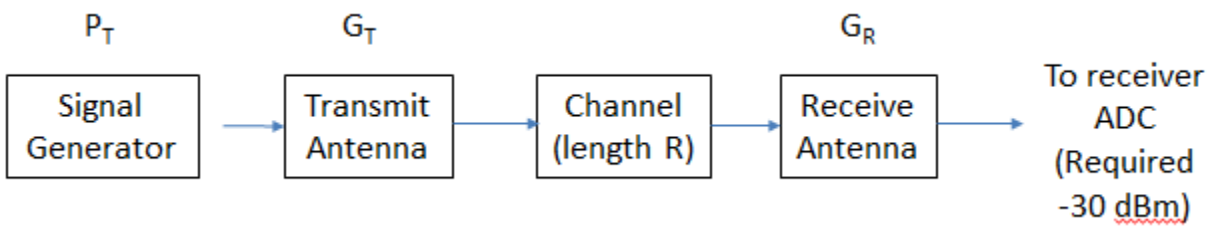

Figure 30: Model of transmitter and receiver configuration for calculating received power.

4.1.4 Specific Hardware

In order to use the Friis transmission equation, hardware dictated parameters, such as antenna gain and signal generator output power level, need to be known. This section will discuss those parameters and give further information on the hardware chosen for the system testing.

Antennas that operated at 2.4 GHz were purchased, as Group 105 had no antennas operating at this frequency, and they can be seen in Figure 31. The Wilson Electronics wide band directional antennas, model number 304411, operate between 700 MHz and 2700 MHz with 8-10.5 dBi gain. They are vertically polarized, utilize N type female connectors, and have a horizontal beamwidth of 70° to 90°. According to the data sheet, when operating at 2.4 GHz, the gain is 10.3 dBi, converting dBi into unitless gain results in a gain of 10.7. Since these antennas were used for both the receiver and transmitter, parameters G_T and G_R are equal to 10.7.

Figure 31: Antenna used for the receiver in the time difference of arrival system. A Wilson Electronics 700 MHz to 2700 MHz wide band antenna with a gain of 8-10.5 dBm.

For the small scale testing that was conducted, the source of the transmit power was an Agilent E4428C analog signal generator, seen in Figure 32. This signal generator outputs up to +27 dBm of power and can do so at the 2.4 GHz that was desired for testing. Converting +27 dBm into Watts results in a value of about 0.5 Watts, which was the value used for P_T. However, in a tighter test geometry it was necessary to use two transmit antennas because the horizontal beamwidth of the antennas was not wide enough to cover both receivers. A Mini-Circuits ZAPDQ-4-S 2000 MHz – 4200 MHz power splitter was used to split the signal to two transmit antennas. The input to both antennas was +24 dBm,

because the power was divided in half, hence a 3 dBm drop. Converting +24 dBm into Watts resulted in 0.25 Watts, which would be that value for P_T.

Figure 32: Agilent E4428C analog signal generator.

4.2 Computing Received Power

The purpose of this section is to explain how received power was calculated. The requirement driving this section is that the ADC needed a signal power of -30 dBm. An error margin of -2 dBm allowed for the system to operate at -32 dBm if necessary. The Friis transmission equation was used to determine the power of the signal at the receiver.

4.2.1 Practical Power Considerations

Using the parameters discussed in the previous sections the initial results of the Friis equation calculations were computed. Shown in Table 2 column one, these results assume the case that the transmit antenna had a wide enough beamwidth to have both receivers in its field of view at the same time. A tighter geometry would require two directional antennas at the transmitter, one pointed at each receiver. This setup would require splitting the power in half, hence the values in Table 2 column two were recalculated based off of a transmit power of 24 dBm. A final calculation was done which took 2 dBm of cable loss into consideration, and these calculations are shown in Table 2 column three.

4.2.2 Result of the Friis Transmission Equation Calculation

Table 2: Results from the Friis equation. The first column lists the distance between the receivers. The remaining columns are dedicated to specific transmit powers.

Distance (m)	P_r (dBm) at 2.4GHz		
	P_t=27 dBm (Max)	P_t=24 dBm (Halved)	P_t=22 dBm (With cable loss)
1000	-52.246	-55.246	-57.246
750	-49.7472	-52.7472	-54.7472
500	-46.2254	-49.2254	-51.2254
250	-40.2048	-43.2048	-45.2048
125	-34.1842	-37.1842	-39.1842
75	-29.7472	-32.7472	-34.7472
50	-26.2254	-29.2254	-31.2254
25	-20.2048	-23.2048	-25.2048

4.3 Test Geometry

A test was designed based on the results from the section on the Friis equation documented in Table 2, as well as the knowledge of actual power limits set forth by the FCC. Assuming that the transmit power is halved and there is a 2 dBm loss in cabling, as represented by Table 2 column three, 50 meters was the maximum distance that would allow around -30 dBm to be input into the ADC at the receiver. As seen in Table 2 column three, the received power at 50 meters transmitted at 2.4 GHz, is -31.2 dBm. This value is lower than the previously determined limit of -30 dBm, but it is within the allowable margin of error of -2 dBm.

For the field test, the receivers were separated by a distance of 50 meters. The transmitter was placed at points along a line parallel to the receiver line. Due to spatial restrictions the transmitter line and receiver line were separated by 5 meters. The described setup is pictured in Figure 33. With this setup it was possible to move the transmitter from a point of high TDOA (very near to one receiver and far from the other) to a point of low TDOA (transmitter approximately in the middle of the receivers). Within this geometry, five discrete points were chosen from which to transmit. These points are shown in Table 3.

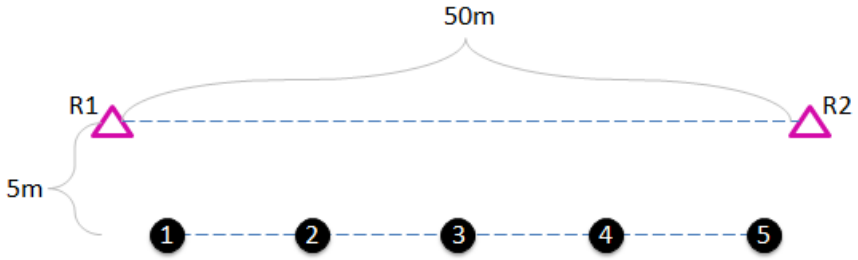

Figure 33: Geometry of the field test, where the triangles denote the receiver locations and the circle denotes the transmitter locations.

Table 3: Choice of discrete transmit points and their distance from each receiver. Distance along transmitter line assumes that zero is on the far left of the line, in line with the first transmitter.

Transmit points	Distance along transmitter line (m)	Distance from receiver 1 (m)	Distance from receiver 2 (m)
1	1	6.0828	49.366
2	12	13.4164	38.4708
3	25	25.7099	25.7099
4	38	38.4708	13.4164
5	49	49.366	6.0828

5. Testing

5.1 Timing Experiment

This section will cover the methods outline, results, and discussion of the physical experiment conducted to determine time offsets between the two GPSDOs. Instead of testing each GPSDO separately to determine if their individual performance met specifications stated on the data sheet, it was decided that both GPSDOs should be tested against each other. There are two main reasons for this choice. First, to test an individual GPSDO, a high precision clock would have to be obtained to act as a time reference. Obtaining such a clock would be expensive and is out of the scope of this project. Second, knowing the offset of the GPSDOs in relation to one another is more useful to this project than knowing individual performance. The reason being that this system takes the time difference of the time of arrival at each receiver; hence, the two clocks need to be precise to one another rather than accurate to UTC.

To test the accuracy of the PPS output from the GPSDOs, it was essential to have an oscilloscope that could measure to at least a single nanosecond of accuracy. Group 105 has a Keysight Infiniium DSO9254A available for use. This oscilloscope has a sampling rate of 20 GSa/s and a 2.5 GHz bandwidth across all four analog channels. The oscilloscope also has a resolution of 5 picoseconds per division, which is accurate enough to test the GPSDOs.

5.1.1 Methods

The GPSDOs do not have internal antennas; therefore the antennas purchased for them were attached in order to characterize the GPSDOs. Once attached to the GPSDOs, the antennas were placed side by side on a windowsill to avoid the introduction of any error that might be a result of location differences between the GPSDOs.

The PPS signal is output from the GPSDO through a cable harness. There are three output choices for the PPS: A 5V CMOS, LVDS differential pair, and an RS-232 level output. The two-receiver geo-location system requires a CMOS level signal, which is output by pin 13 of the GPSDO.

To measure the PPS signal, an Agilent N2873A probe was used. This passive probe has a 4 ft cable, operates DC to 500 MHz, and has a 10:1 attenuation factor. This type of probe measured both GPSDO PPS outputs. One PPS output was measured by channel 1 and the other by channel 4 of the oscilloscope.

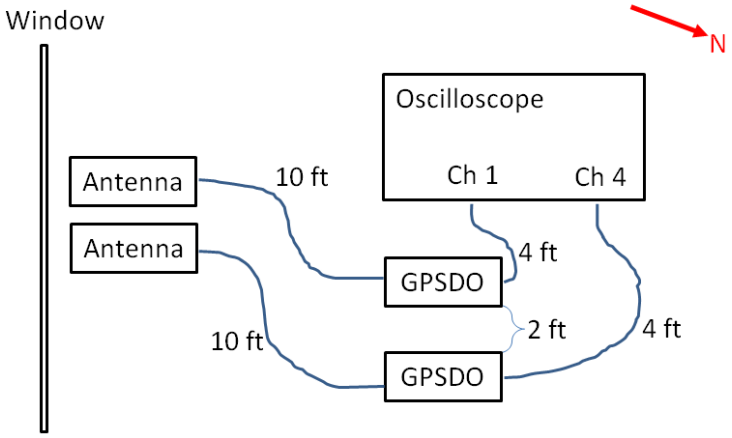

Figure 34: Entire setup of timing experiment. Antenna separation was on the order of centimeters. Figure not drawn to scale.

A diagram of the entire setup is shown in Figure 34. The two GPSDOs were on a lab bench along with the oscilloscope. The two antennas were raised 3 ft from the height of the lab bench and placed on the windowsill.

Before the test discussed in this section could be run, it was necessary to first determine if the oscilloscope was accurate enough. Setting up both of the probes to measure the same signal simultaneously tested the delays in the individual probes and channels. Channels 1 and 4 of the oscilloscope were used for this test because those were the channels decided upon for the main test of timing. By using the same signal in both probes, in this case the PPS output from one of the GPSDOs, the probe's measurements were compared against one another. The result of this measurement is seen below in Figure 35. With this oscilloscope's resolution, the signals are close to identical until 2.5 V where they then diverge, but by no more than 3 ns. This discovery is why 2 V was chosen for the MATLAB script as the point to compare between the two channels.

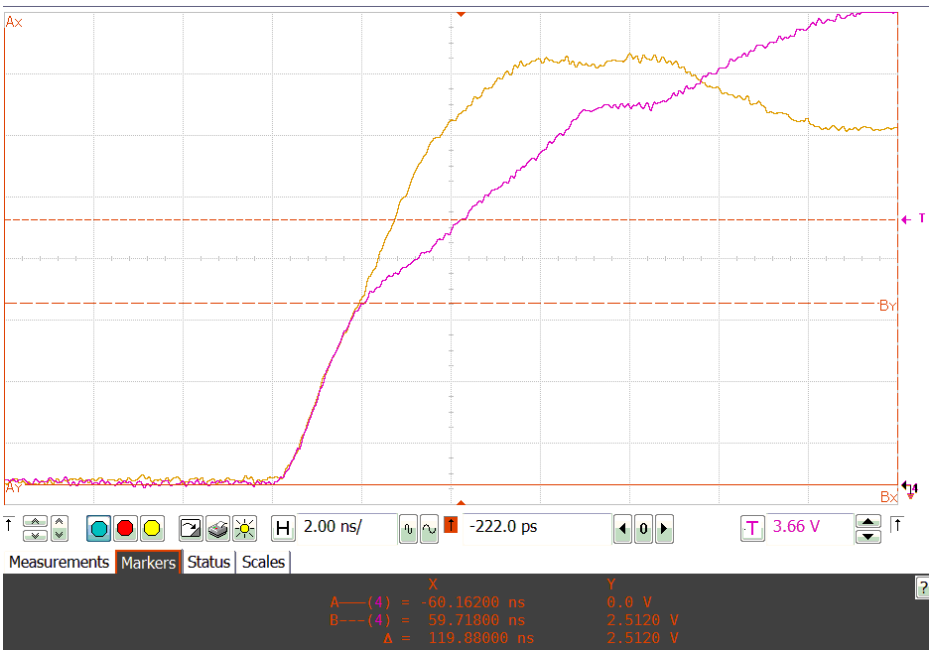

Figure 35: Oscillogram showing the same pulse per second (PPS) signal measured on two probes, through channel 1 and channel 4. The signal diverges at a value of 2.5 V as measured by marker BY.

While testing the oscilloscope with the PPS as a reference, it was observed that one of the GPSDOs would lose synchronization more frequently than the other. To ensure that this loss of synchronization was not due to the antenna or its placement, experiments were conducted with the setup of the GPSDOs. First, the placements of the physical antennas were exchanged with each other. This swap did not have a noticeable effect on the performance of either GPSDO. Second the antennas were exchanged, meaning that the antennas were disconnected from their respective GPSDOs and attached to the other GPSDO. This exchange also did not appear to have an effect on the performance. Finally, the physical location of the test was moved from a bench in the interior of the building to a bench near a window. Moving the location not only improved the performance of the GPSDOs, in terms of precision to one another, but also improved their ability to stay synchronized to the GPS satellites for long periods of time.

To further increase the GPSDOs' ability to stay synchronized, there are software settings that can be adjusted on each GPSDO. The settings on the GPSDOs can be checked and changed through the use of a serial connection with a computer. Some of these settings involve accounting for the delay through the cable between the antenna and the GPSDO,

changing the operation of the PLL, or adding an offset to the PPS output. After experimenting with these settings, it was concluded that the manufacturer's settings were optimized for performance on each GPSDO. The value that did have to be changed was the setting for antenna delay. The GPSDO data sheet specified that a delay of 1.5 ns per foot of cable was typical. Since the antennas being used for both GPSDOs had 10 ft cables, a delay of 15 ns was set with the command GPS:REF:ADEL 15 ns.

Once the physical setup of the antennas was established, the PPS comparison test could take place. Testing the PPS involved capturing the rising edge of the signals in order to determine the time difference between each GPSDO's PPS output. Capturing the rising edges of the PPS signals involved configuring the oscilloscope to be in segmented mode with a sampling rate of 10 GSa/s; 4000 points of memory per channel; and a horizontal time of 20 ns per division for a total of 200 ns, as there are 10 divisions on the oscilloscope. When setting the oscilloscope into segmented mode, one of the PPS signals was triggered at time zero, while the other PPS signal was displayed in time relative to the other. This oscilloscope can capture a maximum of 8192 segments in a single run, which accounts for 136 minutes of PPS signals. To collect an ample supply of data for processing, the oscilloscope was run in segmented mode 11 times, which provided over 24 hours of data.

For each collection of 8192 PPS signals, a MATLAB script determined the time difference between the rising edges of the two PPS outputs. A sample screen shot is shown in Figure 35. The script imported all of the voltage values of the waveform, which the oscilloscope had sampled, from a text file saved on the oscilloscope. The script then searched through the data points for each channel on corresponding measurements until a value greater than or equal to 2 V was located. The point at which each signal was above 2 V was compared and the difference in samples was then converted to a time value. The conversion factor was determined by dividing the total number of samples by the total time in each segment. The conversion factor was approximately 160 samples/ns.

5.1.2 Results

Using the time difference between the outputs, the mean, median, and standard deviation of the time differences were calculated. Also, the percentage of absolute time differences within certain time durations were determined, specifically, 30 ns, 40 ns, and 60 ns. All of these values, for all 11 of the 8192 segment collections, can be seen in Table 4.

Table 4: Statistics of time difference between pulse per second (PPS) signals.

Capture number	Mean (ns)	Median (ns)	Standard deviation (ns)	Percentage of time differences within ±60 ns	Percentage of time differences within ±40 ns	Percentages of time differences within ±30 ns
1	10.7	11.0	30.0	91.1%	82.5%	69.2%
2	-1.7	-10.8	39.5	86.5%	69.0%	58.3%
3	21.8	20.1	30.1	87.1 %	70.7%	63.1%
4	22.6	25.5	31.9	88.1%	68.5%	53.1%
5	22.1	21.9	22.2	97.2%	75.1%	61.3%
6	20.9	15.8	34.2	84.4%	64.7%	56.7%
7	22.7	20.4	33.4	87.8%	70.1%	54.4%
8	25.2	22.2	30.7	88.3%	67.3%	60.2%
9	0.3	0.6	28.0	98.0%	82.7%	69.5%
10	-15.0	-17.7	22.7	97.1%	88.6%	72.7%
11	-8.5	-10.4	34.2	90.1%	68.9%	59.4%
Average	**11.0**	**9.0**	**34.0**	**90.5%**	**73.5%**	**61.6%**

A histogram of all the data can be seen in Figure 36. The histogram shows the signed time differences between the PPS outputs of the two GPSDOs. The overall mean of all the data collected is 11.0 ns with a standard deviation of 34.0 ns. This means that 68% of the data falls between -23 ns and +45 ns, 95% of the data falls between -57 ns and +79 ns, and 99.7% of the data falls between -91 ns and +113 ns. The individual histograms for each capture can be found in Appendix A. Along with the histograms, the time series plots of

each of the 11 captures can also be found in Appendix A. An example of one of the time series plots is shown in Figure 37.

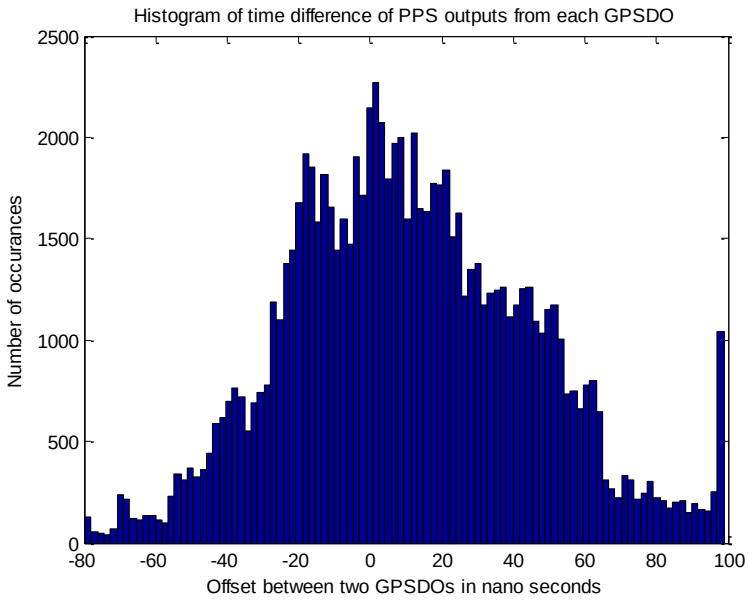

Figure 36: Histogram of signed time differences of the pulse per second outputs from the two GPS disciplined oscillators (GPSDO).

Figure 36 shows an unsigned histogram of the results. As would be expected, there is a peak around zero seconds, and the figure shows a fairly normal distribution, except for the large spike at about 100 ns. In every one of the 11 data collections, there would be a number of differences over 60 ns. These differences could be due to a loss of synchronization to the GPS satellites on the part of the GPS receiver.

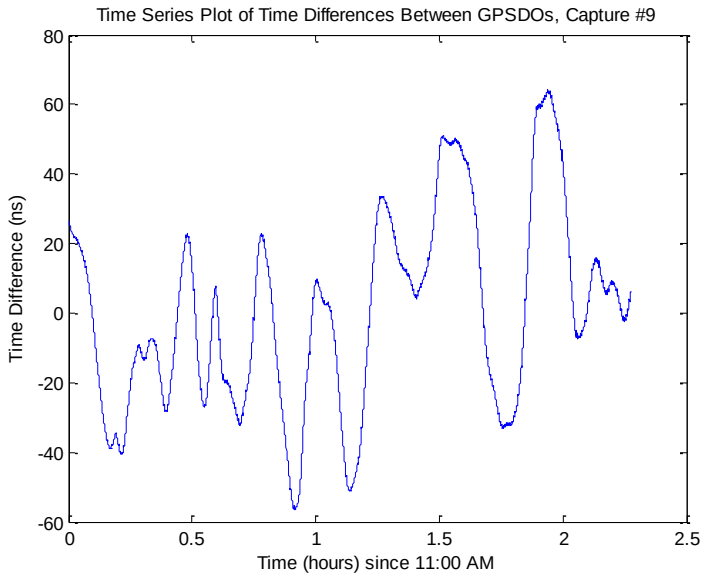

Figure 37: Time series plot of time differences of the pulse per second (PPS) outputs of the two GPS disciplined oscillators (GPSDO) for capture 9.

5.1.3 Discussion

The goal of this section was to determine if the GPSDOs kept sufficiently precise time to meet the requirements of the project. The necessary precision for this system was established through knowledge of the requirements, specifically that the estimated target had to be within 1.5° of the actual location. In other terms, the error from the GPSDOs that the system can tolerate is ±60 ns. As noted in Table 1, when the time error is 90 ns and the target is at any position along the flight path, the associated distance error is greater than the allowed distance error.

A corollary to the 1.5° angle of error restriction is that this requirement only needs to be met 70% of the time. Statistics about the 11 oscilloscope captures, displayed in Table 4, show that a time error within ±60 ns is expected, on average, 90.5% of the time. A 60 ns timing error corresponds to a 60 ns distance error, which is shown in Table 1. Clear from Table 1 is that the distance errors associated with 60 ns would all be within the limits of acceptable error. Therefore, 90.5% of the time the time error is within 60 ns, which means the distance error will be acceptable. From these results it can be concluded that the GPSDOs not only meets the goal for keeping precise time, as defined by the distance error restrictions, but it exceeds the requirements.

However, these results are not capable of verifying all of the data sheet specifications of interest. One flaw in the methodology that was followed was that we were unable to verify the accuracy of either individual GPSDO output. Each GPSDO should output a PPS accurate to ±30 ns UTC RMS. Unfortunately, there was no test done to validate that either GPSDO met this specification. To check this specification, an extremely high precision clock, accurate to within picoseconds of UTC, would have had to been used as a reference for each GPSDO to be compared against.

5.2 Laboratory Test

Tests of the system needed to be conducted to determine if it worked. In order to perform the tests, the hardware components chosen were assembled together. Tests were performed inside of the lab to gather initial data. Once the data were evaluated, a field test was performed in a more realistic application to gather more data on the system's performance.

5.2.1 Methods

An initial test was conducted inside the lab to verify that all components worked together. To perform the test a signal generator, a power divider, the two receivers without antennas, and various lengths of cable were utilized. The antennas were not utilized because the signal generator, acting as the transmitter, was directly connected to the ADC input on each FPGA card. Figure 38 shows the test setup, where the large red dashed lines represent cables of various lengths that simulate different distances between the receivers and the transmitter.

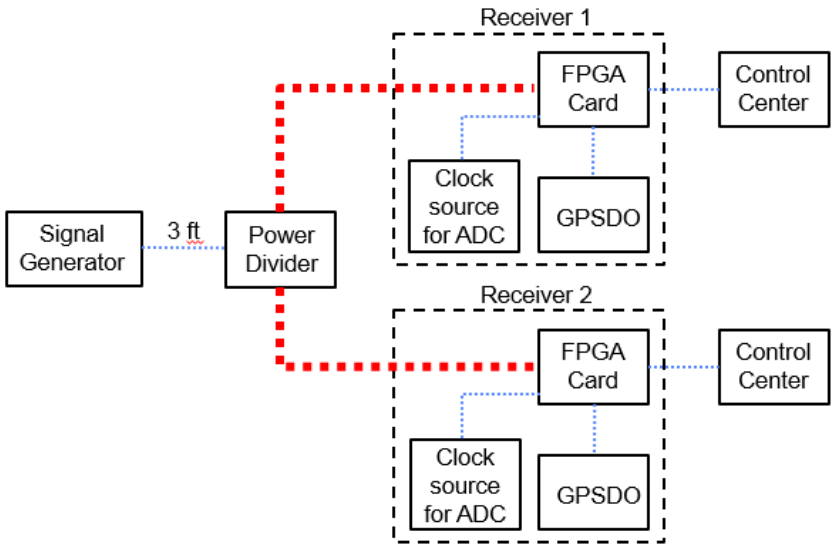

Figure 38: Laboratory test setup, where the large red dashed lines represent the varying cable lengths.

To perform the test, a power splitter was connected to the output of the signal generator by a three-foot coaxial cable. The signal generator was set to output -15 dBm of power at 2.4 GHz. It was also set to pulsed mode with a pulse repetition interval (PRI) of 1 ms and a pulse width of 100 µs. Set in this mode, the signal generator output -15 dBm at 2.4 GHz for 100 µs every one ms. This splitter enabled a signal to be sent to two receivers. One output of the splitter went to each receiver through various lengths of coaxial cable. The long 75-foot length cables used were low loss cable with an expected propagation delay of 1.2 ns/ft. All of the small lengths of coaxial cable under 6 feet used were of a lower quality and had more loss. The configurations of coaxial cable tested are shown in Table 5. Each of these experiments was run for 16 hours, from 5pm to 9am to ensure that a full period of the GPS satellites, about 12 hours, was experienced during a test.

Table 5: Experiments with varying lengths of coaxial cable.

Experiment	Length to Receiver One	Length to Receiver Two	Distance Difference
A	6 ft	6 ft	0 ft
B	81 ft	156 ft	75 ft
C	6 ft	156 ft	150 ft
D	6 ft	231 ft	225 ft

Once varying lengths of cable were tested two different PRIs were tested for the case of zero TDOA. A zero TDOA case is where the distance between the receivers and the transmitter is the same; therefore the TDOA should be zero. The value of the PRI was 1 ms for the first set of experiments. A PRI of 2 ms and 0.5 ms was also tested. These tests were running for 4 hours each.

Next, the startup conditions of the system were observed. First, the GPSDOs was turned off and allowed to cool down for one hour. They were then turned back on, and once both GPSDO had locked to the GPS satellites a test was run for 4 hrs. Second, the entire system was shut down; GPSDO, FPGA, and the ADC clock source. After allowing the system to cool down for three hours another test was run for 18 hrs.

5.2.2 Results

The results of experiments A though D, described in Table 5, are shown in Table 6. Figure 39 is a plot of the data from Table 6, where the slope of the line of best fit is 1.8 ns/ft. The plots that follow Figure 39 show the results of experiments A through D in graphical form. In these plots, the solid red line represents the mean of the TDOA and the red dashed lines represent deviation from the mean of ±60 ns.

Table 6: Table of statistics from figures in this section.

Experiment	Distance difference (ft)	Mean (ns)	Percent within ±60 ns of the mean	Mean counter value at receiver one	Mean counter value at receiver two
A	0	105	86	26456	25830
B	75	-16	87	91612	91157
C	150	-96	88	192540	191940
D	225	-327	95	37978	37107

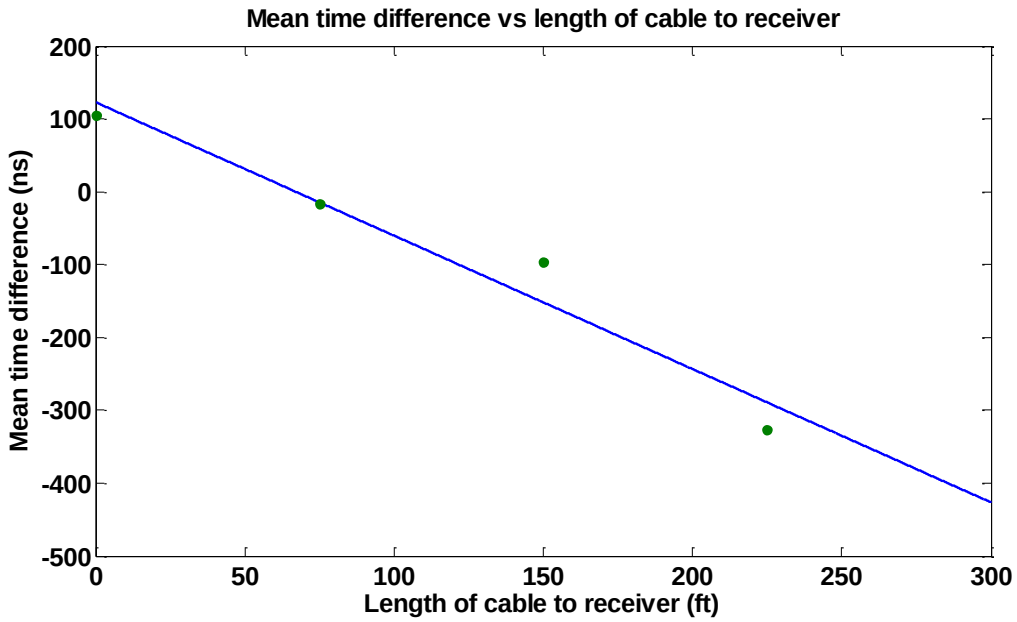

Figure 39: Plot of data from Table 6. Cable length difference against the mean time difference. The slope of the line is 1.8 ns/ft.

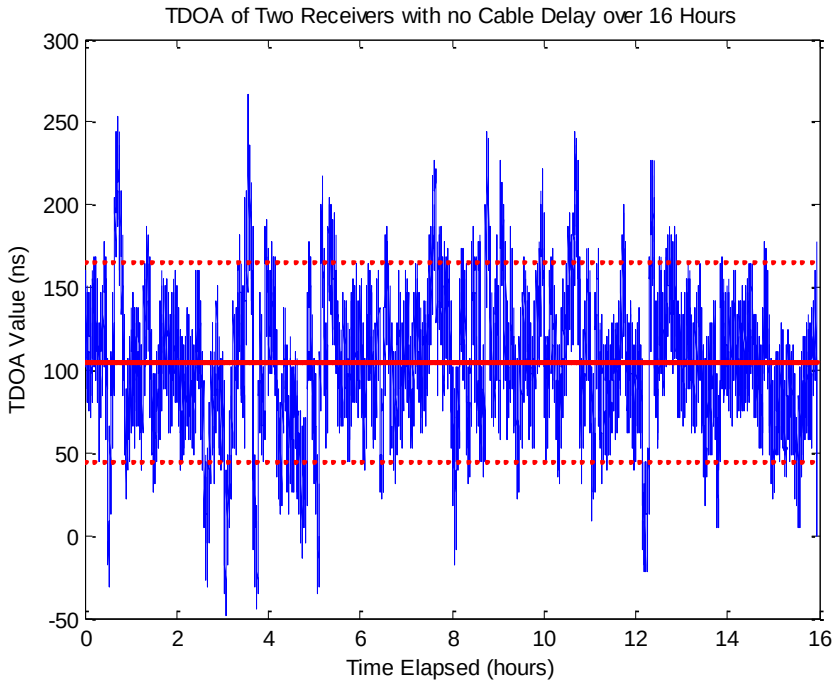

Figure 40: Time difference of arrival (TDOA) experiment A. The solid red line represents the average value of the TDOA. The red dashed lines represent deviation from the mean of ±60 ns.

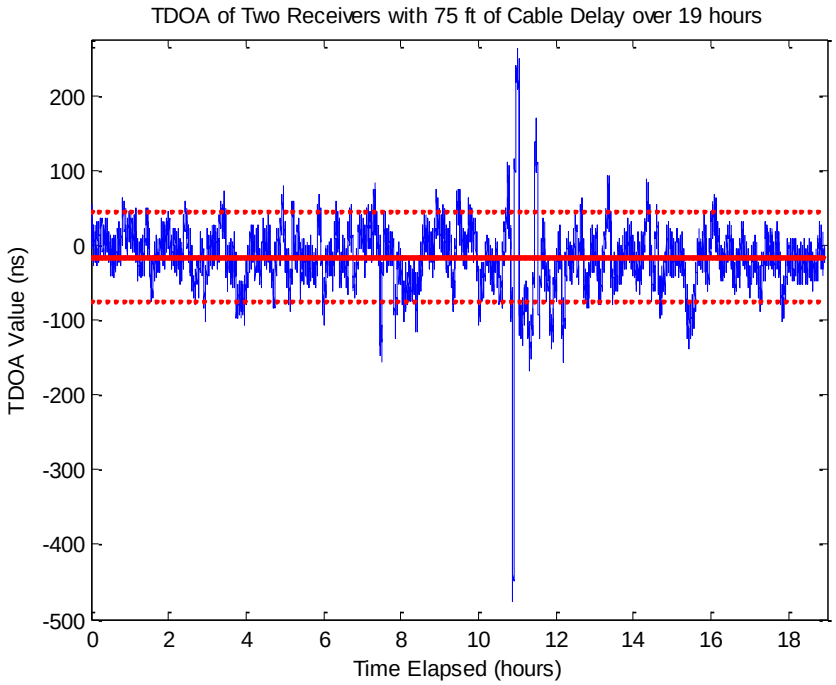

Figure 41: Time difference of arrival (TDOA) experiment B. The solid red line represents the average value of the TDOA. The red dashed lines represent deviation from the mean of ±60 ns.

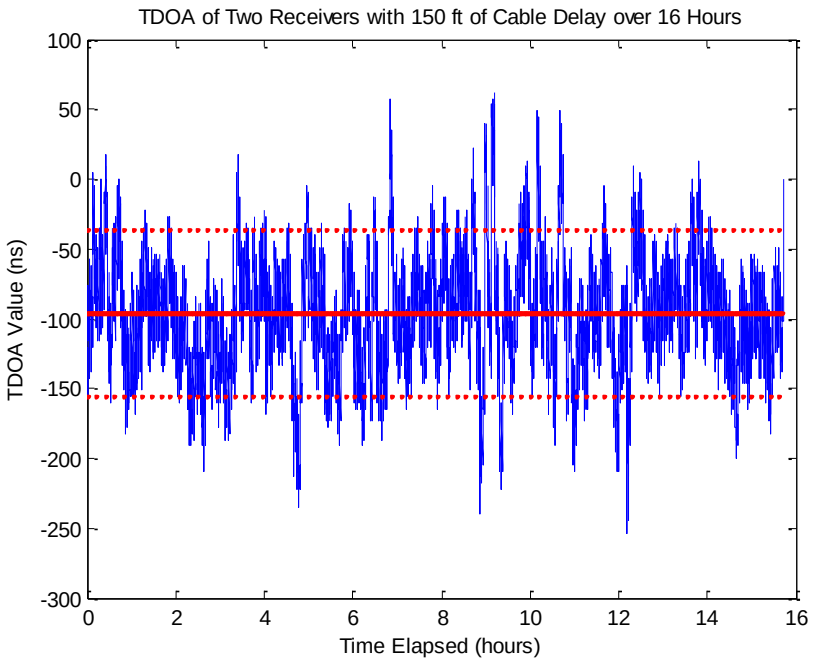

Figure 42: Time difference of arrival (TDOA) experiment C. The solid red line represents the average value of the TDOA. The red dashed lines represent deviation from the mean of ±60 ns.

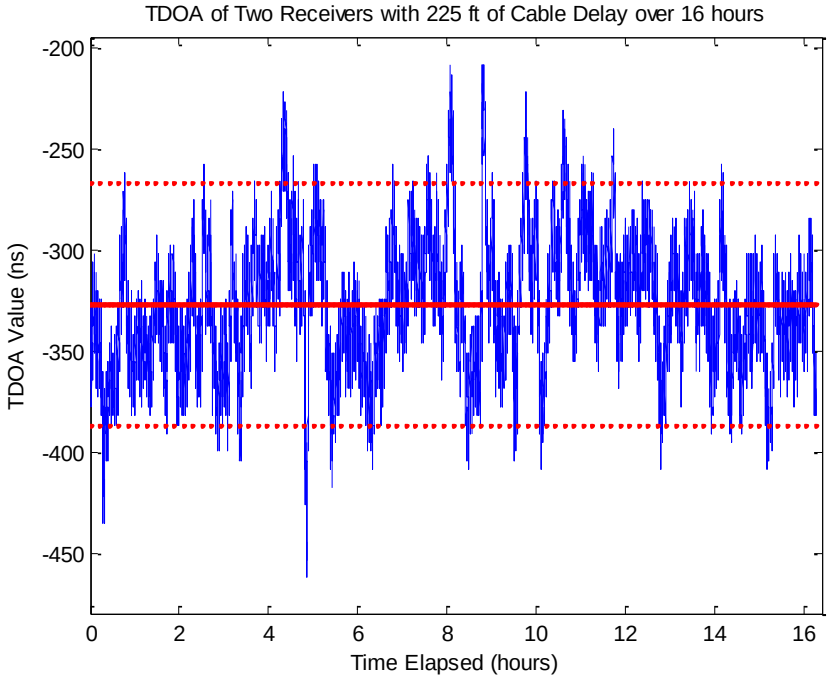

Figure 43: TDOA experiment D. The solid red line represents the average value of the average value of the TDOA. The red dashed lines represent deviation from the mean of ±60 ns.

The next set of results comes from the test of different PRIs. Table 7 displays the results of the test. Data from experiment A is shown as a reference point as the case of one ms. Figure 44 and Figure 45 show the plot of the TDOA over time for half and double PRI respectively.

Table 7: Results of testing the case of zero TDOA with various PRIs

PRI (ms)	Mean (ns)	Percent within ±60 ns of the mean	Mean counter value at receiver one	Mean counter value at receiver two
0.5	33	96	46752	46536
1	105	86	26456	25830
2	58	98	36018	35166

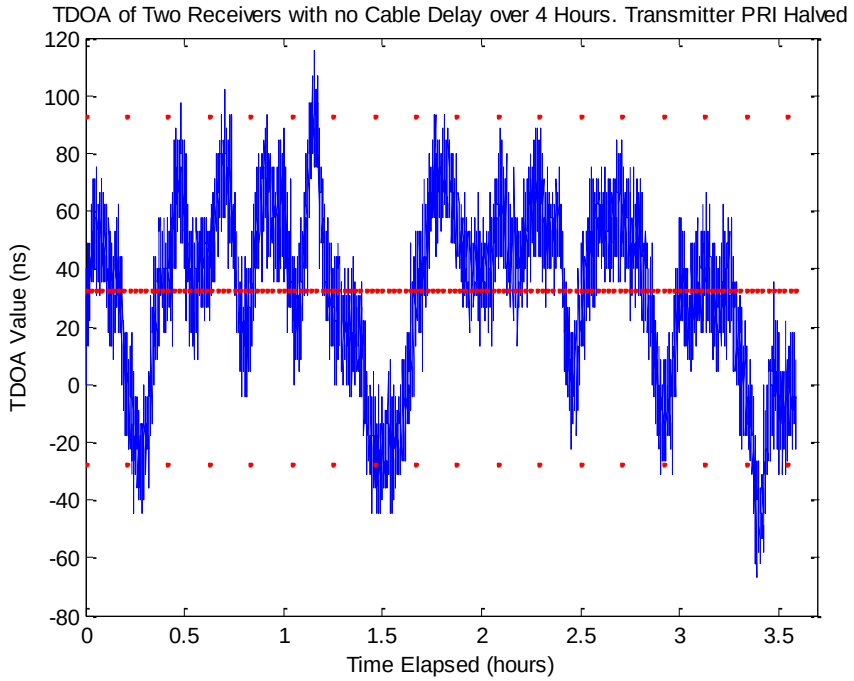

Figure 44: Test where PRI was set to 0.5 ms. The solid red line represents the average value of the average value of the TDOA. The red dashed lines represent deviation from the mean of ±60 ns.

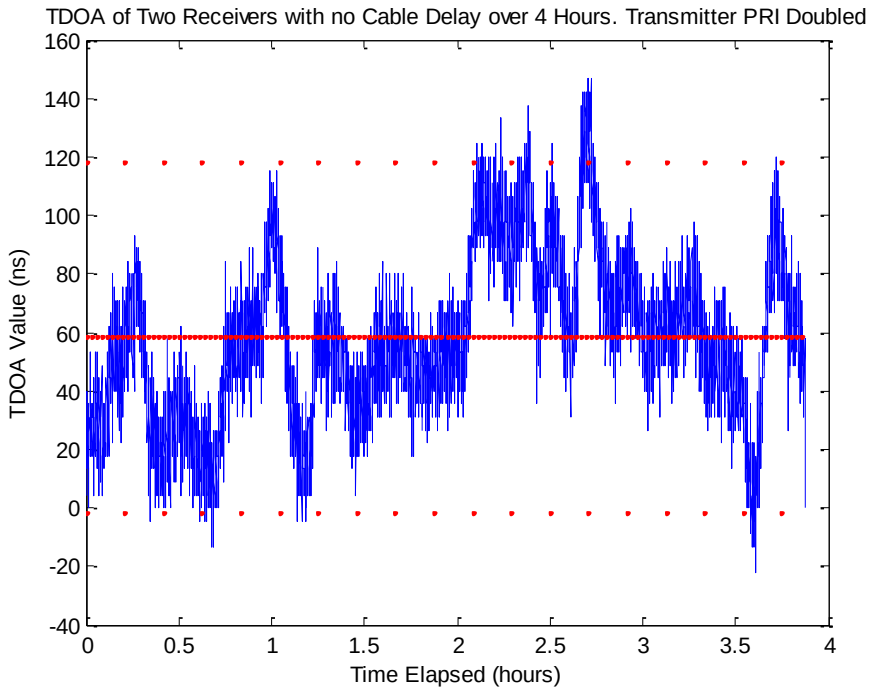

Figure 45: Test where PRI was se t to 2 ms. The solid red line represents the average value of the average value of the TDOA. The red dashed lines represent deviation from the mean of ±60 ns.

Next, the results of the tests considering the effects of startup on the system's performance are displayed. Table 7 shows the results below followed by Figure 46 and Figure 47, which display plots of the TDOA data over time. Figure 48 displays the data from Figure 47 with the first 10000 seconds, almost three hours, removed. The data points removed encompassed the time the TDOA took to stabilize. The mean of the data in Figure 48 is 60 ns and 93% of the TDOAs were within ±60 ns of the mean.

Table 8: Display results of tests after resetting the GPSDO and the entire system.

Reset	Mean (ns)	Percent within ±60 ns of the mean	Mean counter value at receiver one	Mean counter value at receiver two
GPSDO	-16	87	211190	210730
Full System	50	85	112690	112200

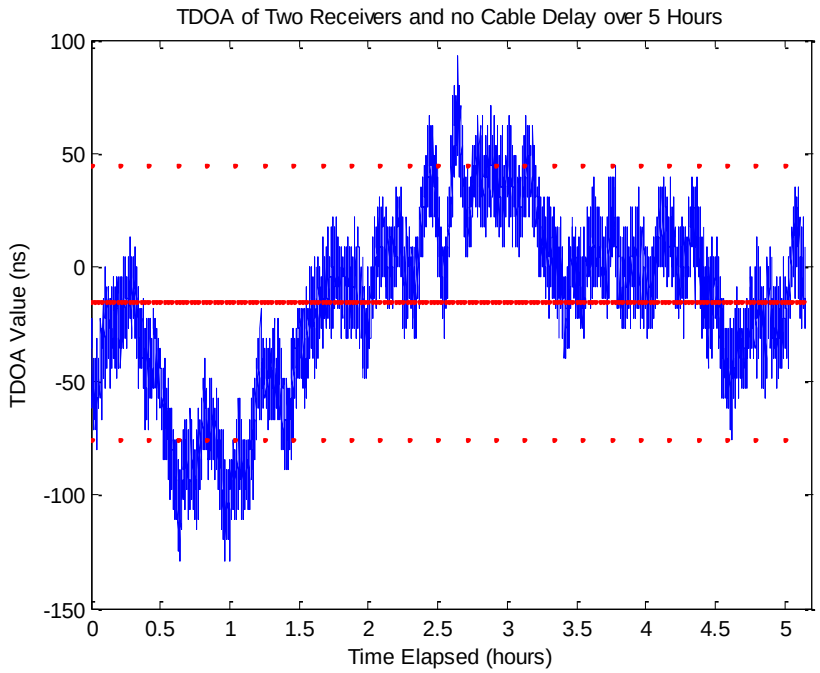

Figure 46: Results of 5 hr test run after the GPSDO had been rest. The solid red line represents the average value of the average value of the TDOA. The red dashed lines represent deviation from the mean of ±60 ns.

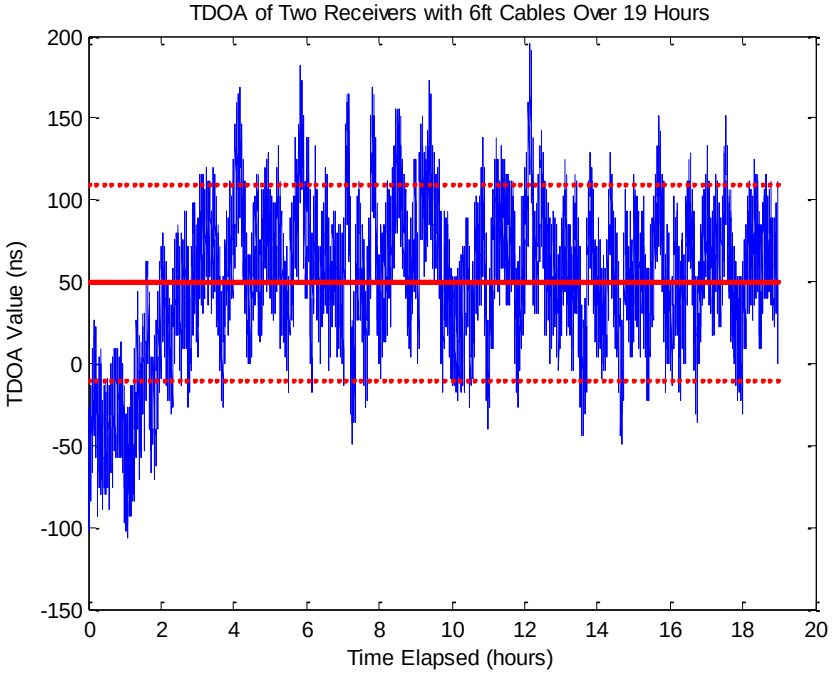

Figure 47: Results of 17 hr test after resting the entire system. The solid red line represents the average value of the average value of the TDOA. The red dashed lines represent deviation from the mean of ±60 ns.

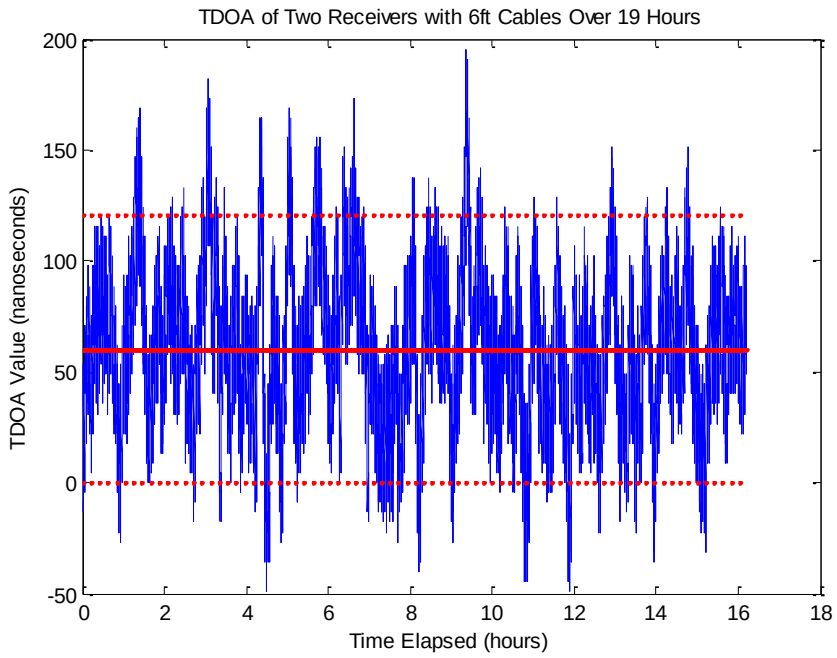

Figure 48: Results from Figure 47 with the first 10000 seconds removed. The solid red line represents the average value of the average value of the TDOA. The red dashed lines represent deviation from the mean of ±60 ns.

5.2.3 Discussion

Experiment A showed very clearly that the system was not producing expected results. As seen in Figure 40, the mean of these data was 105 ns. The test setup that acquired these data should have ideally seen no difference in the time of arrival at each receiver. The reason there should have been no TDOA is because the signal had to travel through the same amount of cable to reach each receiver. Though there was an offset, the observed deviation from the offset was expected. When characterizing the GPSDOs it was determined that, on average, the deviation from the expected value of the TDOA was within ±60 ns 90.5% of the time. For every test conducted in the lab, the percentage of data within ±60 ns of the mean was at least 85% and for the case of experiment A, the value was 86%.

Before considering the source of the error, it is important to realize that the error is not periodic, rather a constant offset. It is also important to understand that the average offset was constant for the entirety of each experiment, for experiments A through D.

One reason for the offset could be that one of the cables used was damaged. If one of the cables was damaged, then an offset could be introduced if it was causing the signal to be

delayed or attenuated. This source of error was ruled out by probing each 6 ft cable on the end where the cable connected to the receiver with an oscilloscope. There was only a 3 ns timing delay, not a 105 ns delay, between the cables. This delay can be seen in Figure 49, where it will also be noted that the amplitude of one signal is slightly less than the other.

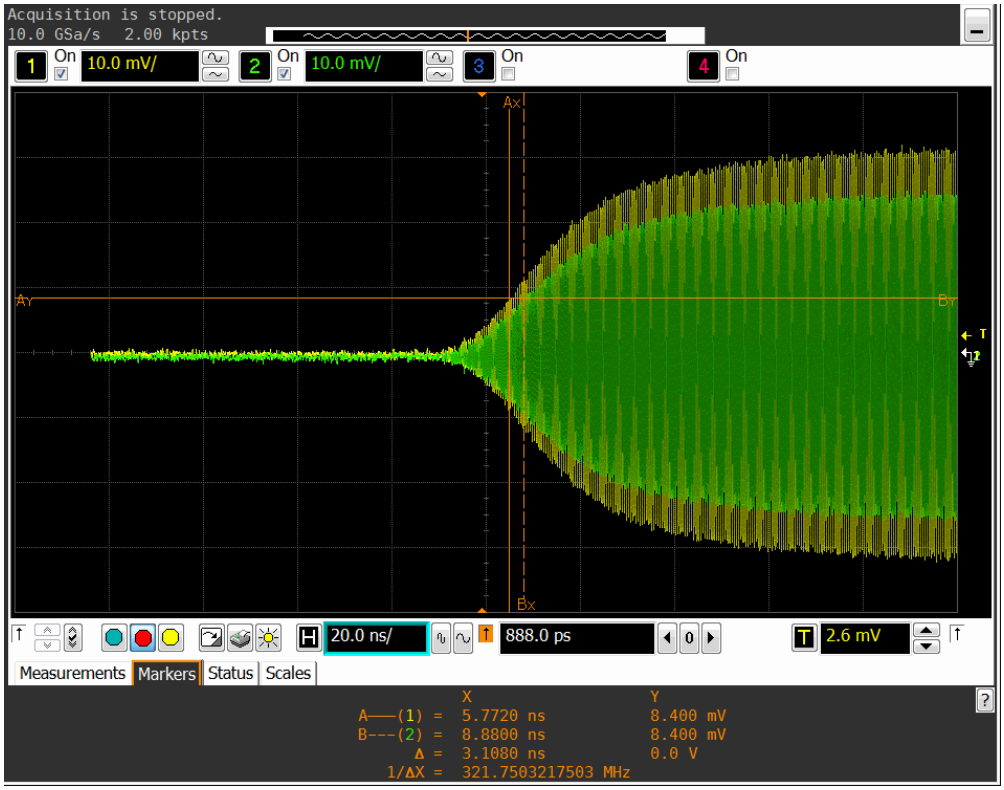

Figure 49: Oscilloscope screenshot of timing offset between the outputs from the splitter attached to the signal generator. The green signal is the signal at the end of a 6 ft cable connected to the power divider and the yellow signal is the signal at the end of another 6 ft cable connected to the power divider. Horizontal scale is 10 mV per division and the vertical scale is 20 ns per division.

To further explore the cables the results from experiments A through D were considered with the offset of experiment A subtracted out. Since the average error is constant it is possible to subtract out the mean from every point. The result of doing so is shown in Table 9. Table 9 also shows the expected TDOA corresponding to the simulated distance differences based on a propagation speed of 2.58 m/s, which is what is specified for the delay cables used. Unfortunately, subtracting out the offset measured in experiment A does not produce the correct results.

Table 9: TDOA of experiments A through D with 105 ns offset subtracted and expected value based on a propagation speed in the cable of 2.58 m/s

Experiment	Distance Difference	TDOA mean with 105 ns offset subtracted	Expected TDOA based on a propagation speed of 2.58e8 m/s
A	0 ft	0	0
B	75 ft	-121	-90
C	150 ft	-201	-180
D	225 ft	-432	-270

The final step taken to understand the cables was to plot the distance difference against the mean TDOA. This plot can be seen in Figure 39. The line of best fit plotted in Figure 39 has a slope of 1.8 ns/ft. The slope represents the delay through the cable. Though the slope shows a delay of 1.8 ns/ft and the expected value was 1.2 ns/ft, the data still plots linearly which shows that offset is independent of the cable length.

Another possible source of the offset error is the 225 MHz clock on the FPGA. This clock acts as the counter, which counts from the time a PPS signal was received to the time a target pulse is received. The 225 MHz clock leads to a 4.44 ns period. If the period of the counter is offset from this value, then, for every increment of the counter more error will be accrued.

For experiments A through D, the PRI on the signal generator was set to one millisecond. This PRI means that the largest count between the PPS and received target would be one millisecond, which corresponds to approximately 225000 counts of 4.44 ns. This maximum count means that a small error could accumulate up the 225000 times. Therefore, changing the pulse repetition rate to 2 ms, or double what it previously was, should double the maximum error. Halving the rate to 0.5 ms would halve the maximum error.

A test was run for both of these cases and the results were not as expected. The case with a 0.5 ms pulse repetition interval is seen in Figure 44. The case with a 2 ms pulse repetition interval is seen in Figure 45. The results displayed in Table 7 are inconclusive. While the mean offset does increase from the case of 0.5 ms PRI to 2 ms PRI, both cases

have a smaller offset than the test with a 1 ms PRI even though all test were run with the same configurations.

This test also showed unexpected results when the counts were observed. By increasing the maximum time expected between the PPS and the trigger it would be expected that the mean count would be greater, and vice versa. However, when looking at the average count value it was observed that the half PRI test had higher counts on average than the double PRI case, and both tests had a lower count value average than the original PRI of 1 ms.

Strange count values were seen in every test. These count values did not seem to depend on the PRI or the length of cable. By looking at Table 6 the lack of correlation between cable length and average count is very clear. It is possible that there were inadequate data to find the true average count but it is more probable that the count was a result of how the test was started. If the signal generator was turned on for a test and the first pulse happened relatively close in time after the PPS, then the counts would be smaller, regardless of the PRI or cable delay then if the test was started and the first pulse was further away from the PPS.

Up to this point, the time when every test was run in relation to one another and if the system had been reset between these test has not been considered. In Table 9 once the offset of 105 ns was subtracted from the results of experiments A through D, the experiment with the least discrepancy from the calculated TDOA was experiment B. Experiment A was conducted on a Wednesday night and experiment B was conducted the next night, Thursday, without ever turning off the system. That Friday, the equipment was moved outside for the field test and the following Monday and Tuesday nights were when experiments C and D were conducted, respectively. When moving the equipment in and out of the lab the equipment had to be turned off. Table 7 shows the results of the varying PRI tests. The 1 ms test was again, experiment A, so it was conducted on a Wednesday. The half and double PRI tests were run on the same day, the Wednesday after experiment A was run.

Given the difference between the mean offsets dependent on either day of the week or if the system had been reset, two tests were run to test the startup conditions of the system. The first test run only explored the startup conditions of the GPSDO, and the results are seen in Figure 46. This test was run for five hours and it can be seen that after some initial high error swings, the mean was beginning to settle at -16 ns, a value different from any other offset of a zero TDOA case. The second test was run after the entire system was reset and the resulting data is seen in Figure 47. This test was run for 19 hours and the mean it settled to, seen in Figure 48 was 60 ns. This result, again, is very different from any other zero TDOA case.

5.3 Field Test

This section covers the field test that was conducted. The field test did not go as planned, however. The methods section describes the plan and the results and discussion section describe what actually happened and the few results that we were able to obtain.

5.3.1 Methods

After completion of the laboratory test, a field test was conducted. The field test was setup in the previously explained geometry. The field test for this system was conducted outside of J-building at MIT LL where there was adequate space to fit the geometry of the system as well as the availability of numerous power outlets. The setup for testing the system in the field is displayed in Figure 50.

Figure 50: A photo depicting the setup for testing the time difference of arrival (TDOA) system. Receiver 1 is in the foreground, receiver 2 is in the background, and the transmitter is in the bed of the truck halfway between the receivers.

Both receivers were placed at the edge of the parking lot about 10 meters away from the building and the receivers were 50 meters apart. The area outside of J-building had standard 120 V_{rms} 60 Hz power outlets to power both receivers. The receiver antennas were mounted on tripods at a height of six ft and pointed toward the transmitter. The full setup of a single receiver can be seen in Figure 51.

Figure 51: A photo depicting one entire receiver setup for the time difference of arrival (TDOA) system. The analog to digital converter (ADC) and the field programmable gate array (FPGA) card are in the black case, the antenna is mounted on the survey stand, the control center is the laptop, and the GPS disciplined oscillator (GPSDO) is in the metal box next to the laptop.

The transmitter was setup in the bed of a pickup truck, as pictured in Figure 52. The power for the signal generator was provided through an inverter from the truck's power. The antenna mount was a metal stand that Group 105 often uses to hold horn antennas. Two antennas were fed through coaxial cables with SMA connections out of a Mini-Circuits 2000-4000 MHz power splitter that was sourced from the signal generator. One antenna was pointed in the direction of each receiver.

Figure 52: Picture of the transmitter used for field-testing the time difference of arrival (TDOA) system.

Multiple measuring tapes were used to place the transmitter at each discrete point of transmission. At each point, all antennas were redirected so that each receive antenna pointed directly at a transmit antenna. Once the antennas were configured, one hour of data, where data were saved once every second, was collected.

The laptop at each receiver collected the TOA at their respective receiver. After the test was complete, the data were compiled and the TDOAs were calculated for each pulse at each transmission point. The TDOA data was then used to compute a location estimate and these estimates were compared with the actual location of the transmitter.

5.3.2 Results and Discussion

When conducting the field test all units were setup as previously stated. The first and most critical result was that the received power was far below the expected values. The transmitter was setup in the back of a pickup truck; a signal generator split into two antennas, where one antenna was pointed at each receiver. The pickup truck was initially set at the first transmit point, 5 meters away from one receiver and approximately 50 meters away from the other receiver. A spectrum analyzer was attached to the output of the receive antenna, 50 meters away from the transmitter, by a 3 ft coaxial cable. With the receive antenna pointed directly at a transmit antenna and power going into that transmit antenna measured to be 22 dBm, the receive power was undetectable. As calculated, the receive power should have been around -31 dBm.

Next the transmitter, in the truck bed, was moved to the central point approximately 25 meters from both receivers. At this point, again, both receive antennas were adjusted to line up with a transmit antenna. Lining up the antennas was done to ensure the signal had the most direct route to the receiver; hence the signal power loss would be minimized. With this configuration, measuring the power out of the receive antenna, in the manner described above, resulted in a power of -42 dBm. The expected received power at a distance of 25 meters was -25 dBm.

A decision was made to run a one hour test at the central point as it was the only place where the transmit signal was detectable at both receivers. For the one hour test the signal generator was outputting 25 dBm to the antennas in a pulsed waveform. The pulses occurred once every ms with a pulse width of 100 μs.

After the test was completed the time of arrival values were observed at each receiver. At one receiver the values of the counter ranged from 200 to 400, randomly jumping around in this range. At the other receiver the counter value started around 50000 and decreased linearly over the hour test by 20000 to a final value of around 30000. All of these numbers correspond to the number of counts from the time the PPS was received to the time the transmit signal was received. This decreasing pattern of the time of arrival count had not been observed in any other setting so it was important to determine the cause.

The first step taken was to switch the GPSDOs at the receivers. This step was completed to determine if the GPSDOs were causing the behavior of interest. After switching the GPSDOs between the receivers, a short ten-minute test was conducted. The linear decrease was observed at the same receiver where it was previously seen. This result showed that the linearly decreasing behavior was independent of which GPSDO was used at a receiver.

The data recorded during these tests were returned to the lab before it was processed. The data collected from the hour-long test is plotted in Figure 53 where the effect of the linearly decreasing counts is clear. Since the TOA at the receiver with the

linearly decreasing behavior was subtracted from the other receiver, the TDOA has a positive slope. This slope is very linear and a line of best fit can easily be derived from two data points. Once this line was formed it was subtracted from the TDOA data in order to remove the linear behavior of the data. Figure 54 shows the results of this subtraction. The results in Figure 54 are still unlike the data originally collected in the lab. It is also important to recognize that the spread of this data is around 400 ns, much greater than the spread measured in the lab, which was slightly greater than 60 ns.

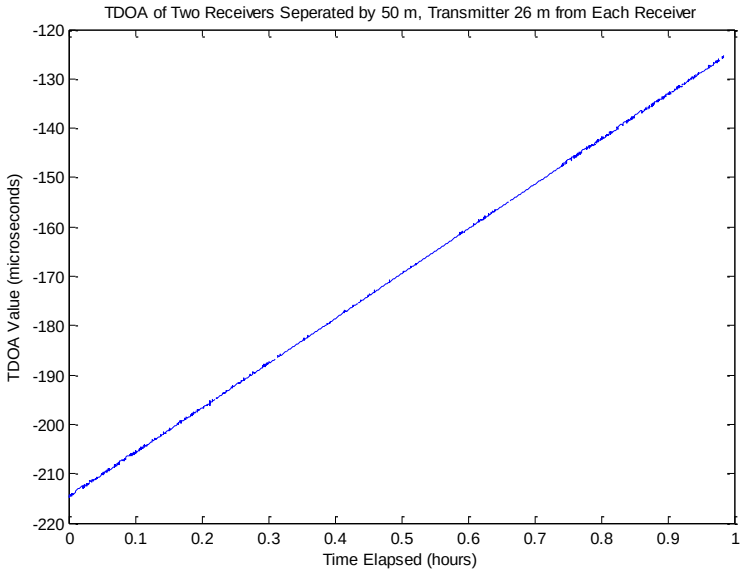

Figure 53: Time difference of arrival (TDOA) over time for field test where transmitter was setup in the middle of the receivers

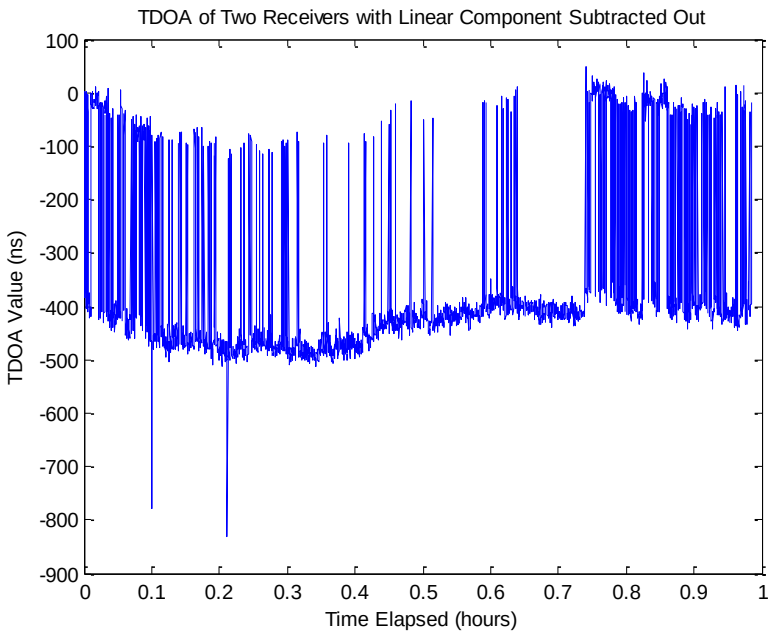

Figure 54: Time difference of arrival (TDOA) over time for field test with linear component subtracted out. Spread is approximately ±200 ns

After what was observed during the test and after the results were obtained, one finding was very clear: the system did not operate as expected. While the receivers were able to acquire the transmitted signal, there was some external interference acting on the signal, or there was an issue with the equipment. Multipath, as an external source of interference, is thought to be a potential reason behind the linearly decreasing count at the one receiver. With the receiver threshold set to such a low level, about -42 dBm, if there were effects from multipath occurring at the same rate every time a signal was received, then the linearity of the count would result.

Testing to determine if multipath was indeed the reason behind the results of the field-test did not occur, as there was insufficient time to repeat the testing. In order to test for multipath effects, a large open field would be needed, as there would be few sources of multipath. The initial testing site was surrounded by numerous buildings and vehicles and on top of asphalt, which are all potential sources of multipath. Testing could also occur in the same location if the power of the received signals was greater. The increased power would allow the threshold for received signals to be set to a higher level, potentially above the level of a received multipath signal. If the receivers were having an issue distinguishing

the received signal from noise, it could also account for the other receiver staying between 200 and 400 counts. If the received signal was received with more power, then the signal should appear above the noise floor, thus affecting the count at that receiver.

6. Future Work

The focus of future work related to this project should be on understanding the results of the lab test and locating the source or sources of error. In trying to locate the source of the offset and timing inaccuracies, the GPSDOs along with the entire system would be better understood and would allow for deployment of this system.

The main reason the source of the offset was not discovered was due to time constraints and other issues that were out of our control. By the time the system was functional, there was little over a week to complete all of the testing desired. The reasons that testing was not conducted until such a late time was primarily out of our control. The main challenge was that the ability to test was highly dependent on members of Group 105 sacrificing their time. One such case is the FPGA cards. A member of Group 105 programmed the cards and testing had to wait until this task was completed. If there was not a time constraint many other tests could have been run to isolate the offset error. The subsequent paragraphs will outline tests that would be useful to conduct to determine the source of the offset.

A very important test to conduct, and the first test that would be run if more time were available, would be to take the GPSDO out of the system. The purpose of the GPSDO is to provide a 1 Hz signal, the PPS, to the FPGAs so that they each start a counter. A signal generator could be set to output a 1 Hz signal to simulate the PPS from the GPSDO. The output of the signal generator would be split with a power divider and sent into both receivers with equal lengths of cable to act as the PPS from the GPSDO. The same signal generator would be used for both receivers to ensure that any error in the signal generator was seen in both receivers, hence it would be subtracted out when the TDOA was calculated. This test would be run for 16 hours. Previous tests have shown that when the system is setup in the zero TDOA case, the system produces a constant output over this period of time. It would also be important to run the 16 hour test multiple times. Between each run it would be important to shut down the system and let it cool down as it was observed that restarting the full system had an effect on the value of the offset. If the results of this experiment still showed a large constant offset then it would be assumed that the error was not in the GPSDO, rather the error would be from somewhere in the rest of the

receiver unit. If the offset was not present, then the error would be assumed to be introduced by the GPSDOs.

If the error was due to the GPSDO, the next step would be to test the different PPS outputs. The GPSDO has a PPS output at three voltage levels: CMOS, 0 V to 5 V; LVDS, ±300 mV; and RS-232, ±6V. Early in the project, the specification given was that the PPS needed should be a 5V CMOS signal. Because of this specification, the focus of the characterization of the GPSDO was on the CMOS output. However, once initial testing of the system commenced it was discovered that the CMOS signal did not work. The control center showed that the signal was not being received, hence the counter was never started and the TOA never recorded. Instead of inputting the CMOS signal the RS 232 signal was tested and the control center showed that this PPS was received as expected and the counter was started. Since preliminary measurement on the oscilloscope showed that the RS 232 level output behaved similar to the CMOS level it was assumed, for the sake of time, that characterization of the CMOS output was sufficient to cover the RS 232 output. However, for future work it would be critical to characterize all PPS outputs in a similar manner to the CMOS output.

Once all outputs were characterized to the level of the CMOS output in this paper, it would be important to analyze the satellite data received by each GPSDO. Each GPSDO outputs real time data about the number of satellites in view, the number of satellites tracked, and the signal to noise ratio of the signal received from specific satellites. To the best of our knowledge this data would have to be continuously monitored and recorded by hand as the GPSDOs do not seem to have a way to output or record this data over time. Recording would have to occur for at least a 12 hour period to capture the full revolution of the GPS satellites. Though this test would be very time intensive it would allow for an understanding of how the satellites that each GPSDO tracks changes over time. The data acquired from this test could also be analyzed to look for source of an offset that could create an offset between the two GPSDOs

A final source of error identified that may originate from the GPSDOs would be multipath in the GPS antennas. Multipath signals being received by the GPS antennas would occur both inside and outside so there is no environment where a test could be conducted where multipath would not have the chance of affecting the results. However, very little

research was conducted to determine how the chosen GPS antennas and GPSDOs respond to multipath. Hence, more research would have to be conducted before a test to determine the effects of multipath could be designed.

If the offset was not coming from the GPSDO, rather some other part of the receiver hardware, there are many more tests that could be run. The first of which would be to simply test points within the FPGA cards with a digital multimeter or an oscilloscope. Points to test would be points where the PPS and trigger signals are travelling into the FPGA cards. Though the control center allows the user to see the signals in the FPGA, it is uncertain if there are delays in the FPGA hardware that would cause delays not seen by the control center.

Another factor to consider is the physical connection of every cable. When the system was moved in and out of the lab all cables were disconnected and reconnected. Similar to testing connections in the FPGA cards, it would be valuable to test the PPS and trigger signals along the entire path. It would also be important to test the connections between the ADC clock source and the FPGA card. Any bad connection or bad length of cable could cause a constant delay, which could be the source of the offset.

If the original test proposed in this section, to remove the GPSDO from the system, was inconclusive there are still other useful tests to consider. It is known that shutting down the entire system, allowing it to cool down, and then restarting causes the system to stabilize to a different offset, after a time period of around three hours. Turning off and on single pieces of equipment to determine if they are the cause of the changing offset or if they change the time it takes the system to stabilize would also be a very good test to isolate the source of the offset. If it was found that one piece of equipment was the source of a large changing offset, this piece of equipment would have to be observed in further testing.

7. Conclusion

This project set out to integrate and test a two-receiver geo-location system with a particular focus on clock synchronization between the receivers. We determined that the difference between the GPSDOs' PPS CMOS outputs were within ±60 ns 90% of the time. Once the GPSDOs were determined to operate within the 1.5° requirement over 70% of the time, laboratory testing was performed. During testing, a 105 ns offset was observed. Other than this offset, the system was still performing within the 1.5° requirement.

The full system was then tested in the field, but the results were inconclusive and a decision was made that there were too many source of error to pursue further field testing in the limited time available. After reviewing the results, another decision was made to perform further testing in the laboratory in order to better understand the system. The secondary laboratory testing provided results that were contradictory to the initial testing. The results proved that the 105 ns offset initially seen was not a constant offset between the receivers. Further testing procedures to determine the source of the error were determined for future work, but the exact source of the error is still unknown.

8. References

Allan, D., Ashby, N., & Hodge, C. (1997). The Science of Time Keeping: Hewlett-Packard Company.

Carr, J. (2001). The Technician's Radio Receiver Handbook: Wireless and Telecommunication Technology. Boston: Newnes. 37-39.

Cristian, F. (1989). Probabilistic clock synchronization. Distributed Computing, Vol. 3, No. 3, 146-158.

Gusella, R.; Zatti, S. (1989). The Accuracy of the Clock Synchronization Achieved by TEMPO in Berkeley UNIX 4.3BSD IEEE Transactions on Software Engineering, Vol. 15, No. 7, 847-853.

Lipsky, S. E. (2004). Microwave Passive Direction Finding: SciTech Publishing. 155-170.

Lombardi, M. A. (September 2008). The Use of GPS Disciplined Oscillators as Primary Frequency Standards for Calibration and Metrology Laboratories. NCSLI MEASURE, 3(3), 56-65.

McCarthy, D.; Seidelmann, P. (2009). TIME From Earth Rotation to Atomic Physics. Weinheim: Wiley VCH. 16-17, 143-144, 151-177, 199-221, 223-232.

Mills, D. (2010). Computer network time synchronization: the Network Time Protocol on Earth and in space. Boca Raton: CRC Press. 2-22.

Shera, B. (July 1998). A GPS-Based Frequency Standard. QST, 37-44.

Timberger, S. (1994). Field-Programmable Gate Array Technology. Berlin: Springer Science & Business Media. 2-4, 22.

Appendices

Appendix A

This appendix contains all of the histograms and time series plots for the data collected to characterize the GPSDOs. The first plots are the histograms of the individual captures. The plots that follow are the time series plots of the same data for each of the captures.

Capture 1 histogram:

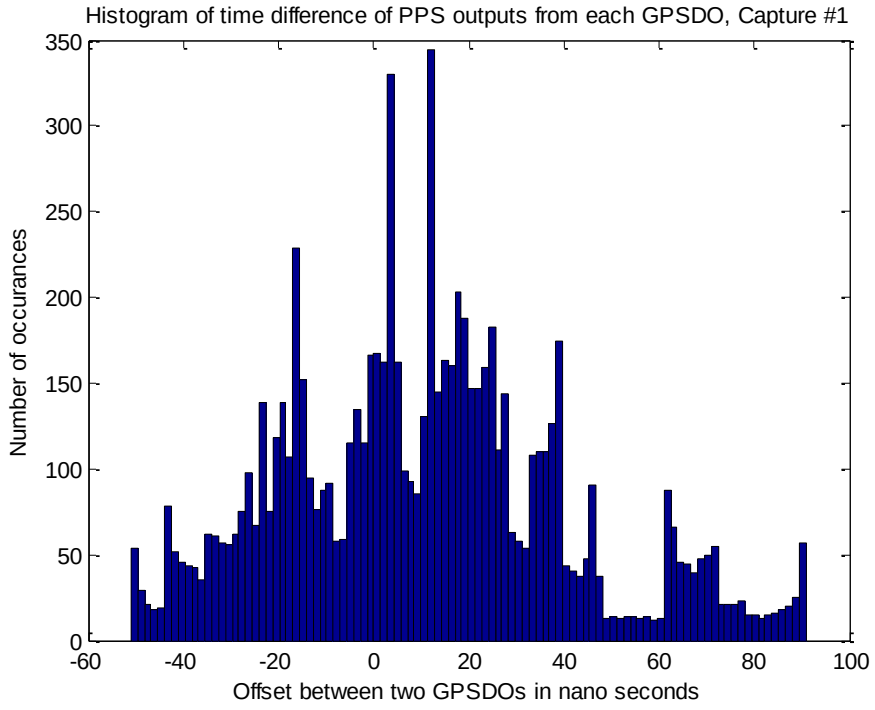

Capture 2 histogram:

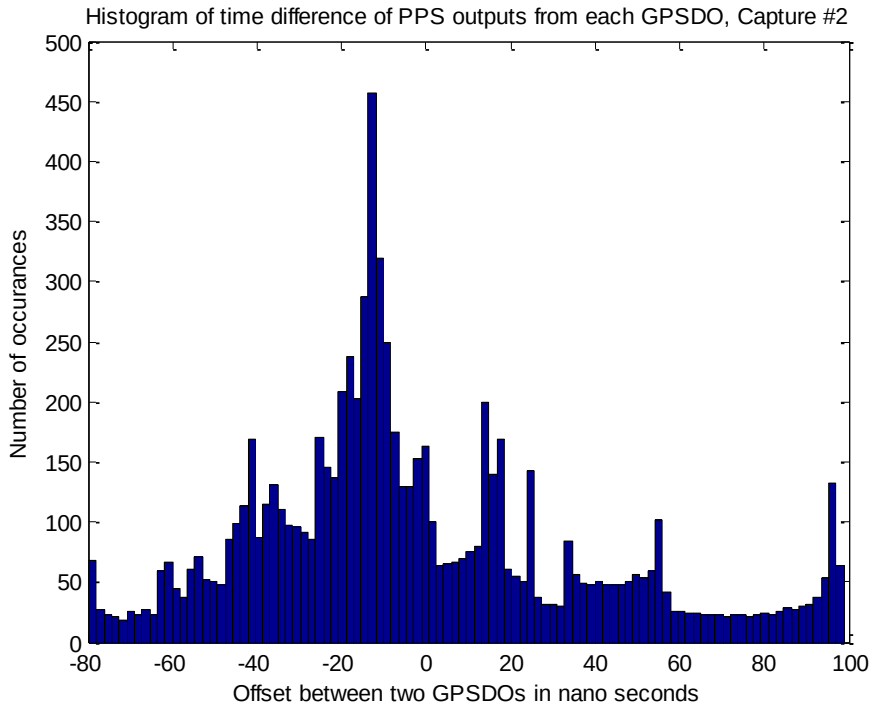

Capture 3 histogram:

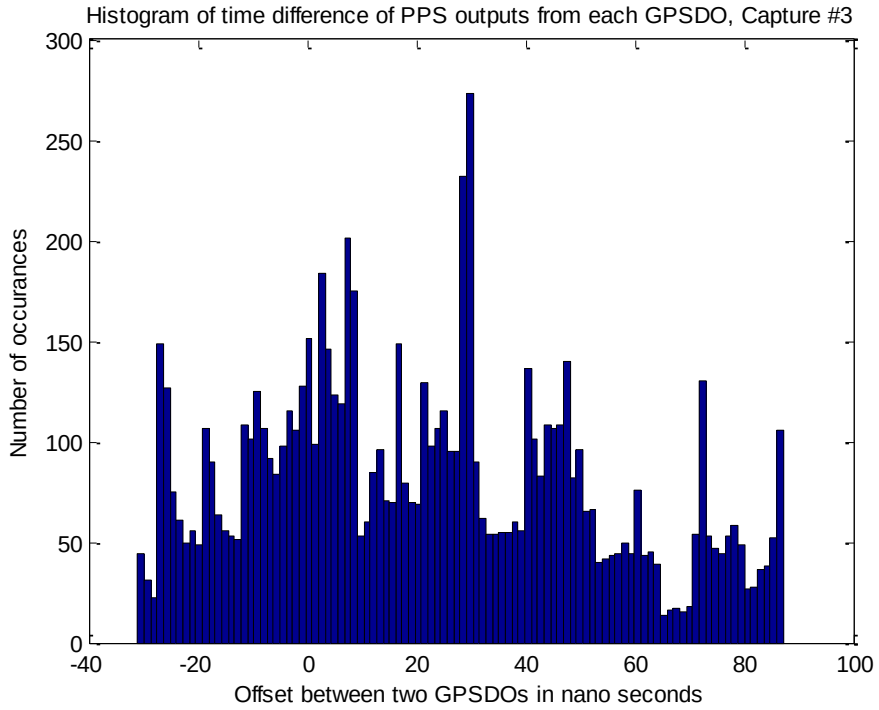

Capture 4 histogram:

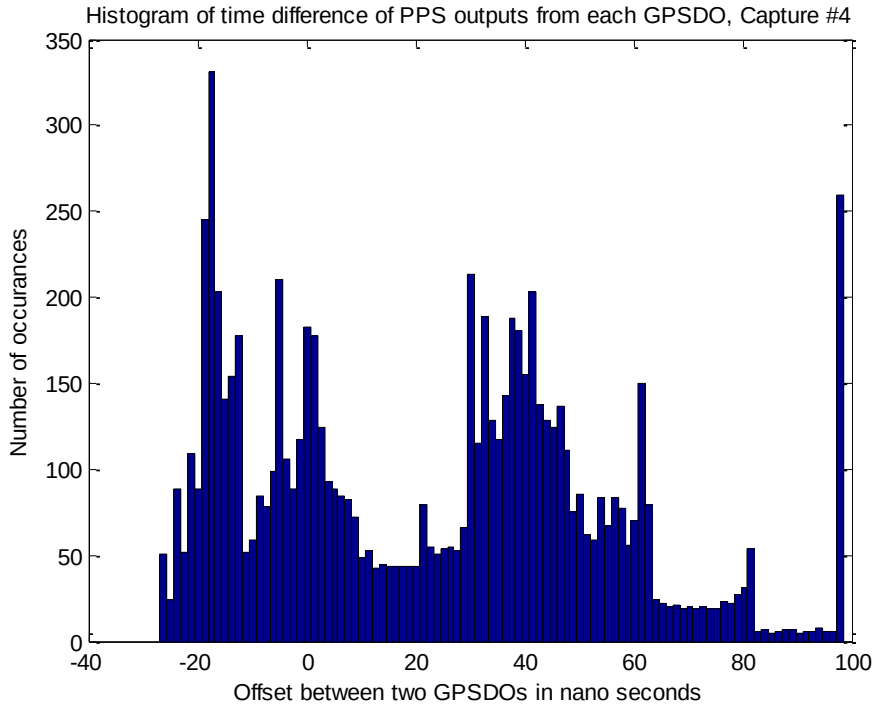

Capture 5 histogram:

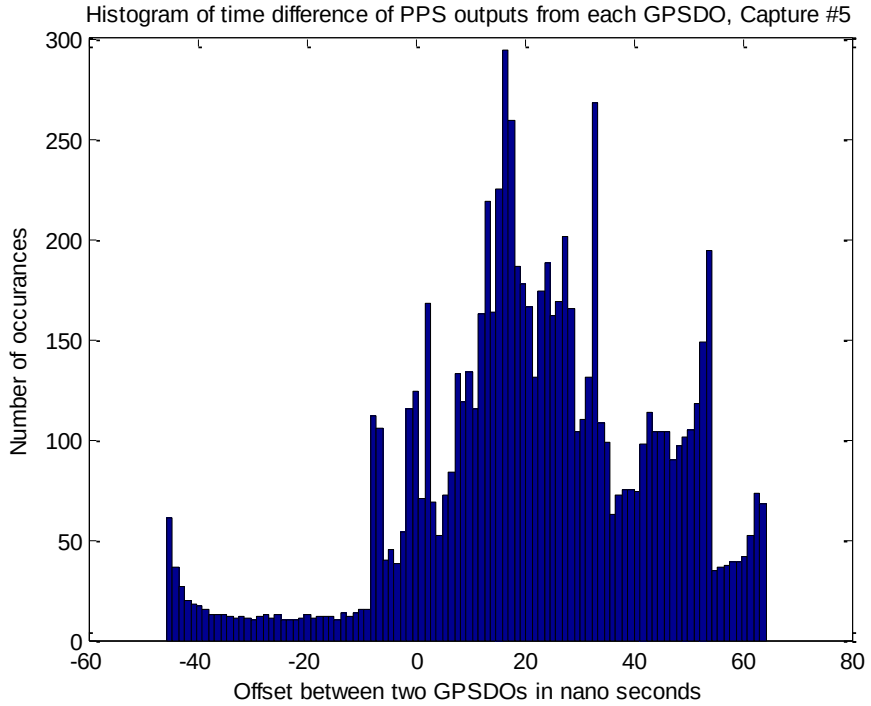

Capture 6 histogram:

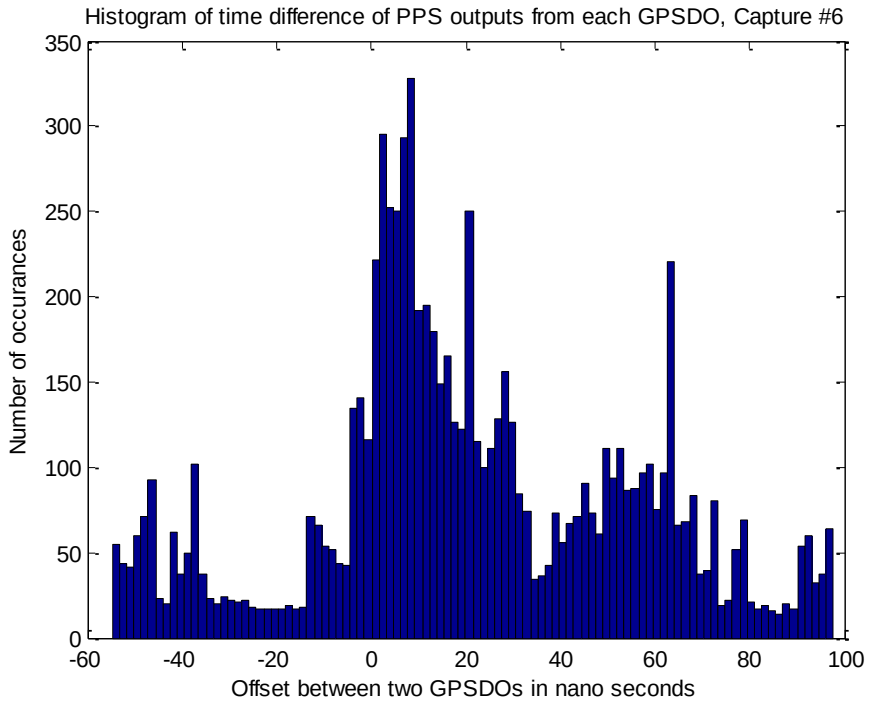

Capture 7 histogram:

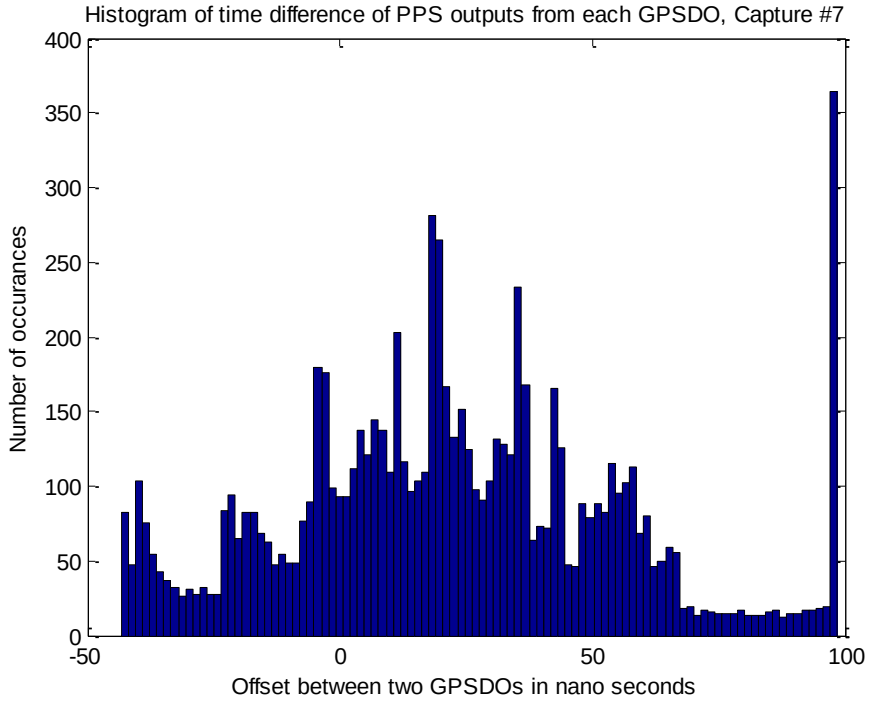

Capture 8 histogram:

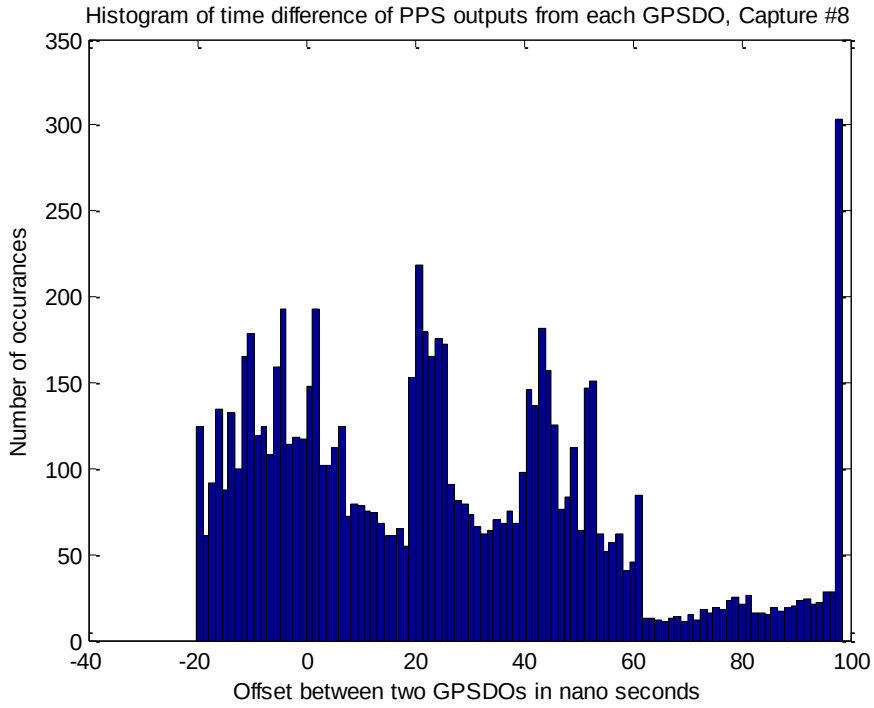

Capture 9 histogram:

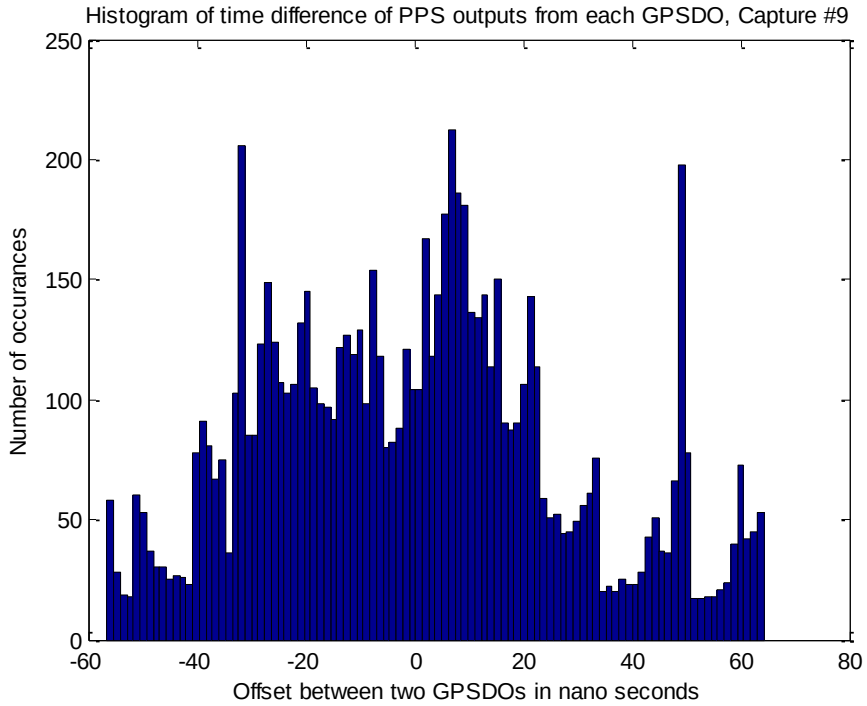

Capture 10 histogram:

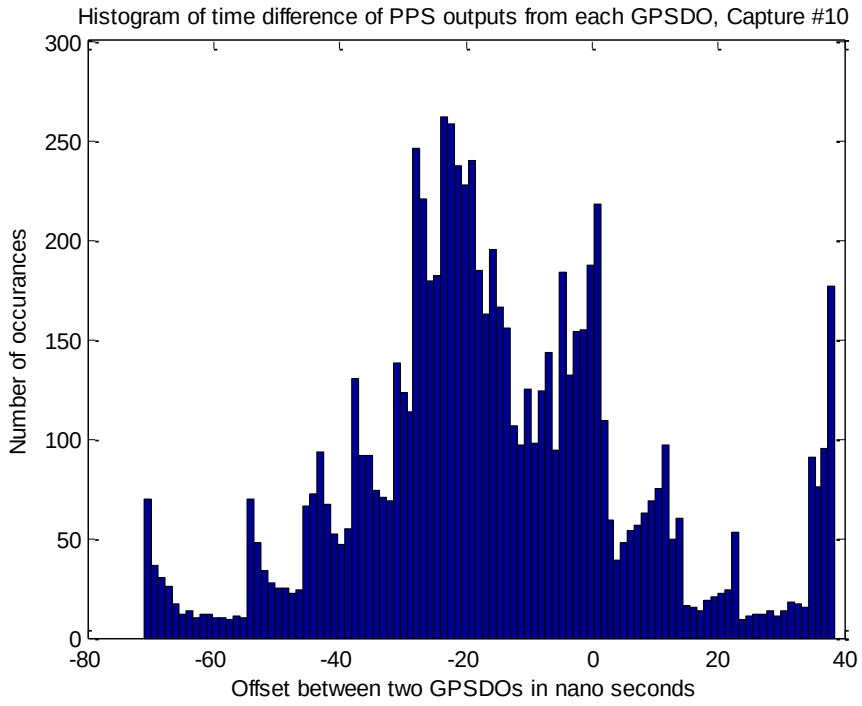

Capture 11 histogram:

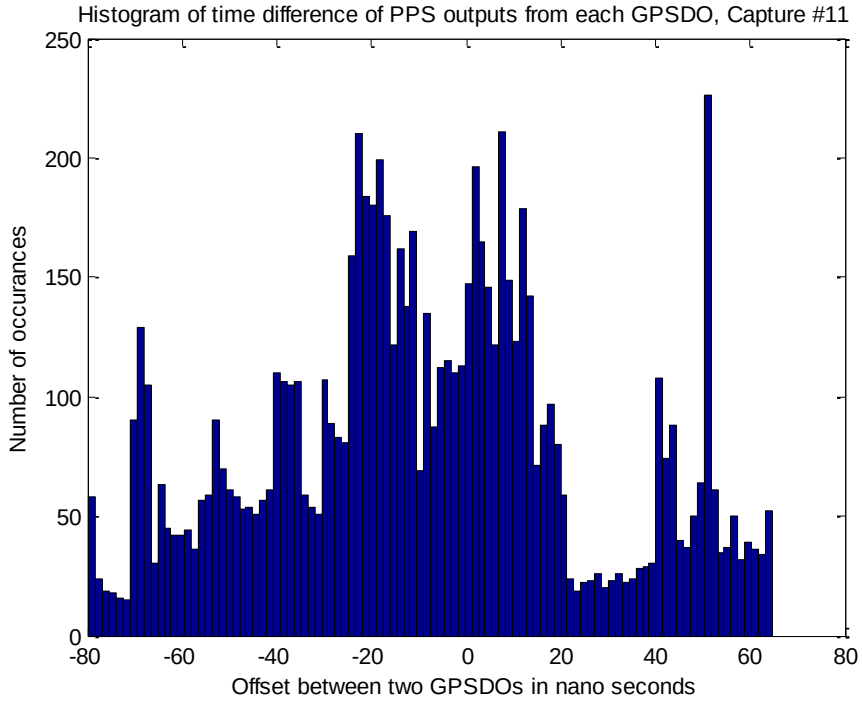

Capture 1 time series plot:

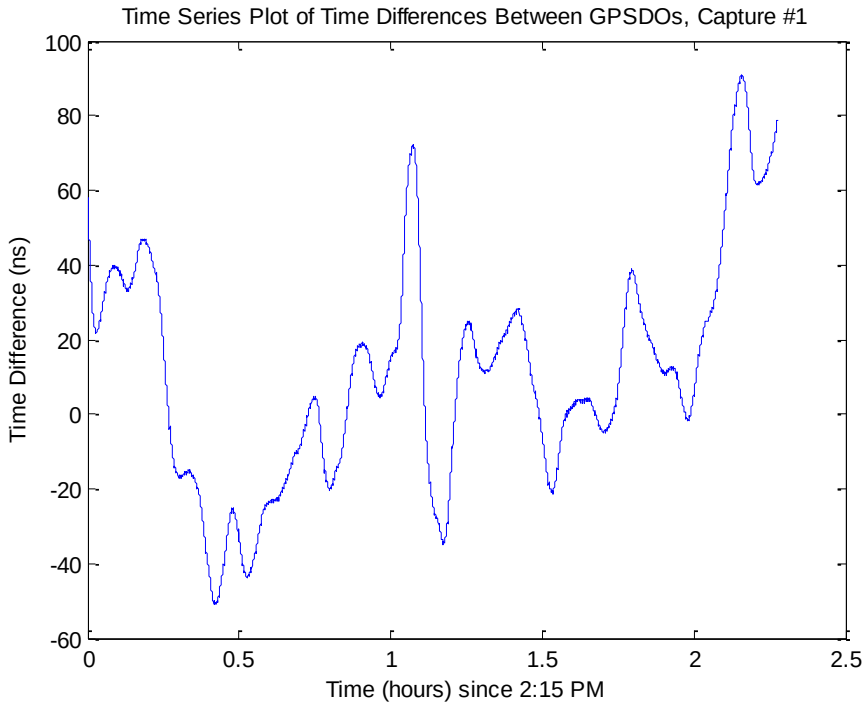

Capture 2 time series plot:

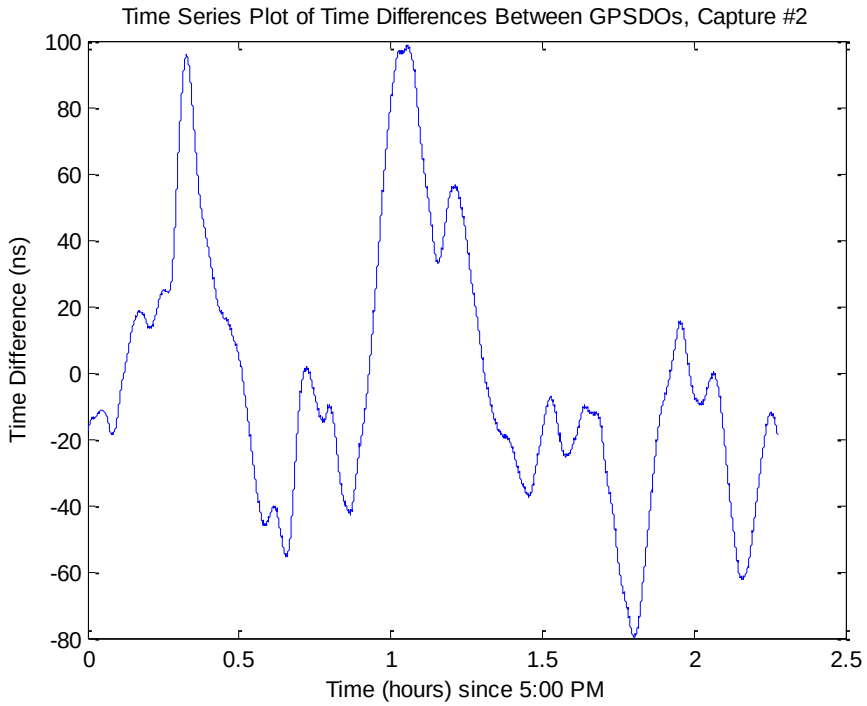

Capture 3 time series plot:

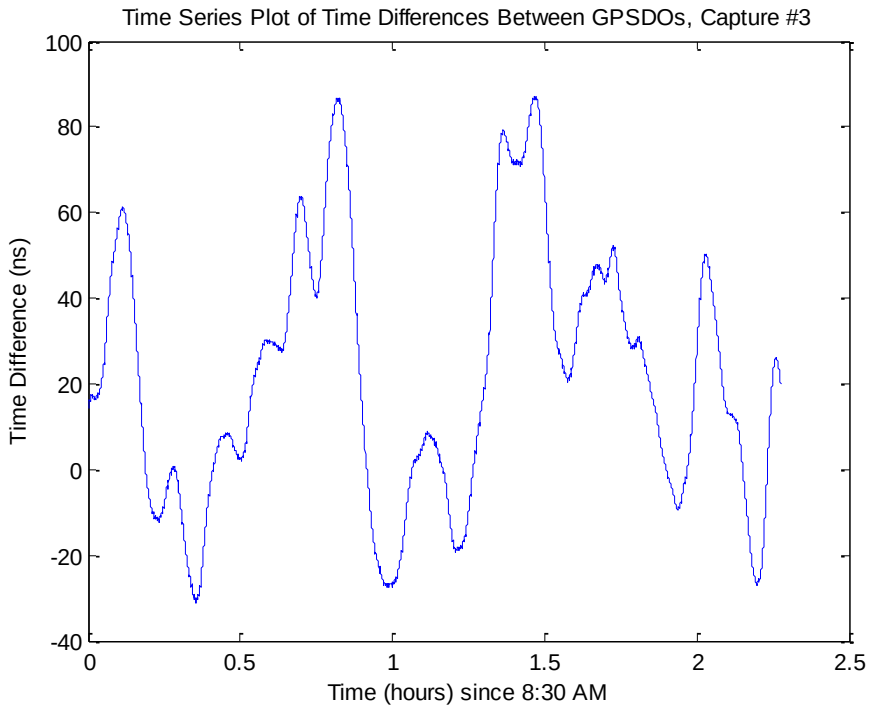

Capture 4 time series plot:

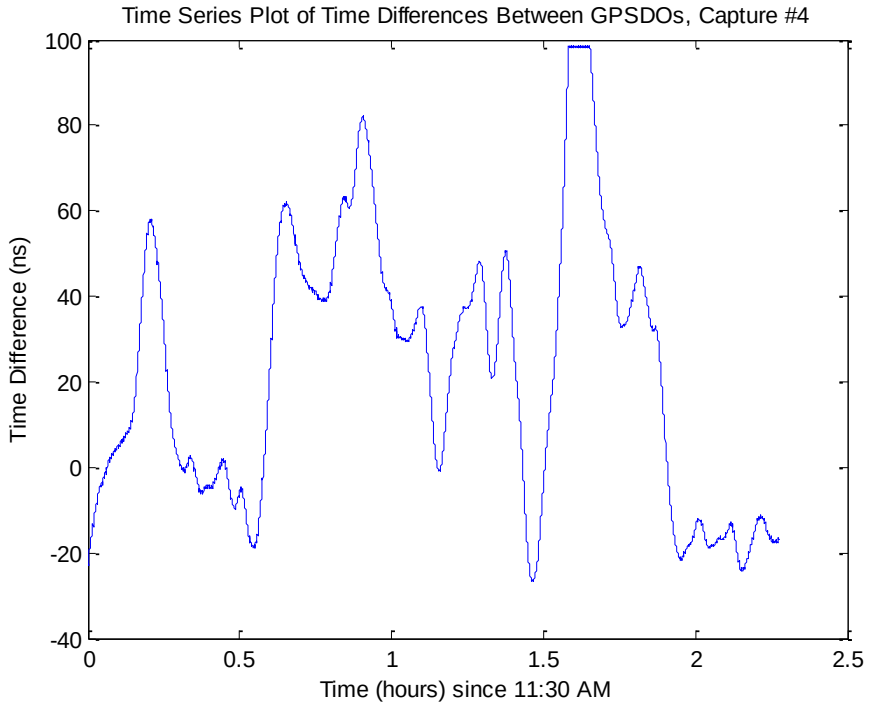

Capture 5 time series plot:

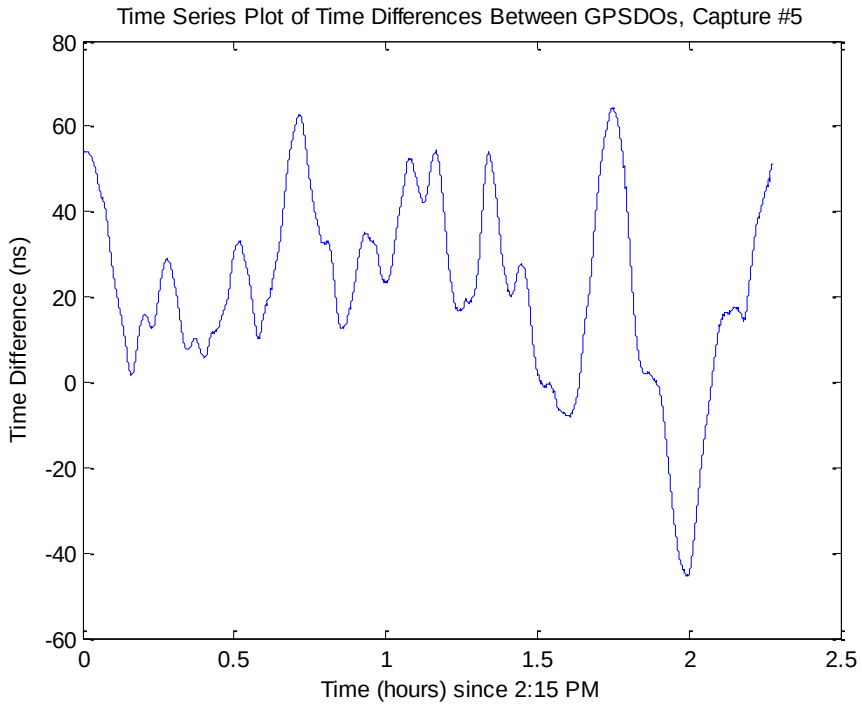

Capture 6 time series plot:

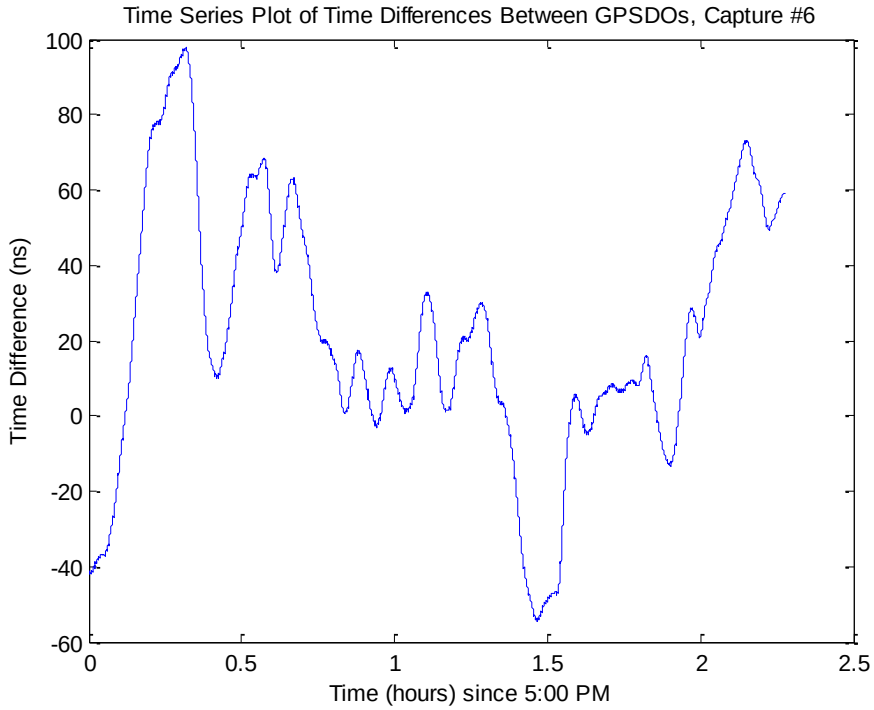

Capture 7 time series plot:

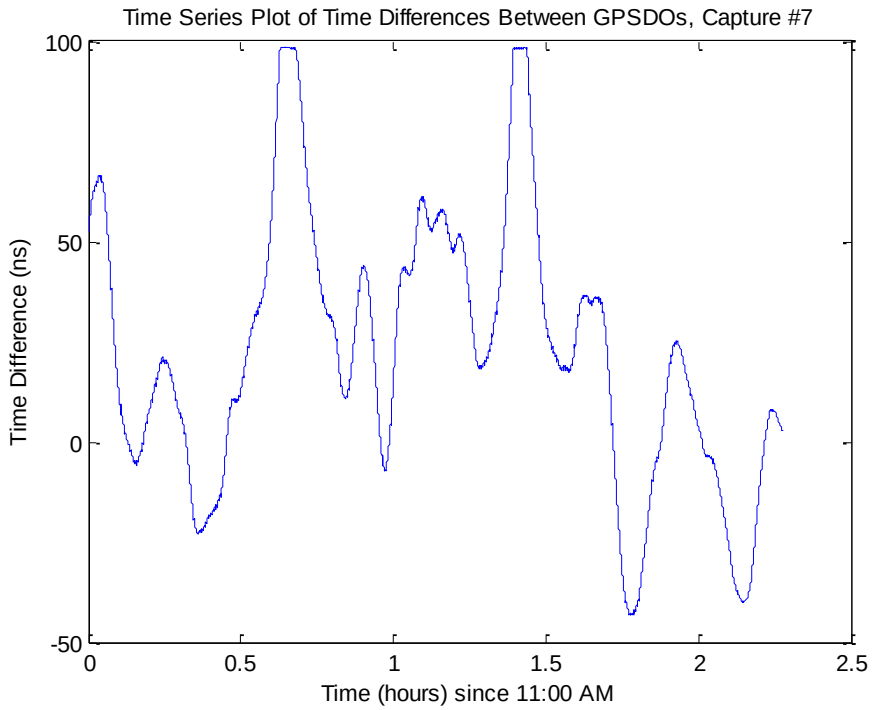

Capture 8 time series plot:

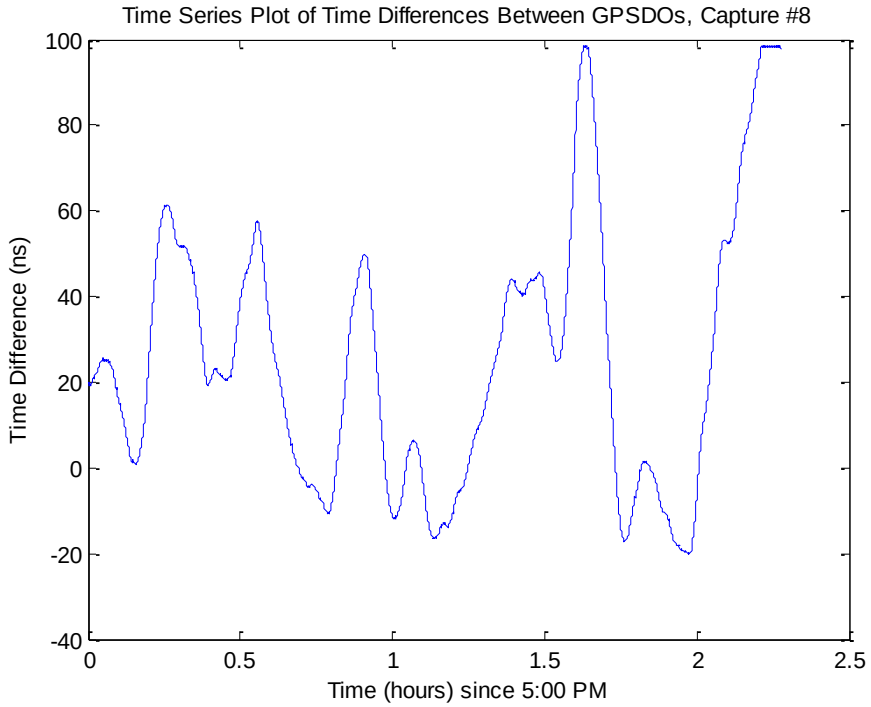

Capture 9 time series plot:

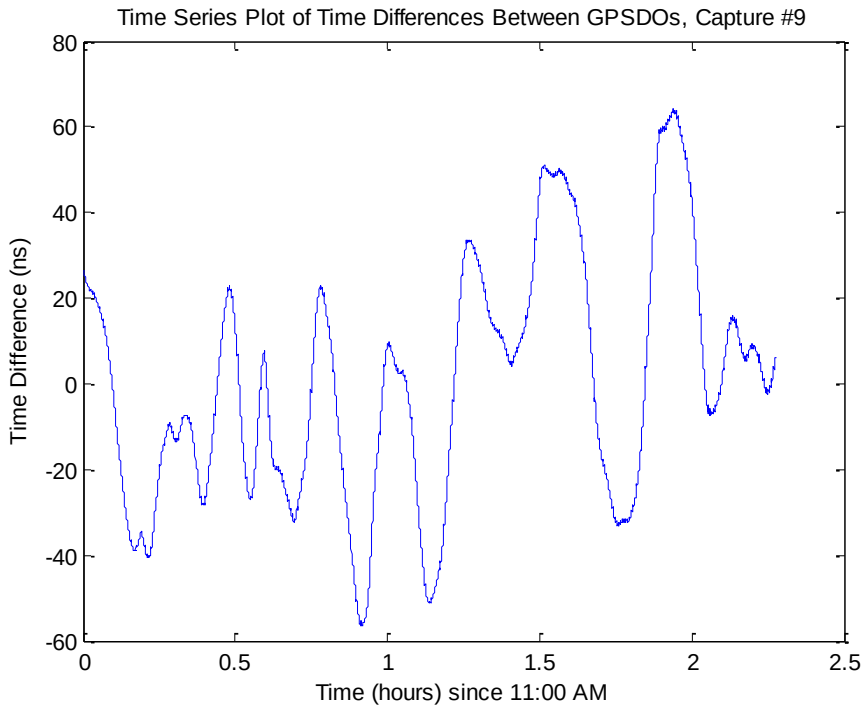

Capture10 time series plot:

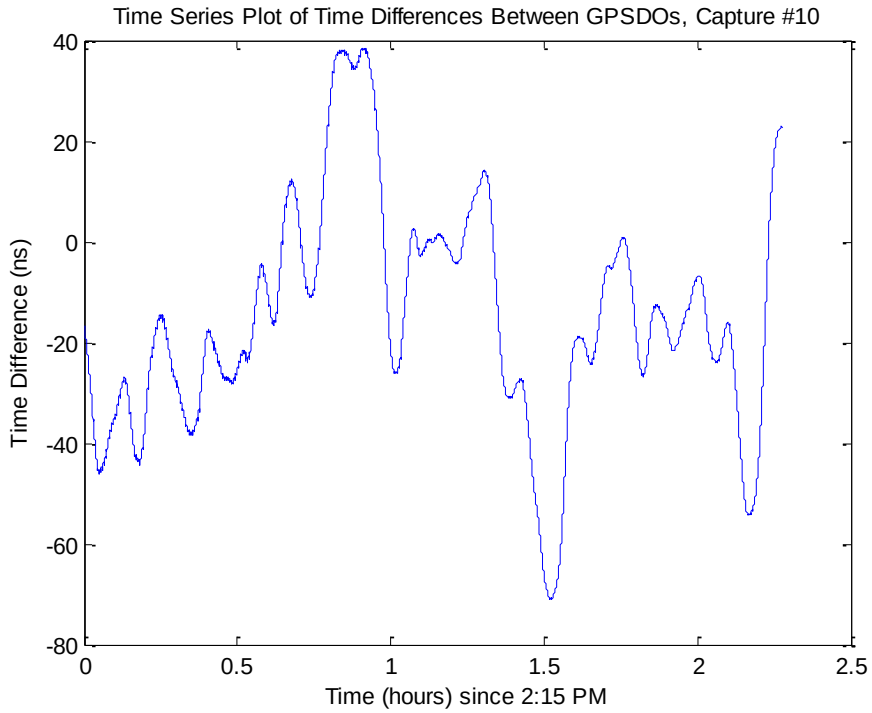

Capture11 time series plot:

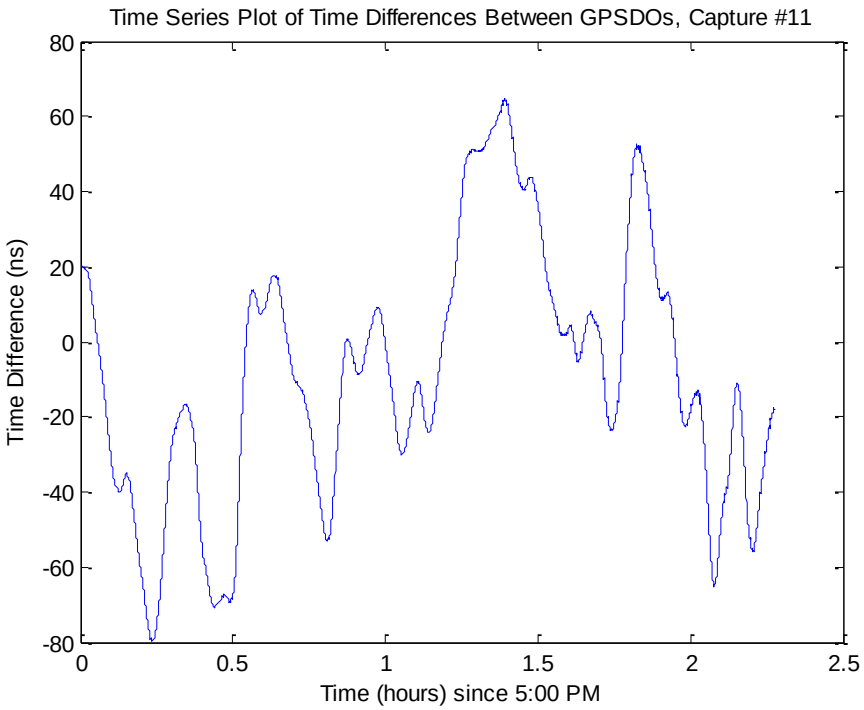

Appendix B

Microvolts/meter is a measure of electric field strength. Since the electromagnetic field created by a transmitter is what actually interferes with other transmitters, many FCC transmit limits are based on electric field strength. The FCC acknowledges that knowing the power limit in Watts is practical and hence gives a simplified equation to convert between microvolts/meter and watts. The equation is:

$$\frac{PG}{4\pi D^2} = \frac{E^2}{120\pi} \tag{1}$$

where P is transmit power out of the antenna, in watts, G is the unit-less gain of the antenna, D is the distance to the measuring point from the transmitter, and E is the electric field strength in volts/meter.

The limit for a signal transmitted at 12 GHz is 12,500 microvolts/meter at 3 meters. Solving for P results in:

$$P = \frac{D^2E^2}{30G} \tag{2}$$

where D is 3 meters, E is 12.5 microvolts/meter, and G is 50.1 which is the 17 dBi gain of the antenna available for Ku band. The result for P is 0.94 watts, or about 29.8 dBm.

Appendix C

The data sheet for the Microsemi GPSDO 2650 utilized for the project can be seen below.

Symmetricom

DATA SHEET

GPS-2600 and GPS-2650

100 MHz DOCXO-based GPS Disciplined Oscillator

Key Features

- High-performance GPS Receiver
- Small footprint and low profile: only 1.5" x 4" x 0.8"
- Excellent holdover stability
- Built-in Distribution Amplifier for multiple outputs at both 100 MHz and 10 MHz
- Low phase noise and very low phase noise floor at 100 MHz
- 1 PPS output accuracy of ±30 ns to UTC RMS (1-sigma), GPS-locked

Applications

- Unmanned Aerial Vehicles (UAV's)
- IED Jammers – fixed, mounted, dismounted
- Radar Systems
- Satellite Communications terminals
- Aircraft Guidance Systems
- Tactical Radios
- Underwater systems using GPS for initialization

The Symmetricom® GPS-2600 and GPS-2650 are 100 MHz Double-Oven OCXO-based GPS Disciplined Oscillators (GPSDO's). The GPS-2600 covers a temperature range of 0°C to +75°C, while the GPS-2650 covers an extended range of -25°C to +75°C. Both units feature a high-performance GPS receiver that can track up to 50 GPS signals, down to levels as low as -160 dBm. The receiver is compatible with GPS, WAAS, EGNOS, and MSAS signals.

Special software functionality supports airborne applications by providing avionics systems with a 3D velocity vector, Attitude/Tilt information, Speed, Heading, Height (both MSL and GPS height), Position, Time, Date, Frequency, Time-stamping, and Health information. For mission-critical applications, the units also provide a direct redundancy feature, allowing multiple units to be daisy-chained to each other for increased reliability.

By providing both 10 MHz and 100 MHz reference outputs in one compact unit, the GPS-2600 and GPS-2650 are an excellent fit for up-conversion subsystems used in radar and satellite equipment, where very low phase noise is critical. The units provide two 10 MHz outputs, one sine wave at +13 dBm, and one with LVDS-compatible levels. They also provide seven 100 MHz outputs, 2 sine wave at +7 dBm each, 4 LVDS-compatible, and 1 5V CMOS-compatible. There are also three 1 PPS outputs, one each with 5V CMOS, LVDS, and RS-232 compatible levels. The 1 PPS output is accurate to within ±30 ns of UTC RMS (1-sigma), once GPS lock has been achieved.

Holdover stability is excellent, at better than ±7 µs over a 24-hour period at +25°C. Phase noise at 10 MHz is <-100 dBc/Hz at a 1 Hz offset, with the comparable number for the 100 MHz output being -118 dBc/Hz at 100 Hz. The noise floor of the 10 MHz output is <-145 dBc/Hz, and for the 100 MHz output it is an extremely low -160 dBc/Hz. The units consume <4W of power at +25°C.

These units can be monitored and controlled through an RS-232 port via standard SCPI commands, and they also can generate NMEA-0183 output sentences for easy integration into existing system architectures.

Page 1 of 2

GPS-2600 and GPS-2650 100 MHz DOCXO-based GPS Disciplined Oscillator

Specifications

ELECTRICAL SPECIFICATIONS

MODULE SPECIFICATION:

1 PPS Accuracy	±30ns to UTC RMS (1-sigma) GPS locked
Frequency Accuracy	Better than ±3.0 E-10 after 1 hour operation with GPS locked
Holdover Stability	±7µs over 24 hour period @+25°C (no motion, after 3 days with GPS)
ADEV	1s to 1000s: 2.0E-11 with GPS lock (typical)
1 PPS Outputs (OCXO Flywheel Generated)	Three outputs: 5V CMOS, LVDS differential pair and RS-232 level output
10/100MHz Outputs (9 outputs total, 7 @ 100MHz, 2 at 10MHz)	4 differential LVDS pairs @ 100MHz, 2x sine 100MHz at +7dBm, 1x CMOS @ 100MHZ, 1x sine 10MHz at +12dBm, 1 differential LVDS pair @ 10MHz
RS-232 Control	Full control via SCPI-99 control commands, NMEA-0183
Avionics Support	3D velocity vector (velocity output for the X, Y, and Z planes), 3D MEMS accelerometer with ±3G range
GPS Frequency	L1, C/A 1574MHz
GPS Antenna	Passive or active, 5V
GPS Receiver	50 channels, mobile, GPS, WAAS, EGNOS, MSAS supported
Sensitivity	Acquisition – 144 dBm Tracking – 160 dBm
GPS TTFF	Cold start – <45 sec Warm start – 1 sec Hot start – 1 sec
TTL Alarm Output	GPS unlock and event indicator
Warm Up Time/ Stabilization Time	<10 min to 1.0E-9 accuracy at +25°C (typical)
Supply Voltage (Vdd)	11.0V to 16.0V DC nominal
Power Consumption	< 4W at +25°C
Operating Temperature	0°C to +75°C (GPS-2600) and -25°C to +75° C (GPS-2650)
Environmental Conformance	MIL-STD-202, method 204, condition I-A
Storage Temperature	-45°C to +85°C

OSCILLATOR SPECIFICATION:

Frequency Output	10MHz and 100MHz
10/100MHz Retrace	±2E-08 after 24 hrs. on, 24 hrs. off, 1 hr. on (no GPS)
Frequency Stability Over Temperature	±2.5E-10 low-g option: ±3E-10 per g per axis
Oscillator Heater Warm-Up Time	<8 min

Phase Noise	100MHz Out	10MHz Out
1Hz	-60dBc/Hz	-100dBc/Hz
10Hz	-95dBc/Hz	-125dBc/Hz
100Hz	-118dBc/Hz	-140dBc/Hz
1kHz	-140dBc/Hz	-142dBc/Hz
10kHz	-155dBc/Hz	-145dBc/Hz
100Khz	-160dBz/Hz	-145dBc/Hz

Designed Lifetime	>10 years

Symmetricom

2300 Orchard Parkway
San Jose, California 95131-1017
tel: 408.433.0910 fax: 408.428.7896
www.symmetricom.com

DS/GPS2600_2650/052112 900-00422-000

Appendix D

```
% Plots 2 receiver TDOA hyperbola with a flight path and intersection point
R1 = [5 0];
R2 = [-5 0];
Tx = [7.874 10];

Rloc = [R1;R2];
v = 2.99e8/1000;%speed of light in km/s
t1 = sqrt((R1(1)-Tx(1))^2+(R1(2)-Tx(2))^2)/v;
t2 = sqrt((R2(1)-Tx(1))^2+(R2(2)-Tx(2))^2)/v;
a = abs(t1-t2)*v/2;
d = sqrt((R1(1)-R2(1))^2+(R1(2)-R2(2))^2)/2;
b = sqrt(d^2 - a^2);
theta = atan(abs(R1(1)-R2(1))/abs(R1(2)-R2(2)));
if R2(2)>R1(2)
    theta = -theta;
end
if R2(1)<R1(1)
    theta = -theta;
end
x_off = 1/2*(R1(1)+R2(1));
y_off = 1/2*(R1(2)+R2(2));
%%
A= [R1(1)-R2(1) R1(2)-R2(2) -v^2*(t1-t2)];
k=-1/2*(v^2*(t1^2-t2^2)+(R2(1)^2+R2(2)^2)-(R1(1)^2+R1(2)^2));
xyt = A\k;
%% plot
figure, hold on
scatter(Rloc(:,1), Rloc(:,2), 'm', '^')
xmax = 100; ymax = 100;
x = linspace(-xmax,xmax,1001);
y=a*sqrt(1+(x./b).^2);
[X, Y] = xfm1(x,y,theta,x_off,y_off);
plot(X,Y)
[X, Y] = xfm1(-x,-y,theta,x_off,y_off);
plot(X,Y)

plot(-30:1/30:30,10,'k')
scatter(7.874,10,'o','filled','g')
legend('Rx', 'Hyperbola', 'Location', 'North');
title('Two Receiver TDOA');
xlabel('distance (km)');
ylabel('distance (km)');
axis([-25 25 -30 30])

% Plots lab test data and computes mean and percentage within +/-60 ns
Rx1 = dlmread('testovernight.txt');
Rx2 = dlmread('testovernight2.txt');

cnt1 = Rx1(1:end,1:end);
cnt2 = Rx2(1:end,1:end);
[r1,c1]=size(cnt1);
[r2,c2]=size(cnt2);
if r2>r1
    rows = r1;
```

```
    columns = c1;
else
    rows = r2;
    columns = c2;
end
j=1; k=0;
dif = zeros(rows,1);
for i = 1:rows-1
        dif(j) = cnt1(i,5) - cnt2(i+1,5);
        j = j+1;
end

dif=dif.*1/(225e6);
rem = find(abs(dif)>1e-6);
dif(rem) = NaN;
mean = nanmean(dif);
display(['mean: ' num2str(mean/1e-9) 'ns'])
gd = find(abs(dif-mean)<60e-9);
display(num2str(length(gd)/rows*100));

plot(dif);
hold on
plot(1:100:rows, mean, 'r')
plot(1:750:rows, mean+60e-9, 'r--')
plot(1:750:rows, mean-60e-9, 'r--')
xlabel('seconds elapsed');
ylabel('TDOA value (seconds)');
title('TDOA of Two Receivers with 6ft Cables over 16 Hours');
```